Fine Coal Beneficiation: Comparison Study of The Separation Efficiency of a Dense Medium Cyclone and Flat-bottom Cyclone

Naledi Lumbela

A dissertation submitted to the Faculty of Engineering and the Built Environment, University of Cape Town, in fulfilment of the requirements for the degree of Master of Science in Chemical Engineering

Supervised by:

Prof. Aubrey Mainza

Dr Paul Bepswa

Plagiarism Declaration

1. I know that plagiarism is wrong. Plagiarism is to use another's work and to pretend that it is one's own.
2. I have used the Harvard system for citation and referencing. Each significant contribution to, and quotation in, this report from the work, or works, of other people has been attributed and has been cited and referenced.
3. This report is my own unaided work, except for assistance received from the teaching staff.
4. I have not allowed and will not allow anyone to copy my work with the intention of passing it off as his or her own work.

Signed by candidate

_____

Signature

Abstract

Near-gravity material (NGM) is the fraction of coal particles with a relative density within a range of ± 0.1 of the relative density of the separating medium during coal washing. High levels of NGM in coal impede classifier separation efficiency because NGM particles have low settling rates, which hinder free particle movement during classification. Low-grade coal has a high ash and near-gravity material content, making it economically unviable to beneficiate.

As near-gravity material concentration increases, the efficient beneficiation of clean coal from middlings and rejects becomes challenging, hindering the reduction of ash-bearing impurities. High NGM levels obscure the separation boundaries between middlings and reject coal, complicating product extraction and handling. This reduces the efficiency of coal beneficiation processes. Therefore, this study is undertaken to investigate which classifier between a dense medium cyclone and a flat-bottom cyclone can optimally beneficiate the NGM-laden coal.

A conventional hydrocyclone was modified into a flat-bottom cyclone with an extended cylindrical section and wide cone angle to promote the formation of an autogenous separating medium. This cyclone is sometimes called a water-only cyclone (WoC) in coal washing. The flat-bottom cyclone (FBC) uses no media except water to create an autogenous medium that promotes separation by density. In contrast, the dense medium cyclone (DMC) drives separation by density by using an external heavy media to create a sharp density difference between the coal, gangue particles and the heavy media.

Each classifier experiment investigated the impact of three parameters on cyclone separation efficiency when beneficiating low-grade coal with high NGM and ash-bearing impurities content. The flat-bottom cyclone parameters included vortex finder diameter, spigot diameter, and solids concentration, each tested at three levels. For the dense medium cyclone, the parameters were vortex finder diameter, spigot diameter, and medium density, also varied at three levels.

The central composite rotatable design (CCRD) was employed to model and numerically optimise the operating variables of the classifiers to minimise the ash

content in the final product coal. Classifier separation performance was analysed through partition curves, density cut-point, sharpness of separation, organic efficiency, and particle misplacement.

The results indicate that for the dense medium cyclone, the vortex finder diameter significantly influences the ash content of the recovered coal yield. In contrast, for the FBC, the spigot diameter is the primary factor affecting ash content. Regression models developed for ash content showed strong agreement with experimental data, achieving R^2 values of 0.78 for the flat-bottom cyclone and 0.80 for the dense medium cyclone. Under optimised conditions, the dense medium cyclone demonstrated sharper separation, lower particle misplacement, and better ash reduction. Conversely, the flat-bottom cyclone showed lower ash removal efficiency, higher clean coal particle misplacement, and poor separation performance.

Acknowledgements

Smakadze, ngaphadlekwakho bengingabayini! Ngiyabonga Nkhosi angicedzi!

I would like to express my deepest gratitude to everyone who contributed to the successful completion of this project. Firstly, I sincerely thank Prof. Aubrey Mainza, Dr. Paul Bepswa and Prof. Narasimha Mangadoddy for their invaluable support and guidance throughout this project. This would not have been possible without you. Thank you!

I am deeply thankful to my parents for their unwavering support and constant encouragement. Your endless calls and prayers, especially you Mama, truly sustained me through this challenging journey. The obstacles I faced along the way were not easy, but your love and belief in me made all the difference. I am grateful to my friends Chiamaka and Same for your endless support during this project.

I am also grateful to the staff at the Centre for Minerals Research who assisted with my project: Shireen Govender, Nqobile Dingilizwe, Monde Bekaphi, Gary Groenmeyer and Kenneth Maseko. Additionally, I would like to thank Clint, Abraham, Egshaan, and Curwin for their help with my rig.

Table of Contents

List of Figures

List of Tables

Glossary of Terms

Abbreviations

ANOVA	Analysis of variance
ASTM	American Society for Testing and Materials
DMC	Dense medium cyclone
DW	Degree of washability
ESKOM	Electricity Supply Commission
FBC	Flat-bottom cyclone
ISO	International Organisation for Standardization
NGM	Near gravity material
NGMI	Near gravity material index
RA	Recovery of ash
RD	Relative density
RNA	Recovery of non-ash
RoM	Run of mine
SG	Specific gravity
VSD	Variable speed drive
WoC	Water-only cyclone
XRD	X-ray diffraction

1 Introduction

1.1 Background

This study aims to compare the separation efficiency of the dense medium cyclone and flat-bottom cyclone (also known as a water-only cyclone) in coal beneficiation. The goal is to determine the most efficient classifier for beneficiating low-grade fine coal with high ash-bearing impurities and near-gravity material content. The coal is sourced from a colliery in the Highveld Coalfield in Mpumalanga. A conventional hydrocyclone was modified to create a flat-bottom cyclone with a long cylindrical section and a wide cone angle, which promotes the formation of an autogenous separating medium. For the dense medium cyclone, a magnetite suspension, an external heavy medium, was introduced into the conventional hydrocyclone to promote separation by density in the classifier.

South Africa aims to gradually shift from fossil fuels to clean renewable energy in the following decades. However, the challenge is the heavy reliance of the state-owned electricity producer, Electricity Supply Commission (Eskom), on coal for energy generation. Close to 53% of the domestically produced market value coal is used for electricity generation (Eskom, 2016). The country has abundant reserves of coal and approximately 336 million tonnes of coal is produced annually. However, close to 74.8 million tonnes of the produced coal is discarded into slurry ponds and tailings dams because of its low-grade characteristics according to Mulambazo (2016).

Nyoni, Bwalya and Chimwani (2020) suggest that, at the current coal consumption rate, high-grade coal reserves will be depleted in 60 years. To meet current and future energy demands in South Africa, it is crucial to consider the beneficiation of discarded tailings and low-grade coal. These materials contain significant ash-bearing impurities and near-gravity material, and their beneficiation is expected to increase over time (Nyoni, Bwalya & Chimwani, 2020).

High ash-bearing impurities and near-gravity material content render coal economically unviable for washing and quality upgrading (Hembrom & Suresh, 2018). NGM is a mix of clean coal particles and impurities or gangue particles with a relative

density (RD) range within ±0.1 of the RD of the separating medium during coal washing (Kumar & Kumar, 2018). High levels of NGM in coal impede classifier separation efficiency because NGM particles have low settling rates, which hinder free particle movement during separation. This results in an increase in material retention time which leads to particle misplacement to the wrong stream during coal washing (Sripriya et al., 2007).

The commonly applied processes of beneficiating fine coal include flotation, water-only cyclones and dense media cyclones. Flotation is commonly used for the beneficiation of ultrafine coal (Ramudzwagi, Tshiongo-Makgwe & Nheta, 2020). The efficient beneficiation of low-grade coal in a heavy medium classifier depends on the density contrast between the clean coal particles and the ash-bearing impurities (Holuszko & Grieve, 1994). A substantial density difference between clean coal particles and gangue material enhances the efficiency of density-based classifiers, such as in dense medium cyclones, leading to improved beneficiation processes (De Korte, 2008).

Dense medium cyclones and water-only cyclones are commonly used in coal beneficiation. These classifiers function similarly: a mixture of coal feed and separating medium is introduced tangentially under pressure through the feed inlet, creating a swirling vortex. This vortex creates a low-pressure area along the vertical axis, forming an air core extending through the centre of the cyclone and connecting to the outside via the spigot opening.

Within the cyclone, particles experience opposing forces: centrifugal forces which force the particles denser than the separating medium towards the inner cyclone wall and down to the spigot for discharge. Drag and pressure differential forces guide low-density particles towards the axial axis, where they are directed to the overflow stream through the vortex finder (Wills & Finch, 2016; Bai et al., 2017; Aketi et al., 2021).

The dense medium cyclone (DMC) can beneficiate coal with a minimum particle size of 0.5 mm (Ramudzwagi, 2020; Sobhy, 2022; Phengsaart et al., 2023). It uses an external dense medium, magnetite or ferrosilicon, to separate fine coal particles based on density differences. Ferrosilicon can achieve relative density values as high as 6.8 and magnetite as high as 4.8. However, ferrosilicon is less frequently employed in coal

beneficiation processes due to its relatively higher cost, making it less economical for treating low-grade coal.

A drawback of the DMC is the loss of fine magnetite to the clean product overflow which impacts separation efficiency and coal quality (Ramudzwagi, 2020). The flat-bottom cyclone (commonly known as the water-only cyclone in coal beneficiation) uses water as the separation medium without chemicals or external heavy media. Structurally, it comprises a short wide-angle conical bottom, a long cylindrical section, and an extended vortex finder, which distinguishes it from a dense medium cyclone which has a long narrow conical section.

1.2 Motivation

The declining reserves of high-grade coal in South Africa coincide with increasing domestic demand. Therefore, the abundant low-grade coal resources have the potential to help meet the current and potential future coal demand. De Korte (2015) suggests that the remaining reserves of high-grade coal in South Africa are projected to be nearly depleted by 2040 as a result of the over excessive mining of the coal owing to high local and international demands for coal.

However, many collieries lack the necessary processing capacity and efficient equipment to improve the quality of low-grade coal. This coal is characterized by a low carbon content and calorific value, and a high moisture and ash content. Additionally, the coal contains significant near-gravity material (NGM) content which makes it less amenable to washing and difficult to process. This makes low-grade coal economically unviable to beneficiate and upgrade its quality.

The extraction and handling of low-grade coal results in the generation of large volumes of coal fines, owing to its natural friability, which accumulates in waste ponds and tailings dams. Despite extensive international research on low-grade coal beneficiation, insufficient attention has been given to South African low-grade coal. By 2016, approximately 2.4 billion tonnes of low-value coal had been discarded, due to inefficient beneficiation processes in the coal mining industry. This has resulted in the pollution of water bodies and air contamination from coal particulates. Addressing

these challenges requires research to develop classifiers that can efficiently handle low-grade coal or optimize existing ones to reduce the volume of coal fines ending up in tailings dams.

1.3 Hypotheses

1.3.1 Hypothesis 1

The combination of the dense medium cyclone operated at an optimised relative density, vortex finder diameter and spigot diameter would enhance the separation efficiency of the classifier. This is because optimised vortex finder diameter and spigot diameter minimise the misplacement of clean particles into the underflow stream and gangue pales into the overflow stream. The optimised relative density promotes sharper density separation which produces a high-quality clean coal product with a significantly reduced ash content.

Key Questions

To determine the validity of the proposed hypothesis for this study, the following questions were formulated:

1. Can the separation efficiency of the cyclone be improved by changing the density of the separating media?
2. How do the cyclone spigot and vortex finder diameters affect the product coal ash content, clean coal yield and separation efficiency of the cyclone?
3. What operating conditions maximize the separation efficiency for the dense medium cyclone?

1.3.2 Hypothesis 2

The separation process in a flat-bottom cyclone (FBC) is predominantly influenced by density rather than particle size. This is attributed to the presence of a hindered settling

regime, which facilitates the formation of an autogenous medium within the cyclone, thereby enhancing density-driven separation efficiency.

Key Questions

To test the hypothesis the following questions were developed:

1. Is the classification process in the flat-bottom cyclone primarily influenced by particle size or density?
2. How do the feed solids concentration, cyclone spigot and vortex finder diameters affect the product coal ash content, clean coal yield and separation efficiency of the cyclone?
3. What operating conditions optimise the separation efficiency of the flat-bottom cyclone when processing high near-gravity material containing fine coal?

1.4 Research Objectives

The primary aim of this study is to determine and compare the effectiveness of separating fine and ultrafine coal using a flat-bottom cyclone against a dense medium cyclone. To achieve this research aim, the following specific objectives have been developed to guide the investigative study:

1. Conduct coal characterization to assess quality, ash content, and near-gravity material content, and evaluate their influence on cyclone separation efficiency.
2. Determine the effect of the vortex finder diameter, spigot diameters and medium density on the classification of fine coal in the dense medium cyclone.
3. Determine how the feed solids concentration, vortex finder diameter and spigot diameter will influence the separation efficiency of the flat-bottom cyclone.
4. For every dense medium cyclone, and flat-bottom cyclone separation experiment, collect the overflow/concentrate throughput and determine the ash content to determine its separation performance.
5. Optimise the operating conditions of the flat-bottom cyclone and the dense medium cyclone and compare which classifier optimally beneficiates high ash and NGM-containing coal.

1.5 Thesis Layout

This thesis consists of five chapters. Chapter 1 outlines the research background, motivation, hypothesis, key questions, and objectives. Chapter 2 reviews the existing literature on fine coal beneficiation. It discusses the impact of separating medium density, vortex finder diameter, and spigot diameter on the performance of the dense medium cyclone. Additionally, it explores the effects of solids concentration, vortex finder diameter, and spigot diameter on the performance of the water-only cyclone, also referred to as the flat-bottom cyclone. It also discusses the effect of the quantity of near-gravity material in coal on classifier performance.

Chapter 3 discusses the research methodology, outlining the experiments conducted, including the characterization of magnetite and coal. It also describes the modification of the conventional hydrocyclone into a flat-bottom cyclone, known as a water-only cyclone in coal washing, and a dense medium cyclone. These modifications were employed for classifier experiments, followed by the analysis of underflow and overflow coal products.

Chapter 4 is the results and discussion section where the outcome from magnetite and coal characterization, and classifier experiments for low-grade fine coal beneficiation, are presented and critically discussed. Chapter 5 concludes the thesis by summarizing the key findings and presenting recommendations based on the research. It highlights the significant results and proposes recommendations for future studies.

2 Literature Review

This chapter discusses and reviews the literature on near gravity material (NGM) and its effect on density-based classifier separation performance. It discusses the effects of key variables on cyclone separation performance. For the dense medium cyclone, these variables include vortex finder diameter, spigot diameter, and feed medium density. For the water-only cyclone, the study focuses on vortex finder diameter, spigot diameter, and solids concentration, specifically in the beneficiation of NGM-laden coal.

2.1 Near Gravity Material

NGM is a fraction of coal, composed of both clean coal particles and ash-bearing impurities. NGM has a relative density within a range of ± 0.10 of the relative density of the separating medium during coal washing (Bhattacharya, Maheshwari & Panda, 2016a). Dense medium separation efficiency primarily depends on the density contrast between the clean coal particles and the gangue particles. A significant density difference enhances the separation of coal from its impurities in density-based classifiers (De Korte, 2008). Consequently, the distribution and quantity of NGM in coal directly impact the separation efficiency of density-based classifiers (Aketi et al., 2017).

In a hydrocyclone, tangential feed introduction induces strong centrifugal forces, which force particles denser than the separating medium towards the hydrocyclone wall and down to the underflow. Drag forces push low inertia coal particles inwards towards the inner vortex and report to the overflow (see Figure 1). However, NGM particles tend to exist within a low-velocity envelope towards the conical section of the cyclone body where the centrifugal and drag forces achieve equilibrium (Aketi et al., 2017). Consequently, the NGM particles experience a prolonged residence time, which can result in particle misplacement during separation in the classifier, leading to overall poor separation performance.

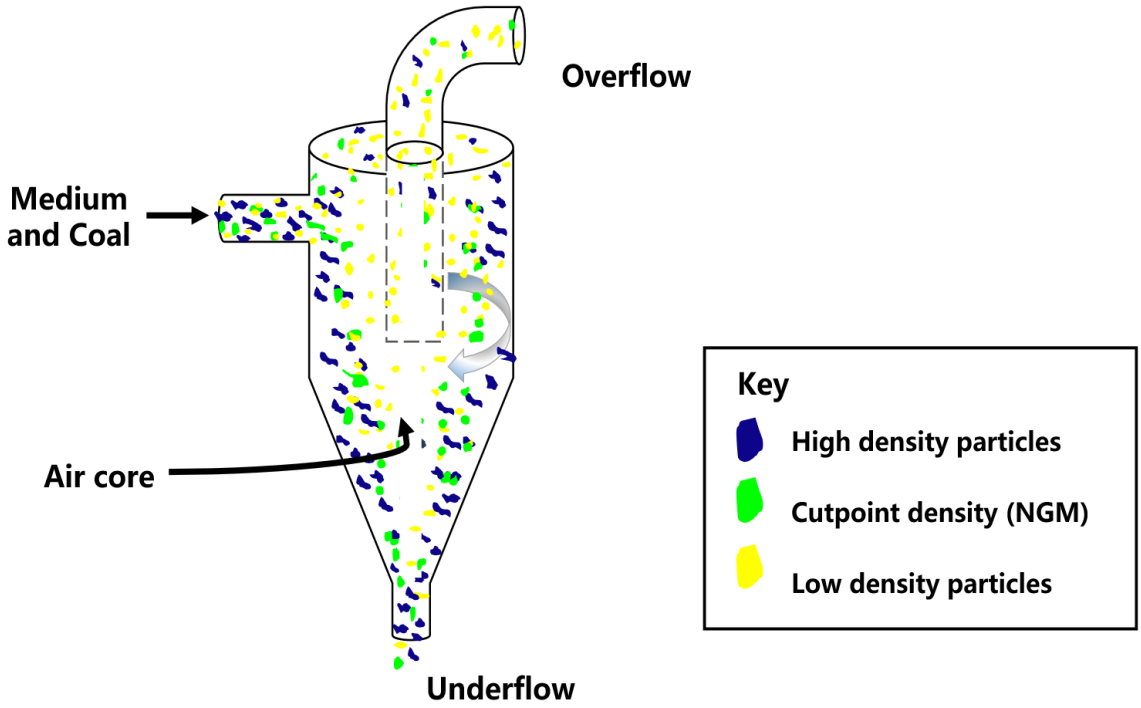

Figure 1: High NGM coal particle flow pattern inside a hydrocyclone during beneficiation

2.1.1 Effect on Coal Washability

Several studies have corroborated the negative impact of increasing near-density material content on coal washing efficiency. When the concentration of NGM increases, the separation of clean coal from middling or reject coal becomes progressively more challenging. In some cases, distinguishing between middling and reject coal, as well as effectively extracting the separated products, also becomes more difficult (Anupam, Bhattacharya & de Korte, 2020).

Table 1 shows Bird's classification of coal, which depicts the increasing difficulty of washing coal in a classifier as the coal feed NGM content increases, irrespective of the separation cut density. Coal with a NGM content exceeding 25% poses significant challenges in terms of washing and upgrading coal quality. Therefore, De Korte (2008) recommends that the feed rate of the NGM-laden coal must be low to achieve efficient separation in a density-based classifier.

Table 1: Effect of NGM concentration on the washability behaviour of coal (De Korte, 2008)

NGM (%)	Degree of difficulty	Process Recommendation
0-7	Simple	Any process applicable, high feed tonnage
7-10	Moderately difficult	Efficient process at high feed tonnages
10-15	Difficult	Efficient separation at medium feed tonnages
15-20	Very difficult	Efficient separation at low feed tonnages
20-25	Exceedingly difficult	Efficient separation at low feed tonnages
>25	Formidable	Highly efficient classifiers, low feed tonnages

The limitation of the NGM content, however, is that it fails to represent the inherent characteristics of the coal accurately. It provides no insights into the amenability of the coal to washing. While the NGM content serves as a valuable indicator for estimating the capacity of the classifier to efficiently beneficiate the coal, it does not encompass the full complexity of the properties of the coal.

2.1.1.1 Near Gravity Material Index

The near gravity material index (NGMI), as defined by Saida et al. (2022), serves as a metric to determine the optimal cut-point density in coal washability tests. It indicates the density at which coal is most conducive to washing. This index represents the ratio of the enclosed area between specific gravity values (±0.1) to the area delineated by the ash and non-ash material recovery curves, as depicted in Figure 2. These areas, especially the region under FGHI, vary with different separation densities. The NGMI is calculated using the recovery of non-ash float material (R_{na}) and ash sink material (R_a), employing mathematical formulae introduced by Govindarajan and Rao (1994):

$$R_{na} = \frac{100 \cdot X \cdot (100 - A_i)}{(100 - A_f)} \qquad 1$$

and

$$R_a = \frac{100 \cdot X \cdot A_i}{A_f} \quad (2)$$

where X represents the cumulative coal fractional weight, A_i and A_f are the ash fraction in the float material and the feed material, respectively, at a specific relative density (Saida et al., 2022). Furthermore, R_{na} and R_a can be expressed as the following cubic equations:

$$R_{na} = aX + bX^2 + cX^3 \quad (3)$$

and

$$R_a = pX + qX^2 + rX^3 \quad (4)$$

where *a, b, c, p, q* and *r* are constants that have been determined using the least-squares method (Saida et al., 2022). Therefore, the NGMI is expressed as follows:

$$NGMI = \frac{Area\ under\ FGHI}{Area\ under\ curve\ ABC\ and\ ADC} \quad (5)$$

In this equation, curve ADC represents the non-ash recovery curve (R_{na}), while curve ABC represents the ash recovery curve (R_a), as defined by equations 3 and 4. The NGMI ranges from zero to one, where zero indicates coal that is easy to wash, and one indicates coal that is challenging to wash (Saida et al., 2022). Washing coal at a specific gravity corresponding to a high NGMI value results in reduced separation efficiency and yields a lower-quality final clean coal product. The enclosed area between the recovery curves is calculated as the difference between the areas under ADC and ABC in Figure 2, as described by equations 3 and 4. Therefore, the NGMI can be expressed as:

$$NGMI = \frac{\int_{\alpha}^{\gamma}(aX + bX^2 + cX^3)\,dX - \int_{\alpha}^{\gamma}(pX + qX^2 + rX^3)dX}{\int_{0}^{1}(aX + bX^2 + cX^3)\,dX - \int_{0}^{1}(pX + qX^2 + rX^3)dX} \quad (6)$$

where α and ϒ represent the minimum and maximum cumulative fractional weight floated at points H and I, respectively, shown in Figure 2. Overall, the NGMI equation becomes:

$$NGMI = \frac{\{[6(a-p)X + 4(b-q)X^2 + 3(c-r)X^3]/12\}_\gamma}{[6(a-p) + 4(b-q) + 3(c-r)]/12} - \frac{\{[6(a-p)X + 4(b-q)X^2 + 3(c-r)X^3]/12\}_\alpha}{[6(a-p) + 4(b-q) + 3(c-r)]/12} \quad (7)$$

The advantage of the NGMI is its adaptability to the specific characteristics of each coal sample. As the area near the specific gravity of separation varies for different coal samples, the enclosed area under FGHI also fluctuates (see Figure 2), resulting in a variable NGMI value. This variability makes the NGMI a valuable metric for coal washing and preparation, enabling efficient optimization of these processes.

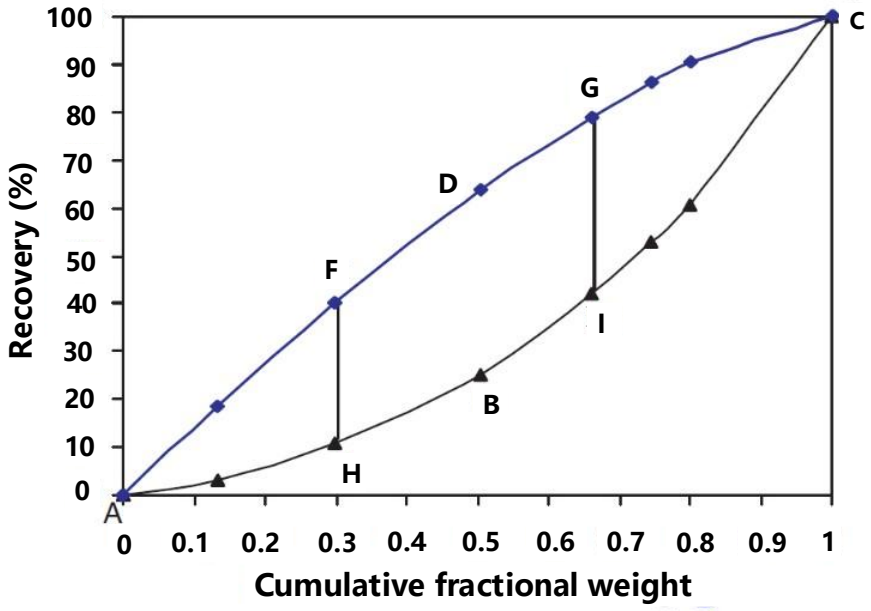

Figure 2: Coal ash and the non-ash recovery curves (Majumder & Barnwal, 2004)

2.1.1.2 S-value

The S-value is an additional metric used to evaluate the washability of specific coal types, derived from the degree of washability index (DW). The S-value ranges from 0 to 1, with values near one indicating that the coal is easy to wash, while lower values suggest that the coal is more challenging to wash. The S-value is calculated as follows:

$$S - value = \sqrt[4]{DW_{1.3} + DW_{1.4} + DW_{1.6} + DW_{1.8}} \quad 8$$

where DW_i is the degree of washability data at a specific gravity of separation calculated as follows:

$$DW_i = tan(tan^{-1}\left[\frac{Y_i}{R_i}\right] - 45) \quad 9$$

Y_i and R_i are the cumulative mass of floats and cumulative ash recovery at a specific gravity, respectively. Based on the S-value metric, the washability characteristics of coal can be graded as follows:

Table 2: Amenability of coal to washing according to the S-value metric (Shahzad & Ali, 2021)

Coal Specification	S-value (%)	Coal Washing Amenability
A+	80-100	Easiest
A	65-80	Relatively easy
B	55-65	Intermediate
C	45-55	Average Difficulty
D	25-45	Difficult
F	<25	Extremely difficult

2.1.2 Effect on Classifier Separation Performance

The presence of high quantities of NGM in the coal feed can have detrimental effects on the operation and separation efficiency of classifiers. NGM particles display a low settling rate in the separating medium, impeding their effective movement and hindering the optimal density-based particle separation in the medium, as noted by Sripriya et al. (2007). Consequently, these particles remain in the suspension for prolonged durations leading to a longer separation time, hence increasing the likelihood of their misplacement into the incorrect stream.

Aketi et al. (2017) observed a correlation between coal feed density, the relative density of the separating medium, and the residence time of coal particles in a dense

medium cyclone, as illustrated in Figure 3. The residence time increases when the coal feed density is within ±0.1 of the relative density of the separating medium, particularly for coal of the same particle size, as shown in Figure 3(a). Additionally, Aketi et al. (2017) found that particle size significantly impacts the separation performance of the classifier, with finer coal particles exhibiting longer residence times in the cyclone.

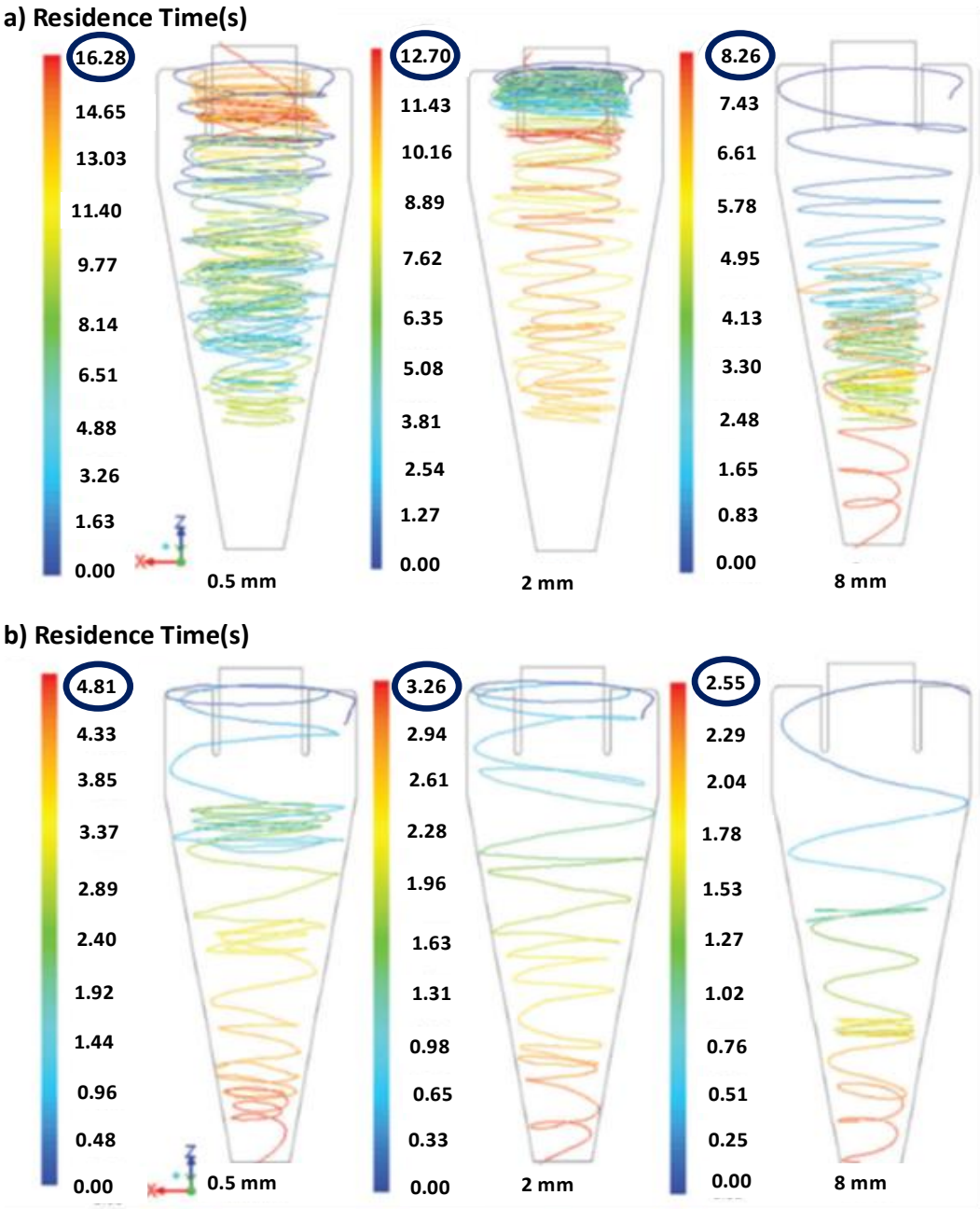

Figure 3: Particle fluid pattern in a dense medium cyclone with a separating medium density of 1300 kg/m^3 where a) feed density is 1290 kg/m^3 and b) feed density is 1600 kg/m^3 (Aketi et al., 2017)

In a dense medium cyclone, De Korte (2008) observed that as the NGM content in the feed increased, the fraction of misplaced coal particles also increased. There is a correlation between the fraction of NGM material in the feed coal and the fraction of the coal that reports to the wrong stream during separation as shown in Figure 4.

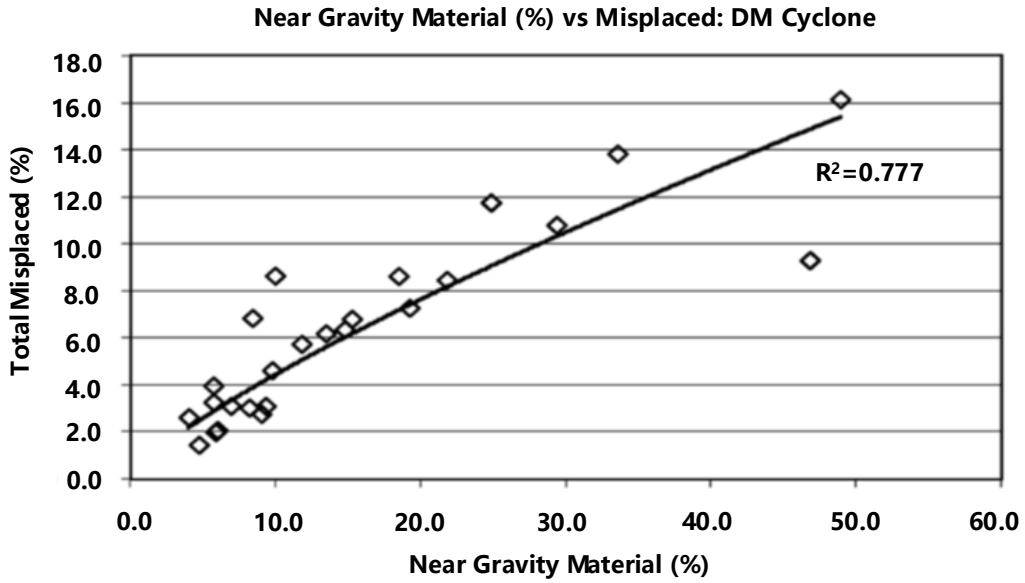

Figure 4: Correlation between NGM and particles misplaced during a dense medium cyclone (De Korte, 2008)

A considerable portion of the data points suggests a clear positive link between the proportion of NGM in the coal feed and the occurrence of particle misplacement in the dense medium cyclone. This relationship is evident from the coefficient of determination (R^2) of 0.78, signifying a strong linear positive correlation in Figure 4.

These findings align with a study by Kumari et al. (2015) who also found that coal particles with densities close to the density of the separating medium have longer residence times in dense medium cyclones. This prolonged residence time and low settling rate of NGM particles lead to their misplacement within the hydrocyclone. This results clean coal particles to end up in the rejects stream and ash contaminants to infiltrate the clean coal stream (De Korte, 2008; Bhattacharya, Maheshwari & Panda, 2016a; Aketi et al., 2017).

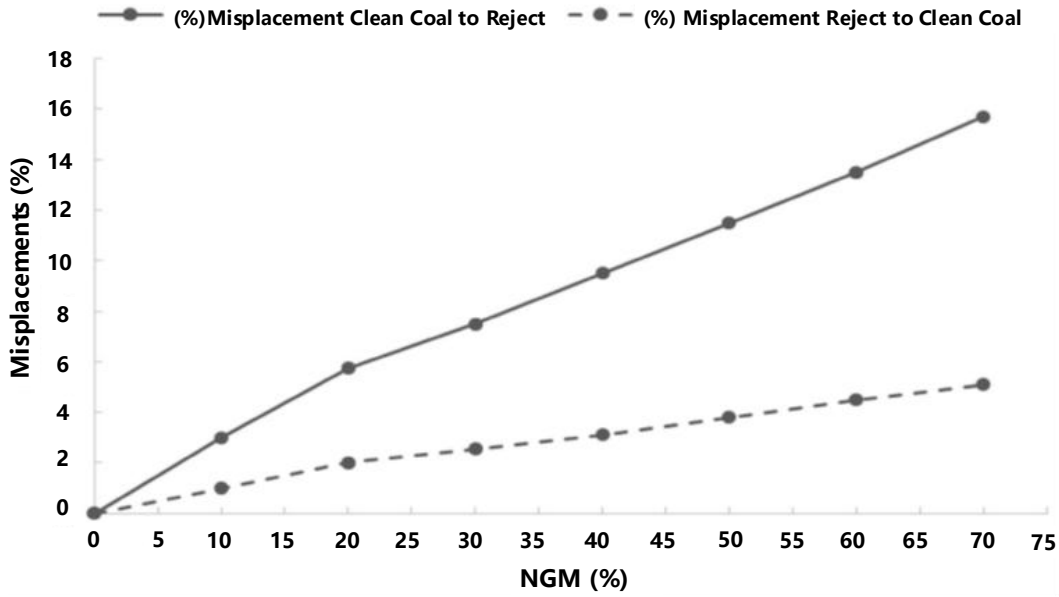

Figure 5: Correlation between NGM and particle misplacement for coal (J. O. Claassen, 2013)

A study by Claassen (2013) on coal from Witbank found a similar pattern: clean coal particles often end up in the underflow stream while impurities and ash report to the overflow stream, supporting the findings of De Korte (2008) and Kumari (2015). As shown in Figure 5, the fraction of clean coal in the underflow increases with the amount of NGM in the coal, resulting in lower organic efficiency and reduced clean coal yields from the dense medium separator. Coal yield is the fraction of coal feed that is recovered as the product after beneficiation (Wills & Finch, 2016).

2.2 Dense Medium Separation

In the minerals processing industry in South Africa, dense medium separation is commonly used for coal, manganese, and iron ore processing. The aim of dense medium separation is to produce a low-density clean product and a reject product with a density higher than the separating medium density from a feed that comprises dense gangue material (Gupta & Yan, 2016). For coal beneficiation in South Africa, the dense medium cyclone and the water-only cyclone are commonly used classifiers, and they are discussed in this section.

2.2.1 Balance of Forces on Particle During Classification

The main forces prevalent in the cyclone during separation are centrifugal forces, pressure gradient forces, gravitational forces, and drag forces as shown in Figure 6. The separating medium used in the classifiers is viscous, which introduces resistance or drag forces to the unimpeded movement of particles as they navigate through the fluid during the separation process.

The centrifugal forces, caused by the rotational motion of the feed inside the centrifugal classifier, impart an outward force on the particles, pushing them towards the hydrocyclone wall. In contrast, the drag force exerts an inward pull on the particles, facilitating the migration of low-inertia particles toward the vortex finder.

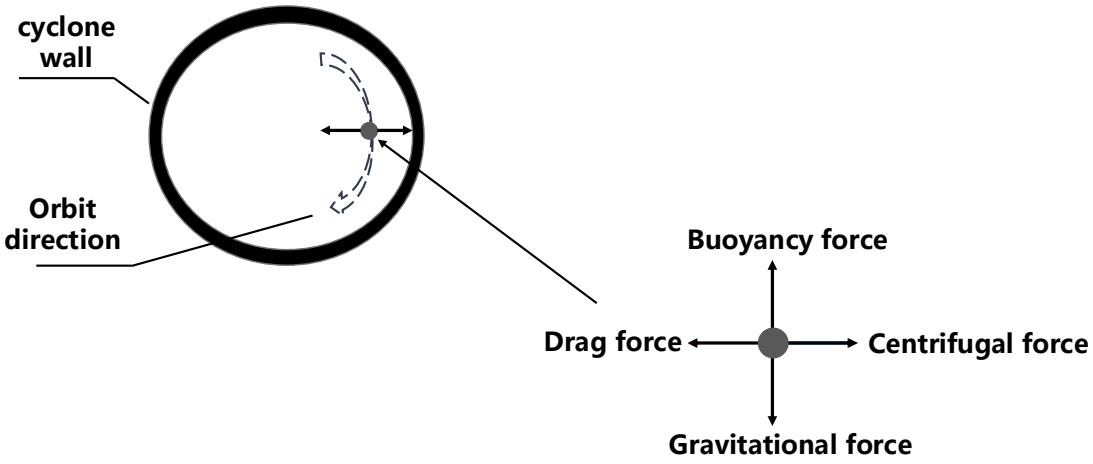

Figure 6: Forces acting on a particle in a classifier

The gravitational force contributes a downward influence on the particle, whilst buoyancy is induced by the pressure gradient inherent within the body of the classifier and the displaced separation medium as the particle moves through (Wills & Finch, 2016). Consequently, the descent velocity of particles in the classifier is influenced by the net forces acting on them (Wills & Finch, 2016).

2.2.2 Particle Settling Theory

The separation efficiency of a classifier is influenced by two main particle settling modes: free falling and hindered settling. In low solid concentrations, free settling dominates with minimal particle-to-particle interactions. However, when the solid concentration exceeds 15% by weight, hindered settling becomes significant, increasing particle interactions and reducing settling rates (Wills & Finch, 2016).

This effect is especially pronounced in classifiers using heavy media, which increase viscosity resistance. During free settling, the particle terminal velocity is determined by the forces acting on them, and for particles less than 100 μm in diameter, this velocity follows Stokes' equation (Gupta & Yan, 2016; Wills & Finch, 2016):

$$v_t = \frac{d^2(\delta - \rho)g}{18n} \qquad 10$$

Conversely, particles with a diameter exceeding 1 mm adhere to Newton's equation to describe their settling rate:

$$v_t = \sqrt{\frac{10(\delta - \rho)gd}{3\rho}} \qquad 11$$

Wherein v_t is the terminal velocity, n is the medium viscosity, δ is the density of the particle, ρ is the density of the liquid, d is particle diameter, and g is acceleration due to gravity. In the laminar flow region, Stokes' equation highlights that the medium viscosity influences the settling rate of particles. For turbulent flow patterns inside the hydrocyclone, Newton's equation indicates that the medium viscosity has a negligible influence on the settling rate of particles in a turbulent flow regime (Osborne, 2013).

Additionally, equations 10 and 11 point out that the variation density (δ-ρ) also influences the settling rate of particles. As a result, for material such as coal with a high NGM content, the density differential will be very low, hence the particles will have a slow settling velocity. In a density-based hydrocyclone, slow-settling particles experience prolonged residence times, remaining suspended in the separating

medium for extended periods. This increases the probability of these particles being misdirected into the incorrect overflow stream. When the near-gravity material contains a considerable proportion of gangue particles, it can result in a coal product of reduced quality.

2.2.3 Hydrocyclone Operation

The operational principle of both the dense medium cyclone (DMC) and the water-only cyclone (WoC) is the same. A mixture of coal feed and a separating medium is introduced tangentially under pressure into the hydrocyclone through the feed inlet, generating a vigorous swirling flow pattern and forming a vortex (Wang et al., 2009; Aketi et al., 2021).

Within the hydrocyclone, this vortex creates a low-pressure region along the vertical axis, developing an air core that extends through the centre of the hydrocyclone and connects with the outside atmosphere via the spigot opening. The presence of this air core in the central section of the hydrocyclone is essential to ensure the correct directional movement of low inertia particles towards the vortex finder (Sobhy, 2022).

2.3 Dense Medium Cyclone

The DMC is a centrifugal classifier used in coal beneficiation, capable of processing coal fines and ultrafines down to 0.5 mm (Sobhy, 2022; Phengsaart et al., 2023). It has a narrow long conical section with a cone angle of about 20°, which structurally differentiates it from the water-only cyclone.

For optimal separation of coal, it is recommended that the DMC should be angled 15° to 20° from the horizontal and operated at a low feed pressure (Gupta & Yan, 2016; Sobhy, 2022). This inclination helps prevent the gravitational forces from pulling the heavy dense medium towards the spigot opening which would block the inner vortex during separation resulting in reduced separation efficiency (Sobhy, 2022) and facilitating easy medium drainage during shutdown according to Gupta and Yan (2016).

Fine coal separation in dense medium cyclones relies on the use of an externally introduced medium, typically magnetite or ferrosilicon, to exploit density differences between particles. Ferrosilicon has a higher relative density value of 7 compared to magnetite with a density of 4.9 to 5.2 (Waanders & Rabatho, 2005; Handayani et al., 2024). Ferrosilicon is primarily used for high dense medium separation due to its ability to achieve medium densities varying from 3.2 to 4.2 g/cm³ (Grobler, Sandenbergh & Pistorius, 2002). It is less commonly applied in coal beneficiation, largely due to its higher cost, which limits its economic feasibility for processing low-grade coal.

Therefore, the DMC uses mainly magnetite (Fe_3O_4), for coal density separation. Magnetite can be repeatedly recovered and reused, and it forms a stable medium when mixed with water to achieve various specific gravities for separation. The density of the medium is controlled by mixing water with finely powdered magnetite, ideally 90% finer than 5 µm for optimal separation (Sahu, Chaurasia & Suresh, 2019a).

However, a challenge with the use of fine magnetite is the loss of the magnetite to the clean coal product overflow which results in a reduced product quality (Ramudzwagi, Tshiongo-Makgwe & Nheta, 2020). Additionally, fine magnetite increases the medium viscosity, destabilising the medium and lowering the separation efficiency of the DMC (GJ de Korte, 2012).

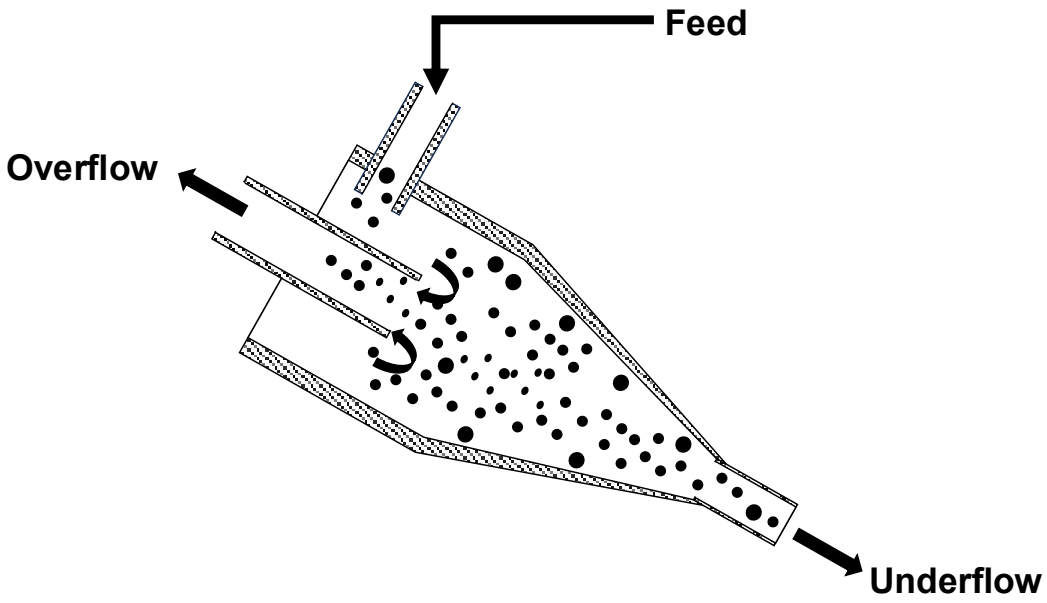

Figure 7: Dense medium cyclone flow pattern schematic

Standard DMC design specifies that the feed inlet diameter should be 15-20% of the hydrocyclone diameter, the vortex finder diameter should be 43-50%, and the spigot diameter should be 30-40% of the DMC diameter for optimal separation performance (Osborne, 2013). The DMC diameter is important as it affects the quantity and quality of the recovered products. Smaller diameter DMCs are more effective for separating fine coal and shale particles due to the increased centrifugal forces generated by their reduced hydrocyclone diameter size (Liu et al., 2018).

However, the feed pressure also influences centrifugal forces in the DMC according to a study by B. Liu et al. (2018). Gupta and Yan (2016) state that industrial DMCs typically operate at pressures around 140 kPa. This pressure can be developed by having a 5 to 6 m hydraulic head above the DMC feed inlet or by directly mixing the ore in a sump tank and pumping it directly to the DMC.

GJ de Korte (2012) recommends hydrocyclone diameters of 250 to 350 mm for optimal fine coal beneficiation, although smaller diameters can also be effective in beneficiating coal. Sahu et al. (2019) demonstrated this by using a 76 mm diameter

hydrocyclone to beneficiate -3 mm fine coal, achieving an ash content of 15.38%. Additionally, B. Liu et al. (2018) used a three-product DMC with 710/500 mm dimensions, achieving a 10% ash content in clean coal.

2.3.1 Separating Medium Properties

He and Laskowski (1994) found that the properties of the separating medium in a DMC significantly impact the separation of fine and ultrafine coal particles. The main factors affecting DMC performance include the rheology and stability of the medium, which are influenced by its composition. Critical composition factors include the concentration of medium solids, magnetite particle size and distribution, separating medium contamination level, and the degree of demagnetization.

Utilising fine magnetite enhances separation efficiency in DMCs by stabilizing the medium and reducing particle movement (He & Laskowski, 2007, 1994). Fourie and Van Der Waltt (1980) recommend that at least 50% of the magnetite be finer than 10 µm.

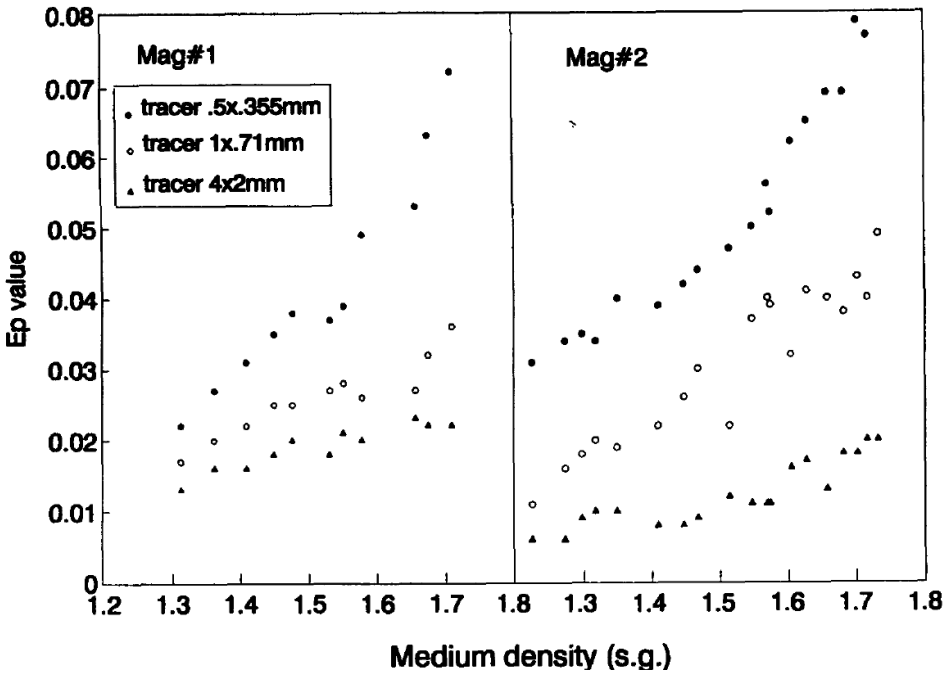

Figure 8: Relationship between the separation efficiency, change in the medium density and magnetite particle size in a DMC (He & Laskowski, 1994)

Figure 8 shows that the DMC achieves higher separation efficiency for relatively coarser tracer particles when utilizing coarser magnetite (Magnetite #1). In contrast, finer magnetite (Magnetite #2), as detailed in Table 3, enhances the separation performance of the DMC when classifying finer particles (He & Laskowski, 1994).

Table 3: Magnetite sample particle size distribution (He & Laskowski, 1994)

Sample	$D_{63.2}$ (µm)
Magnetite #1	30.5
Magnetite #2	18.0
Magnetite #3	33.0
Magnetite #4	4.3

The difference in density between the overflow and underflow in a DMC also has an impact on the separation efficiency. He and Laskowski (1994) explained that magnetite particles experience similar forces to coal particles during DMC separation. Large density differences can create density zones within the separating medium, leading to periodic hydrocyclone overloading and the DMC surging.

According to Sanders (2007), surging can cause low-density particles to report to the underflow, leading to poor separation efficiency. Therefore, to achieve optimal DMC performance, a density differential of 0.2 to 0.5 relative density is recommended by He and Laskowski (1994).

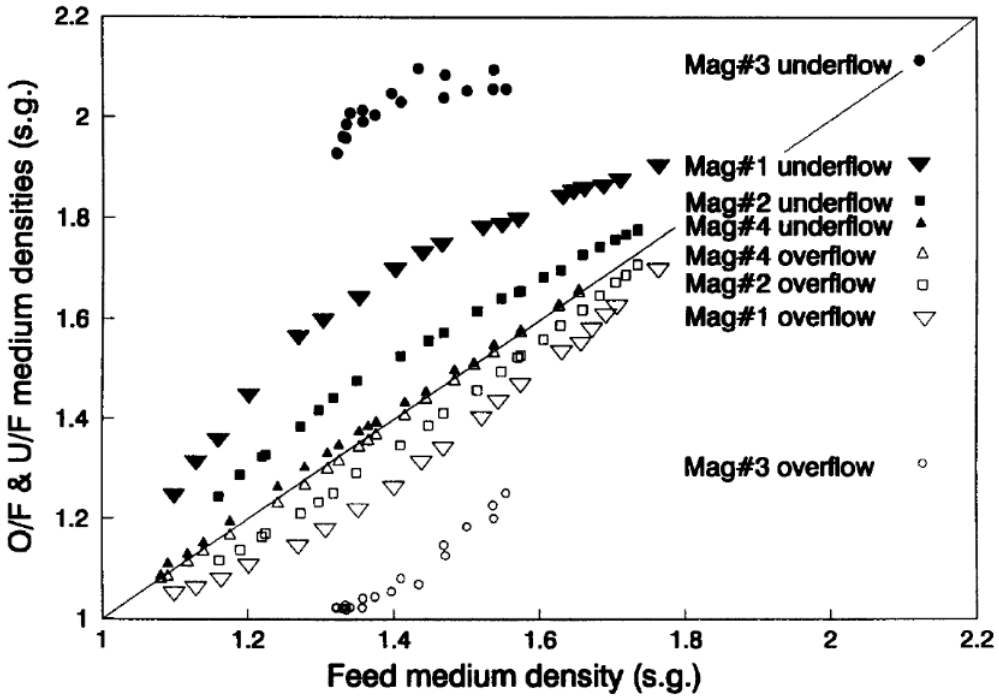

Figure 9: Relationship between magnetite particle size, feed medium density and the density differential of the underflow and overflow mediums in a DMC (He & Laskowski, 1994)

Figure 9 shows that both medium density and magnetite particle size significantly influence the density differential in a DMC (He & Laskowski, 1994). Magnetite #3 results in a steep underflow and overflow density difference, indicating low medium stability and poor separation efficiency, while ultrafine magnetite #4 exhibits high stability and improved separation efficiency. He and Laskowski (1994) found that increasing the medium density raises the density differential, and larger magnetite particle size increases the density differential for the same medium density, reducing separation efficiency.

2.4 Water-only Cyclone

The water-only cyclone (WOC) is a density-based classifier that uses water as a medium of separation (Majumder & Barnwal, 2011a). Unlike froth flotation and dense-medium cyclone processes, WOCs do not require chemicals or artificial media, making them more sustainable and cost-effective (Ramudzwagi, 2020). According to Hembrom and Suresh (2018), WOCs effectively beneficiate oxidized coal and can achieve specific density cut-points as low as 1260 kg/m³ due to their ability to separate materials at gravitational forces 50-500 times stronger than normal gravity (Hembrom & Suresh, 2018).

WOCs have a wide-angle conical bottom, a long cylindrical section, and an extended vortex finder (see Figure 10), which distinguishes them from dense-medium cyclones which have a narrow-angled cone (Wang, Wei & Cui, 2022; Phengsaart et al., 2023). The short conical section and a wide cone angle structural design of the WoC result in improved separation performance by improving the density of the separating medium, according to Sobhy (2022). WOCs typically feature cone angles up to 120°, though angles as wide as 143° have been utilized in coal beneficiation applications (Majumder & Barnwal, 2011).

The inclination angle of the water-only cyclone (WOC) to the horizontal during hydrocyclone operation significantly impacts the ash content in the clean coal output (Abbas & Muhammad, 2017). Increasing the angle of inclination to the horizontal reduces the ash content in the recovered coal yield. However, this results in a decrease in the coal yield at the overflow (Abbas & Muhammad, 2016) .

The separation mechanism in a water-only cyclone relies on a hindered settling environment created in its conical section, where particles are separated by density and enhanced by centrifugal forces (Supriya Maharana & Suresh, 2020; Sobhy, 2022). Denser particles accumulate and re-circulate at the bottom of the cylinder and the conical section, forming a solids suspension that promotes hindered settling. This prevents low-density particles from penetrating the autogenous medium (Osborne, 2013).

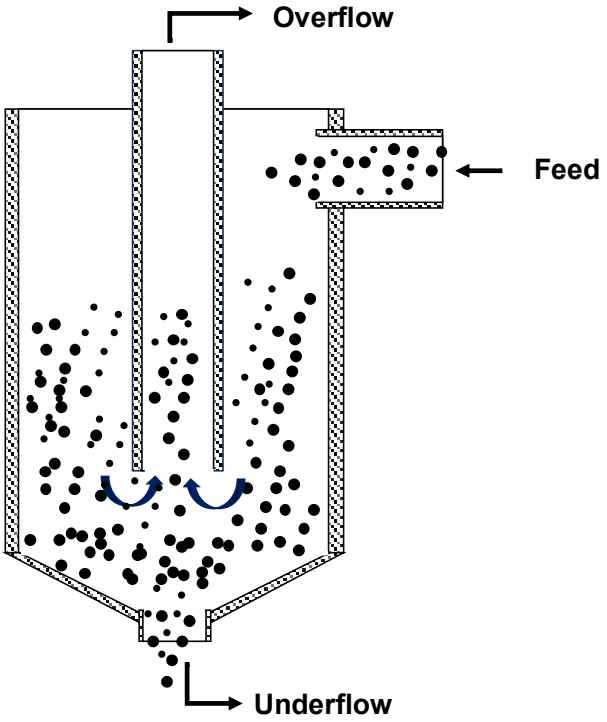

Figure 10: Schematic of a water-only cyclone

Consequently, denser particles settle and move towards the underflow apex, while lighter particles move upward towards the vortex and report to the overflow stream via the vortex finder (Supriya Maharana & Suresh, 2020). The vortex finder, extending close to the underflow opening, shortens the vertical path for particles in the central upward flow, ensuring that large, low-density particles are collected and discharged with the lighter fraction.

2.5 Effects of Variables on DMC and WoC Separation Performance

2.5.1 Effect of Vortex Finder Diameter

Su and Zhang (2022a) found that the vortex finder diameter (VFD) influences the air column shape and overflow stream flowrate during density-based separation in a hydrocyclone. A larger VFD creates an oversized air core, which decreases separation efficiency by shortening the short-circuit flow path. This increases the likelihood of feed bypassing density-based classification to reach the overflow pipe. Although a larger VFD aids in the enrichment of fine particles in the overflow, a smaller VFD reduces the

particle cut size, enriching coarse particles in the underflow. Hacifazlioglu (2012) further observed that a smaller VFD lowers the overflow yield and reduces coal ash content.

2.5.2 Effect of Spigot Diameter

The spigot diameter (SPD) impacts the separation efficiency of the WoC and DMC. The SPD influences both the fluid volume directed to the underflow and the discharge velocity through the spigot. Wang et al. (2011) observed that in a DMC, when the spigot diameter increases the fraction of the medium that reports to the overflow decreases. This results in a decrease in the separation performance of the DMC. Similarly, Hacifazlioglu (2012) observed that in a WoC increasing SPD reduced the pressure difference across the hydrocyclone from 20 kPa to 5 kPa under constant feed pressure and rate.

This low-pressure drop causes more slurry to report to the underflow, reducing the feed residence time inside the WoC and preventing the formation of an autogenous bed medium, thereby decreasing separation efficiency and clean coal yield in the overflow. Consequently, the WoC will undergo separation by size over separation by density (Hacifazlioglu, 2012). The work of Dou, Liu & Yang (2022), and Abbas and Muhammad (2017) support these findings, showing that increasing SPD initially reduces clean coal throughput and ash content in the overflow, however, further SPD increases lead to a sharp decline in clean coal yield and a gradual rise in ash content.

2.5.3 Solids Concentration and Separating Medium Density

The solid content of the slurry feed directly affects the density and viscosity of the separation medium (Hacifazlioglu, 2012a). An increase in the solids concentration increases the density and viscosity, leading to more slurry in the conical section of the WoC (Abbas & Muhammad, 2016). This results in higher coal yield with a higher ash content. A study by Hacifazlioglu (2012) confirmed this, showing that increasing solids

concentration from 10% to 30% raised clean coal yield from 22% to 26%, along with a higher ash content.

The relative density of the separating medium significantly influences the separation efficiency of the DMC. He and Laskowski (1994) observed that an increase in medium density results in decreased separation efficiency, as shown in Figure 8. At elevated density cut points, a significant proportion of coal containing considerable gangue particles is directed to the overflow stream, resulting in a lower-quality final coal product.

2.6 Dense Medium Classifier Empirical Models

For dense media separation, common empirical models include the Wood Model and Osborne Model. These models are based on empirical relationships among separation density cut point, separation efficiency, hydrocyclone geometry, and operational parameters like medium stability during separation (Clarkson & Wood, 1993).

2.6.1 Osborne Model

This model was specifically designed for heavy media separators, proposing that the efficiency of the separator (Ep) can be calculated using the following formula:

$$E_p = E_s \cdot f_1 \cdot f_2 \cdot f_3 \qquad 12$$

here, E_s represents the device-dependent factor, as described by Pural, Sirkeci & Boylu (2023). It is determined through the formulae provided in Table 4:

Table 4: Calculation for the device-dependent factor E_s

Classifier	**Formula for E_s**
Dense medium cyclone	$0.027\rho_{50}$-0.01
Dense medium vessel	$0.047\rho_{50}$-0.05

Additionally, according to Gerald H. Luttrell et al. (2005), the factors f_1, f_2, and f_3 are functions correlated with particle size, equipment dimensions, and manufacturer

guarantees, respectively. Notably, for the dense medium cyclone, the guarantee factor (f_3) of the manufacturer is assumed to be 1. Furthermore, according to Pural, Sirkeci & Boylu (2023), the particle size-related factor f_1 can be expressed by the following equation:

$$f_1 = d^{-0.35} \cdot 1.566 \qquad 13$$

where d is the diameter of the particle size. Lastly, the equipment size factor for the dense medium cyclone is assumed to be 1, if it has a diameter of 500 mm.

2.6.2 Wood Model

This model is used frequently in the design and optimization of the dense medium cyclone (Pural, Sirkeci & Boylu, 2023). The predictions of the Wood model are specific to coarse coal, but with a simple relational modification, the applicability of the model may be extended to all coal size ranges. This empirical framework consists of nine component sub-models or equations that are specifically designed to predict the operational efficiency of an ideally functioning dense medium cyclones.

The primary parameters encompassed within these models are medium density, behaviour and split, coal partitioning, and hydrocyclone geometry, collectively contributing to the prediction of separation efficiency and separation density cut points. Ultimately, the determination of partition numbers is facilitated through the application of the Whitten equation, as outlined by Holtham, Brennan & Managadoddy (2008). The sub-models that build up the Wood model, as described by Clarkson and Wood (1993), include a component model that estimates the flowrate of the heavy media suspension and the feed. It is described as follows:

$$Q_f = 76 \cdot D_r^{1.93} \cdot Head^{0.45} \cdot \left[\frac{D_u}{D_o}\right]^{0.15} \qquad 14$$

where Q_f is the slurry flowrate, D_r is the diameter of the cyclone, D_u and D_o are the diameters of the spigot and the vortex finder, respectively. Sub-model 2 is used to determine the medium split and is calculated as follows:

$$\frac{Q_{um}}{Q_{fm}} = \frac{Q_{um}}{Q_{um} + Q_{om}} \quad 15$$

where Q_{um} is the medium slurry flow to the underflow and Q_{fm} is the flowrate of the medium slurry to the overflow of the dense medium cyclone. The underflow density of the slurry stream exiting via the spigot is then determined as:

$$\rho_{um} = 0659 \cdot \rho_{fm} \cdot \frac{Q_{um}}{Q_{fm}} \cdot 0.194 \cdot {\rho_{fm}}^{-2.04} \cdot {P_{RR}}^{0.17} \cdot Head^{0.082} \cdot D_c^{-0.1} \quad 16$$

where ρ_{fm} is the density of the feed medium. The overflow density can be described as:

$$\rho_{om} = \rho_{fm} \cdot \frac{1 - \frac{Q_{um} \cdot \rho_{um}}{Q_{fm} \cdot \rho_{fm}}}{1 - \frac{Q_{um}}{Q_{fm}}} \quad 17$$

The following sub-models were developed to determine the coal partitioning. The series of equations are as follows starting with the separation density for coarse particles which are particles that have a particle size that is greater than 4 mm:

$${\rho_{50}}^{A} = 0.196 + 0.36\rho_{fm} + 0.532\rho_{om} + 0.274\rho_{um} \quad 18$$

The following sub-model is for the determination of the upper density limit of particle retention which is applicable to feed particles that have a size range of 0.04 to 0.05 of the diameter of the hydrocyclone. The model can be determined as follows:

$$\rho 50_d = {\rho_{50}}^{A} + 0.088 \cdot \left[\frac{1}{d} - \frac{1}{10}\right] \quad 19$$

where *d* is the diameter of the particle. Therefore, the separation efficiency of the separation medium is determined as follows:

$$Ep_d = \frac{0.037}{d} \quad (20)$$

Therefore, the partition number for the density-based classifier can be determined using the Whiten Equation which is expressed as follows (Holtham, Brennan & Managadoddy, 2008):

$$PN = \frac{100}{1 + e^{1.099} \cdot \left[\frac{\rho 50_d - \rho d}{Ep_d}\right]} \quad (21)$$

2.7 Classifier Performance Indicators

The different design and operational parameters of a density-based cyclone influence its separation performance and the quality of the final product during coal beneficiation. A range of performance indicators are employed to evaluate and compare the separation efficiencies of DMC and WoC.

2.7.1 Partition Curve

The partition curve is important for evaluating and comparing the separation performance of classifiers. According to Wills and Finch (2016), it shows the distribution of coal material mass fractions of the feed reporting to either the overflow or underflow streams based on various density fractions of clean coal. Partition curve determination requires evaluating the product float fraction, reject sink fraction, and feed properties.

The partition curve graph is typically an S-shaped curve, where the curve steepness indicates separation efficiency. An ideal partition curve shows perfect separation, with particles denser than the cutpoint density reporting to the underflow and lighter less dense particles to the overflow, depicted as a step curve with a straight line through the cutpoint density (ρ_{50c}), unlike the standard S-shaped curve as shown in Figure 11.

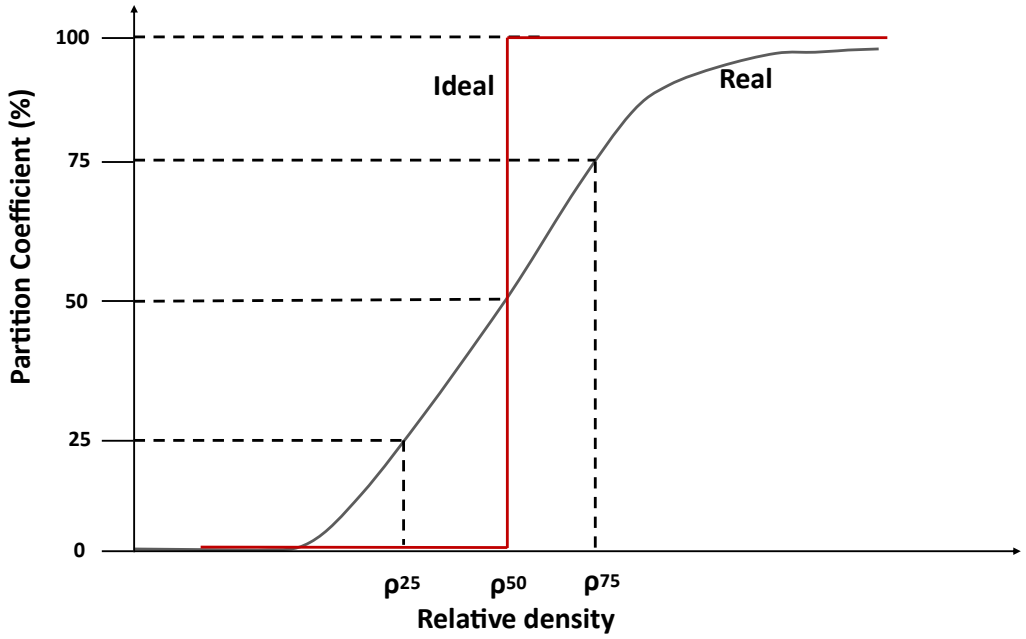

Figure 11: Ideal and real partition curve (Wills & Finch, 2016)

The real, standard S-shaped partition curve shows that separation efficiency decreases near the cutpoint density in the classifier but improves at densities further from it. The overlap between the ideal and real S-shaped curves indicates particle misplacement. The gangue dense particles report to the overflow and the lighter clean coal particles report to the underflow, represented by the shaded areas in Figure 12. This is known as the error area (Wills & Finch, 2016). However, the partition coefficients do not account for differences in ash content in the clean coal or its impact on separator performance (Shahzad & Ali, 2021).

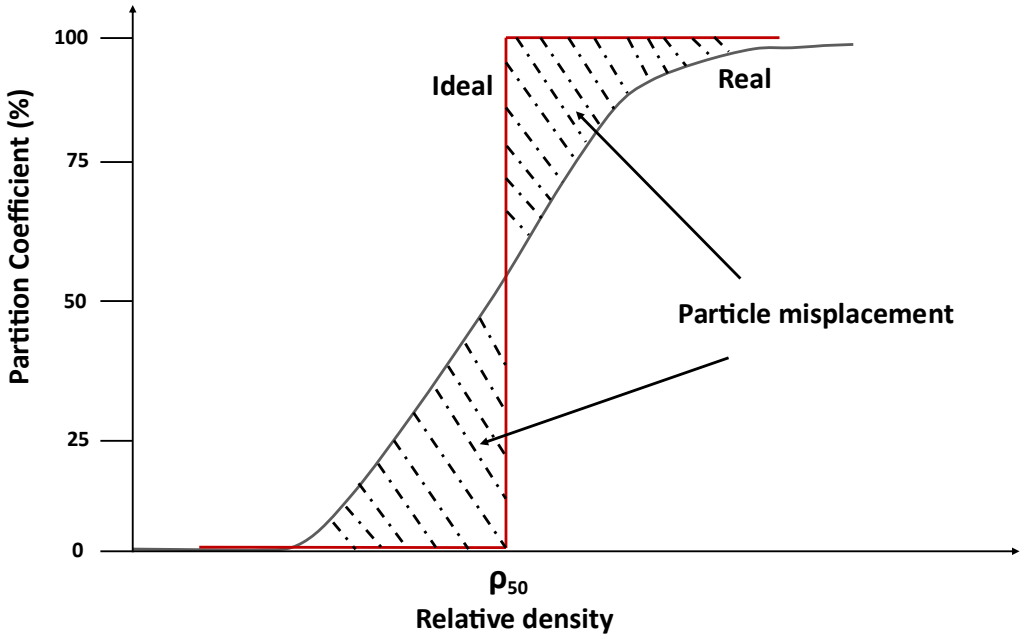

Figure 12: Partition curve showing particle misplacement in a classifier

According to De Korte (2008), the real partition curve in a classifier does not always conform to the conventional S-shaped curve and can exhibit asymmetrical characteristics. Depending on the separation performance of the classifier and the materials being processed, the partition curve may display either a high-density tail, a low-density tail, or even both. These deviations from the standard curve indicate the separation performance achieved in the density-based classifier.

The density tails in the partition curve can be attributed to the misplacement of high-density particles to the overflow stream. This phenomenon can be attributed to rafting which occurs when denser particles resist settling at the bottom of the separating medium and instead remain suspended within the medium itself (De Korte, 2008).

2.7.2 Separation Efficiency

The separation efficiency (E_{pm}) can be quantified by calculating the probable error, which constitutes half the absolute difference between the relative density values corresponding to the 75% and 25% partition coefficient values (ρ_{75} and ρ_{25} in Figure 11) (Sripriya et al., 2001). It is a dimensionless value that mainly measures how much the actual partition curve has shifted from the ideal curve (Paul & Bhattacharya, 2021). It is described by the following equation:

$$E_{pm} = \frac{\rho_{75} - \rho_{25}}{2} \quad (22)$$

Sripriya et al. (2001) explains that a lower E_{pm} value shows a superior separation efficiency, with the recommended range typically falling between 0.04 and 0.05 for gravity separators such as the dense medium cyclone and the water-only cyclone. Conversely, Wills and Finch (2016) suggest that the E_{pm} should ideally range from 0.01 to 0.10 to maintain an efficient separation process.

A steeper curve or one that closely aligns with the ideal partition curve between the 25% and 75% distribution coefficients signifies lower calculated E_{pm} values which means that the separation efficiency is high. The limitation of the E_{pm} value, however, is that it does not indicate the amount of ash contained in the coal product recovered from the classifier operating at the specific relative density.

2.7.3 Separation Density Cutpoint

The cutpoint density (ρ_{50}) value represents the density at which a particle has an equal chance of reporting to either the overflow or underflow streams of the hydrocyclone (De Korte, 2008; Wills & Finch, 2016). The cutpoint density is rarely ever equal to the separating medium density because the cutpoint is influenced by the operating conditions of the classifier (Sripriya et al., 2007).

2.7.4 Imperfection or Sharpness of Separation

The sharpness of separation, according to De Korte (2008), can be defined by the imperfection in the dense medium separation process, which is also known as the generalised partition error (Kumar & Kumar, 2018). The separation efficiency of the classifier can be made unconstrained of the washability properties of the coal and only influenced by the classifier or coal washer. Imperfection is defined as follows for dense medium separations:

$$I = \frac{E_{pm}}{\rho_{50}} \quad (23)$$

For water-based separations, imperfection can be described as follows:

$$I = \frac{E_{pm}}{\rho_{50} - 1} \qquad 24$$

A low imperfection value in a classifier is favourable over a high imperfection value. The latter indicates a poor separation performance in the classifier.

2.7.5 Organic Efficiency

This metric describes the relationship between the actual coal yield achieved by the classifier and the theoretical clean coal yield extrapolated from washability data, considering a consistent fraction of ash within the coal (Paul & Bhattacharya, 2021). An organic efficiency (E_{org}) value approaching 100% signifies a state of ideal separation, where no coal material is misplaced or directed into the wrong stream during the separation process.

On a larger industrial coal processing scale the E_{org} is utilised in financial viability assessments of coal washing and handling plants (CWHP). By quantifying the potential revenue impact by providing an estimate of the amount of clean coal yield lost to the rejects stream. E_{org} aids in assessing the consequences of deviations from the standard organic efficiency value of the classifier. A decline in the standard E_{org} could result in revenue losses, while an enhancement in classifier organic efficiency might culminate in additional revenue streams.

The E_{org} has limitations. Based on data from South Africa and Canada, Paul and Bhattacharya (2021) found a direct correlation between relative density cut-point and organic efficiency in different particle size ranges of the same coal. A higher relative density cut-point leads to a higher organic efficiency. It does not indicate the ash content in clean coal yield or its quality. A high Eorg can represent various coal combinations, such as high combustible recovery with low ash or moderate combustible recovery with high ash content. Additionally, the organic efficiency is sensitive to the relative density cut-point of the classifier.

2.8 Statistical Design and Analysis of Experiment

Effective statistical analysis and experimental design for classifier experiments depend on using an appropriate design of the experiment. The full factorial method, commonly used to explore parameter and interaction effects, requires a large number of experiments (Aslan, 2008). In this study, a three-level full factorial design would be ideal, but limited time and resources make this impractical (K. Palanikumar, 2021).

As an alternative, Aslan (2008) recommends the central composite rotatable design (CCRD), which has been effective in various studies. This design requires fewer tests than the full factorial method while still providing reliable results for steady-state process experiments (Cilliers, Austin & Tucker, 1992; Crozier, 1992). The CCRD includes three key components: a standard 2^k factorial design centred at the origin, axially fixed 2k points from the centre, and a central point (Aslan, 2008).The CCRD is determined as follows:

$$N = 2^k + 2k + n \qquad 25$$

where k denotes the number of parameters and n is the number of centre point repetitions. For three parameters, six centre repetitions are recommended for an unbiased estimate of experimental error (Box & Hunter, 1957). This ensures consistent variance and an impartial error estimate (Obeng, Morrell & Napier-Munn, 2005). The axial points are carefully selected to ensure rotatability, maintaining consistent variance in model predictions across all points equidistant from the design centre, as shown in Figure 13 (Box & Hunter, 1957).

After determining the target parameter ranges, the next step is coding these values for the factorial, centre, and axial points. Factorial points are coded as ±1, centre points as 0, and axial points as ±β, representing the variable parameters' minimum and maximum values (Obeng, Morrell & Napier-Munn, 2005). The range of interest for each parameter, as shown in Table 5, is used to calculate these codes.

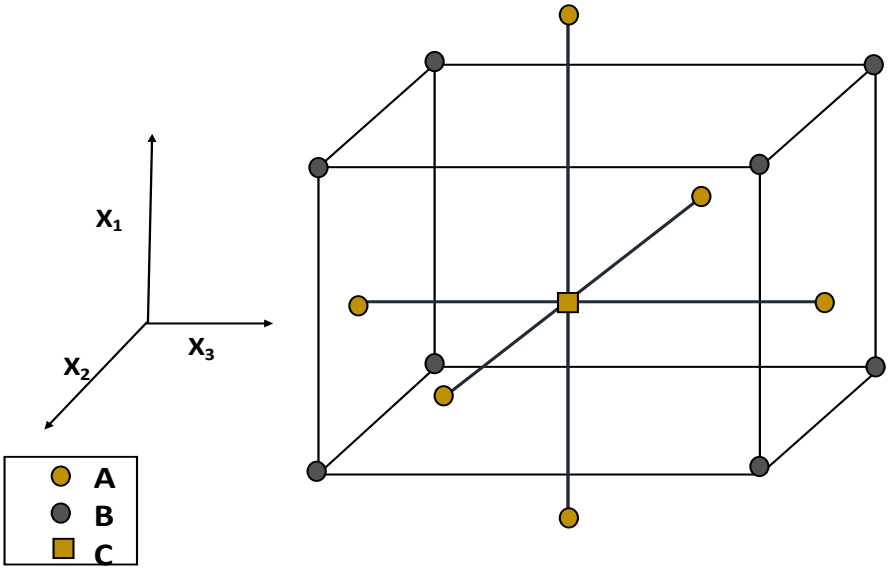

Figure 13: CCRD for 3 parameters (X_1, X_2 and X_3) where A marks the axial points, B marks the 2^k factorial design and C is the centre

Table 5: The relationship between the coded values and the actual values when applying the CCRD approach where α is k/4 and k is the number of varied parameters

Code	Actual value of variable
- β	x_{min}
-1	$\frac{(x_{max} + x_{min})}{2} - \frac{(x_{max} - x_{min})}{2\alpha}$
0	$\frac{(x_{max} + x_{min})}{2}$
+1	$\frac{(x_{max} + x_{min})}{2} + \frac{(x_{max} - x_{min})}{2\alpha}$
+ β	(x_{max})

According to Obeng et al. (2005), a response model can be developed from the CCRD. For a three-level parameter experimental design, the response model would be as follows:

$$y = (b_o + \varepsilon) + \sum_{i=1}^{3} b_i x_i + \sum_{i=1}^{3} b_{ii} {x_i}^2 + \sum_{i=1}^{3} \sum_{j=1}^{3} b_{ij} x_i \, x_j \quad (26)$$

where (b_o), (b_i), (b_{ii}) and (b_{ij}) can be established from the experimental data through a computer simulation using the least squares method (Aslan, 2008). According to Obeng et al. (2005), the response model is valuable as it can allow for the interpolation of data and the development of a response 3-D surface graph which can better portray the influence of the parameters under investigation.

2.9 Summary

The reviewed literature underscores the adverse impact of NGM on the operational performance and separation efficiency of dense medium cyclones and water-only cyclones in coal beneficiation processes. NGM particles, due to their densities being close to the separating medium, exhibit low settling velocities, resulting in prolonged residence times within the cyclone during coal washing. This increases the probability of particle misplacement into the incorrect stream.

The literature highlights that extensive experimental work has been undertaken to study the impact of NGM content in the coal feed and the fraction of misplaced particles in dense media separation. Despite the comprehensive analyses, notable gaps remain. Current studies inadequately address the interplay between the distribution and quantity of clean coal and gangue particles in near gravity material. This critical composition, unique to each coal feed, directly impacts separation performance and the final coal product quality. Furthermore, while substantial research has been conducted on density-based classifiers utilising external media, limited experimental work has addressed NGM behaviour in classifiers with autogenous media.

Extensive experimental work has been conducted to critically analyse how key operational variables—the vortex finder diameter, spigot diameter, and feed medium density—affect the separation efficiency of dense medium cyclones. Similarly, it evaluates the impact of vortex finder diameter, spigot diameter, and solids concentration on the performance of water-only cyclones in beneficiating NGM-laden

coal. The experimental methodologies explored by multiple studies in the literature fail to comprehensively examine the intricate relationships between the quantity and distribution of NGM, operational variables and their cumulative impact on the separation efficiency and performance of the dense medium cyclone and the water-only cyclone.

Additionally, while response surface methodology (RSM) and statistical experimental designs have been utilized to develop predictive empirical models linking ash content with operating variables, these models often neglect the influence of particle size distribution on classifier performance. This oversight limits their applicability. The models are further constrained by their reliance on data specific to particular coal seams and the lack of cross-validation with datasets from coal sourced from other seams.

3 Methodology

This chapter reports the methods followed to obtain the results from the two cyclonic systems used to beneficiate low-grade fine coal with a high NGM and ash-bearing impurities content. A modified conventional hydrocyclone with a long cylindrical section and a wide conical angle was used as a flat-bottom cyclone (FBC) (commonly known as a water-only cyclone in coal beneficiation). It employs only water as the medium of separation to create an autogenous medium that promotes separation by density. In contrast, the dense medium cyclone enhances separation by density by employing a magnetite suspension, as the separation medium, to create a sharp density difference during coal separation.

Each classifier experiment investigated the impact of three varied parameters: vortex finder diameter, spigot diameter, and solids concentration for the FBC, and vortex finder diameter, spigot diameter, and separating medium density for the DMC. Each parameter was varied at three levels to evaluate the separation efficiency and ash reduction potential of the classifiers when beneficiating low-grade fine coal with high NGM and ash-bearing impurities from the Highveld Coalfield, Mpumalanga.

3.1 Experimental Apparatus

A range of equipment was used to characterize and prepare the coal and magnetite to ensure that the research results were reliable and accurate. The coal was screened on a 3.35 mm screen to control the top size. The particle size distribution of the magnetite was determined using the Malvern Mastersizer at the University of Cape Town (UCT). The CHNS elemental analyser from the UCT Chemistry Department was used for the analysis of the carbon, hydrogen, nitrogen, and sulphur content of the coal. The UCT hydrocyclone lab-scale test rig was used for classifier experiments. Other ancillary equipment used included the filter press for slurry dewatering, the muffle furnace to ash the coal, the de-lumping mill, and the oven for drying wet coal samples.

3.1.1 UCT Hydrocyclone Test Rig

The closed flow circuit test rig used in this study is made up of a 100 mm diameter Multotec hydrocyclone fixed vertically onto a steel frame as shown in Figure 14 and Figure 15. The conical section of the hydrocyclone is adjustable to allow for different conical sections with different angles to be mounted. It also enables modification of the length of the cylindrical section, allowing for flexible structural configuration and control. This setup allows hydrocyclones with different configurations to be studied using the same test rig. The height of the steel frame allows for different cylindrical sections to be mounted and modified to the hydrocyclone while it remains in operation.

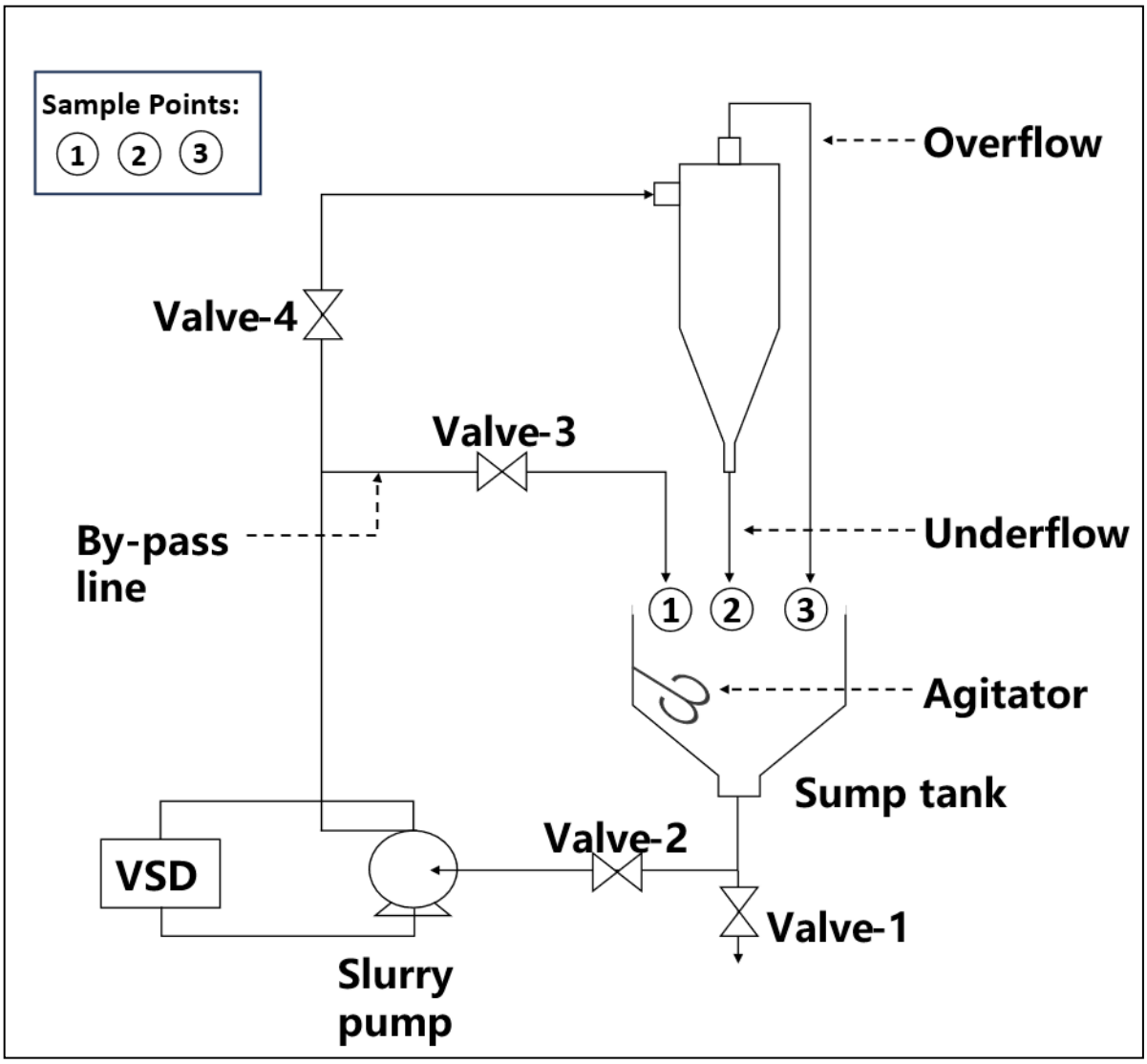

Figure 14: Flow circuit for the UCT 4-inch Multotec hydrocyclone test rig

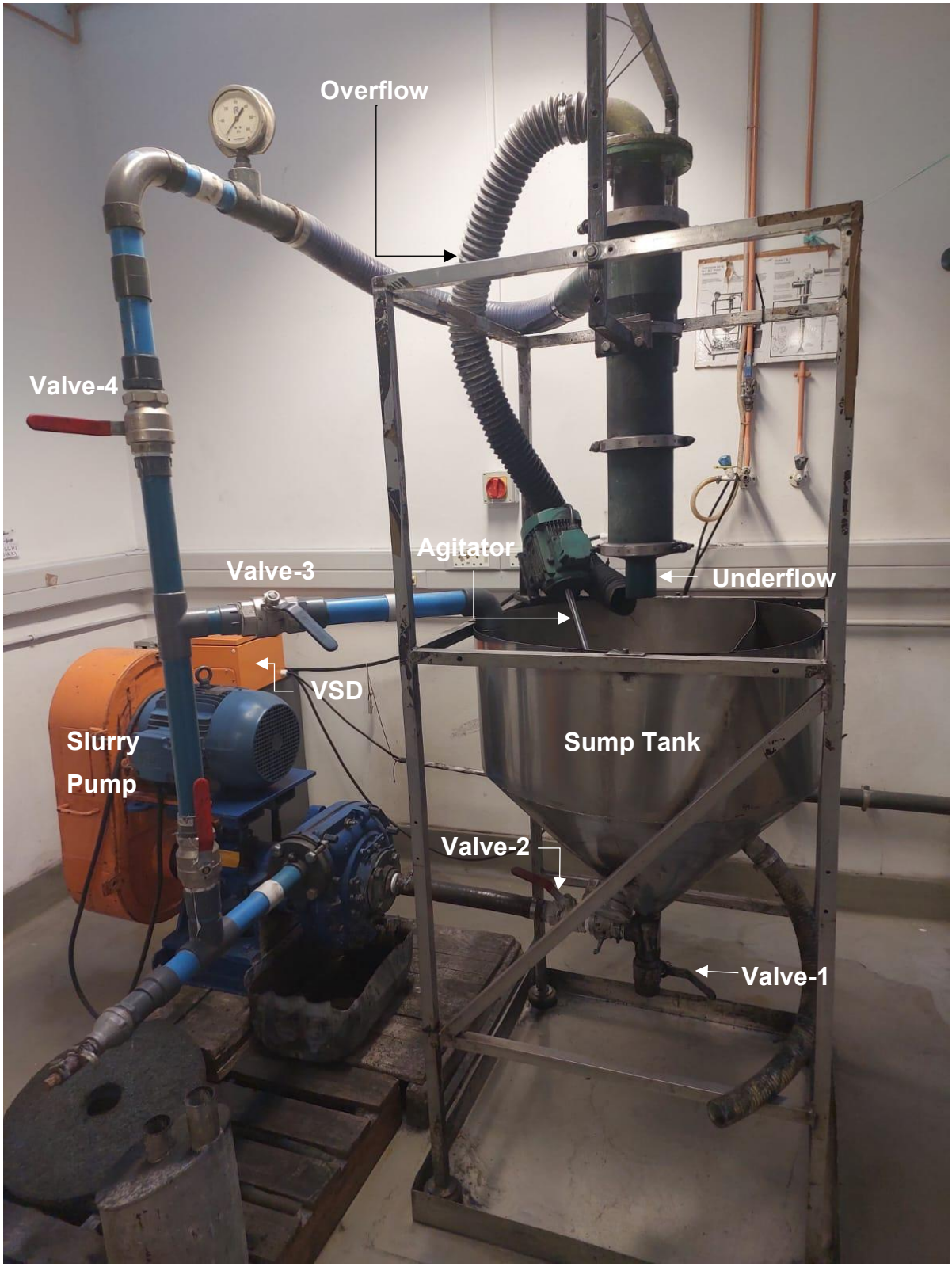

Figure 15: Picture of the UCT hydrocyclone test rig

Feed material is pumped from the 100L capacity stainless steel sump tank by a 5.5 kW Weir-EnvironTech centrifugal pump equipped with a 180 mm rubber-lined impeller. The pump is connected to the Allan-Bradley variable speed drive (VSD) for control.

The pump speed can be adjusted to get the required inlet feed flowrate. To prevent stagnation and dead zones in the sump tank during the experiments, an agitator is installed to mix the coal feed and separating medium. The return flows from the by-pass line, underflow and the overflow discharge streams also assist with mixing.

The hydrocyclone test rig is equipped with four valves placed along the flow line. Valve 1 facilitates the controlled discharge of slurry during the emptying of the slurry tank upon completion of each experiment. Valve 2 regulates the slurry flow into the pump and is kept fully open throughout all experiments. Valve 3 indirectly regulates the flow rate and pressure of the underflow and overflow discharge streams. This is accomplished by adjusting the valve to maintain an underflow stream that falls between the roping and spraying flow pattern conditions. Valve 4 controls the feed flow entering the hydrocyclone. Additionally, there are three sampling points: Point 1 for the feed, Point 2 for the overflow stream, and Point 3 for the underflow stream.

Additionally, the test rig has a bypass line connected to the main feed line to the hydrocyclone. This enables sampling of the feed during experiments. By opening valve 3 and closing valve 4, the conical section, spigot, or vortex finder can be replaced while maintaining the suspension of the feed slurry. The difference between the dense medium cyclone and the flat-bottom cyclone is in the structural design of the hydrocyclone body.

The dense medium cyclone has a long 20° narrow-angled conical section shown in Figure 16B. FBC has a long cylindrical section with a short cone of 160° angle as shown in Figure 16A. A long cylindrical section design increases the average retention time of particles, allowing more time for separation based on density (Hacifazlioglu, 2012). A wide conical angle promotes hindered settling by allowing dense particles to accumulate and recirculate at the base of the cylinder and cone, thereby forming an autogenous separation medium.

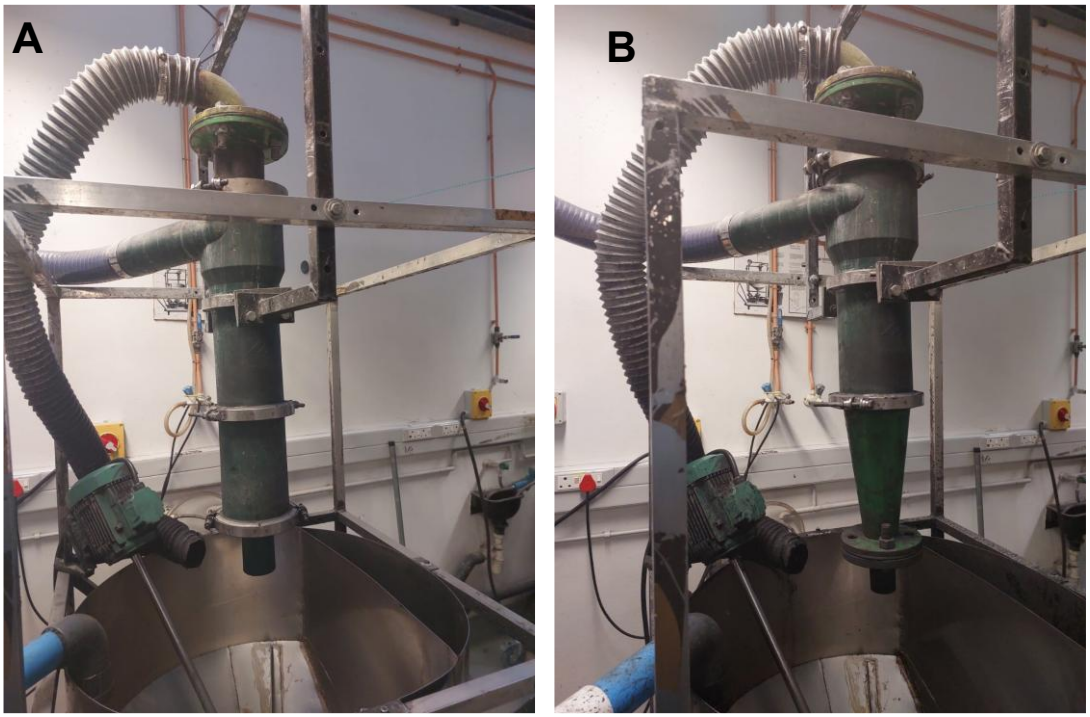

Figure 16: Picture showing the UCT test rig featuring the setup of a flat-bottom cyclone (A) and a dense medium cyclone (B)

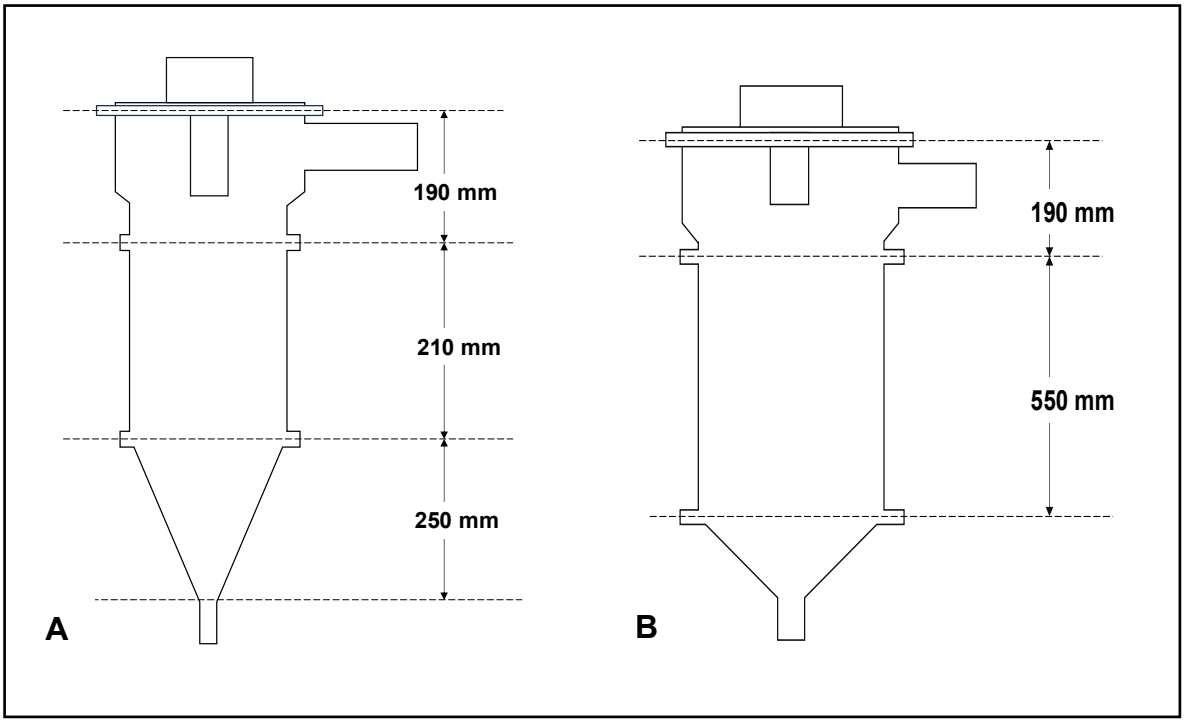

Figure 17: Schematics of the dense medium cyclone (A) and the flat-bottom cyclone (B)

3.1.2 Particle Size Measurement Apparatus

3.1.2.1 Dry Screening Apparatus

In this study, dry screening was used to determine the particle size distribution of the coal feed. Endecotts laboratory test sieves/screens are utilised with a woven stainless steel wire mesh with aperture sizes ranging from 3250 µm to 32 µm with a 100 mm diameter. The test sieves have a stainless-steel outer frame, allowing for sieve stacking and providing structural integrity during screening. The sides and bottom of each test sieve are fully sealed to prevent material loss during screening and have evenly tensioned wire mesh for accurate particle size analysis, and apertures conforming to ISO 3310-1 test standards.

The screens are mounted on a bench-top Fritsch Analysette 3 Pro vibratory sieve shaker, which accommodates up to ten stacked sieves, a sieve lid and a bottom receiving pan simultaneously (see Figure 18). The sieves are stacked in descending order of aperture size. This allows for efficient separation of particles by size, with the coarser particles being retained in the upper sieves and progressively smaller particles passing through to the lower sieves.

A clamping belt system secures the sieve stack during the vibratory screening process, and it can be manually tightened by locking in the tightening screws. The automated amplitude control for the sieve shaker ranges from 0.1 to 3 mm, allowing the selection of an amplitude that minimises particle breakage, ensuring accurate particle size distribution analysis.

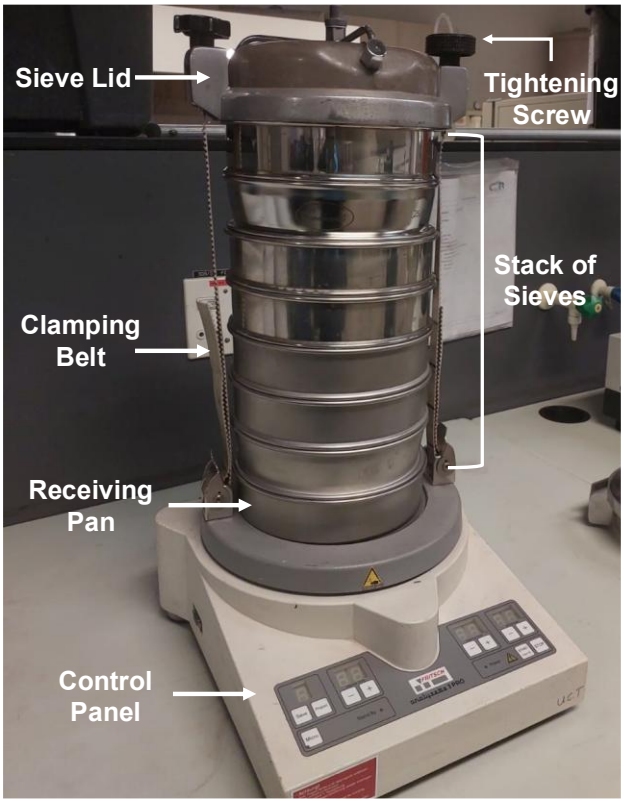

Figure 18: Fritsch Analysette 3 Pro sieve shaker with stacked sieves

The Fritsch Analysette 3 Pro has an electromagnetic drive which creates vertical vibrations in the stacked sieves, lifting the material intermittently off the mesh surface. As the material descends, it is pushed through the mesh of the connected test sieve, separating finer particles which are then collected across different aperture-sized test sieves and the bottom receiving pan on a size-by-size basis.

3.1.2.2 Wet Screening Apparatus

The wet screening apparatus used in this study to determine the particle size distribution (PSD) of the feed, underflow and overflow classifier samples utilizes the same lab test sieves/screens as described in section 3.1.2.1. The screens are stacked in descending order of size above a vibratory unit that induces vibrations to facilitate particle passage through the mesh apertures. A hollow metal sieve cover is placed on top of the stacked sieves to prevent material spillage during wet screening as shown in Figure 19. A water tube connects to the laboratory water supply to evenly distribute water, aiding the wet screening of the coal.

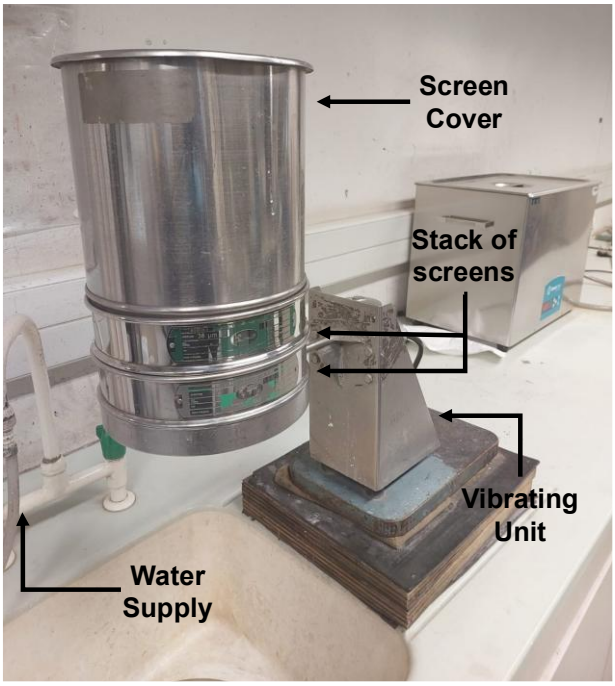

Figure 19: Wet screening apparatus with stacked sieves

3.1.2.3 Laser Diffraction

In this study, laser diffraction was employed to measure the particle size distribution (PSD) of magnetite using the Malvern Mastersizer Hydro 2000G. This device can analyse PSD ranging from 0.2 µm to 2100 µm. The Malvern Mastersizer is made up of three components: the optical bench, the sample dispersion unit and the computer system.

The sample is prepared in the dispenser and is then transferred to the optical bench, where the particle size is measured. The system, controlled by a computer, which has the Malvern Mastersizer software, captures the scattering patterns generated by the magnetite particles being measured. This software then interprets the patterns to determine the magnetite particle sizes.

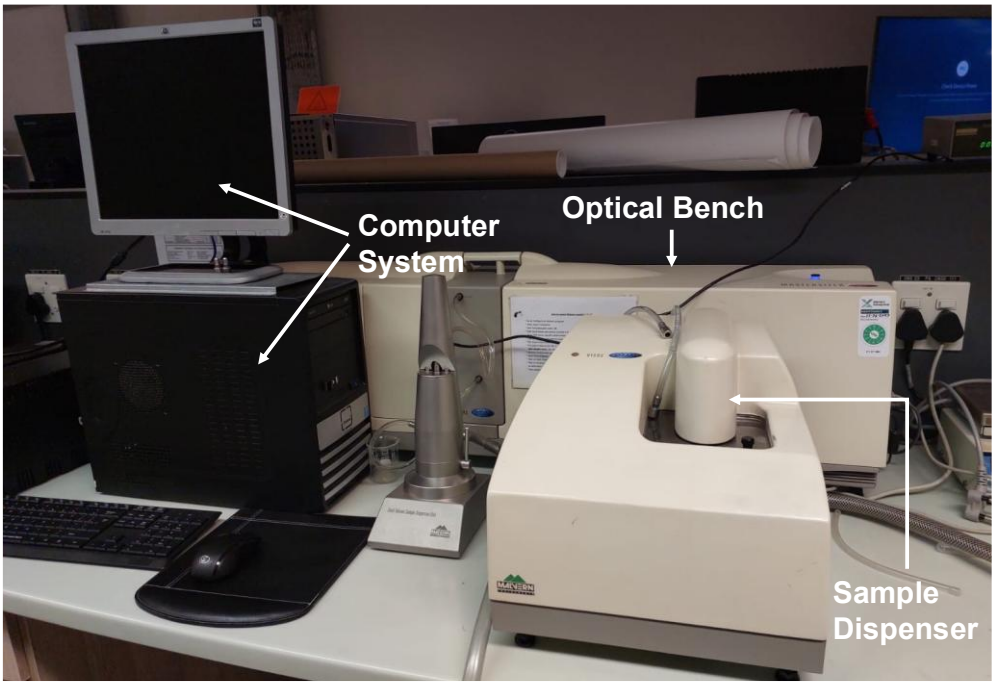

Figure 20: UCT Malvern Mastersizer Hydro 2000G

3.1.3 Float and Sink Apparatus

The float and sink tests were used in this study to determine the washability of the coal feed use an organic solvent as the separating medium. Organic solutions- bromoform, zinc chloride, and tetrabromoethane are carefully mixed in a glass 40L cylindrical see-through drum under a fume hood to achieve the target separating medium density. The drum allows for easy mixing of the coal with the organic solution mixture. The transparent drum allows for easy observation as coal particles denser than the separating medium settle at the bottom, resulting in the division into float and sink fractions.

The cylindrical container has a removable inner woven stainless wire mesh lining with an aperture size of less than 0.5 mm that runs along the full depth of the cylinder. The smallest coal particle size in the float-and-sink test conducted in this study is 0.5 mm. Therefore, a mesh with an aperture size smaller than 0.5 mm ensures full recovery of all coal particles that settle at the bottom as the sink fraction during the test. The container has a 350 mm diameter and a 475 mm depth as shown in Figure 21.

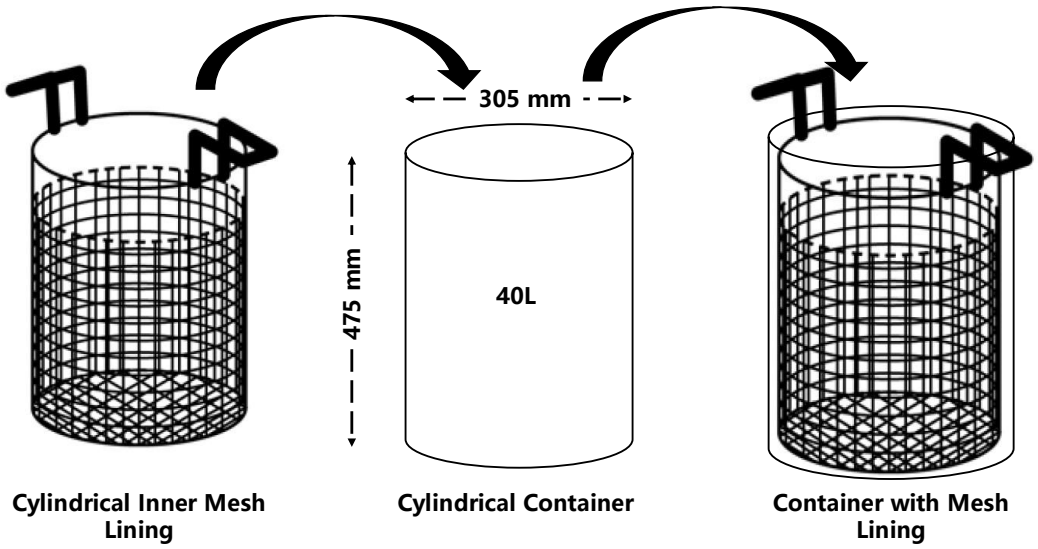

Figure 21: Float and sink apparatus - cylindrical inner mesh lining and container

In this work, a carefully controlled mixture of organic solvents was used to achieve a range of relative densities from 1.3 to 2.0. A hydrometer is used to measure and ensure the accuracy of the relative density of the separating medium.

Figure 22: Float and sink apparatus - wire mesh strainer

A strainer sieve with an aperture smaller than 0.5 mm is used to recover the float fractions from the cylindrical container during the experiment which are then placed on a collection tray. This setup allows the volatile organic solvents to evaporate from the recovered float fractions before measuring their mass.

3.2 Experimental Plan

Coal supplied by a colliery in Mpumalanga was used in the experiments, while magnetite from a commercial source was utilised for the dense media experiments. It

was important for the coal in this study to contain a reasonable fraction of near gravity material along with ash-bearing impurities. The coal preparation before the experiments included: drying, de-lumping, and screening. The coal was blended and split into representative portions. The materials used in this study were characterised. The characterization of magnetite included the chemical composition and particle size distribution (PSD). Proximate and ultimate analyses tests, calorific value, float and sink tests, and ash analysis for each of the float fractions derived from the float and sink tests were performed on the coal.

For each classifier, twenty experiments were performed from which optimally operating conditions were determined. During the experiments, samples were collected from the feed, underflow (UF) and overflow (OF) streams, and these samples were analysed to determine the ash analysis and particle size distribution. The optimised classifier experiments feed, UF and OF samples underwent further float and sink tests and ash analysis content.

3.3 Material Selection and Preparation

The experimental process involved externally sourcing magnetite and low-grade coal. Magnetite was sourced from Martin and Robson Industrial Minerals in Broodsnyersplaas, Mpumalanga. Approximately 1.5 tonnes of damp low-grade fine coal with a top size of 5 mm, high ash-bearing impurities and near gravity material content from a colliery in the Highveld Coalfield, Mpumalanga, South Africa.

The coal received was in the form of a thick slurry paste as shown in Figure 23. Wet coal with a high total moisture content cannot be used for experiments because it would result in inaccurate results. The physical characteristics such as density and mass, will not be a true reflection of the properties of the coal and would introduce inaccuracy in data from the classifier experiments.

Therefore, the coal was air-dried to remove the moisture. Drying was carried out on metal throughs in an open space in the laboratory. Natural air-drying was chosen over artificial heating lamps and the oven to avoid introducing any chemical or physical changes to the inherent chemical composition and properties of the coal. The coal was

turned twice a day using a shovel to speed up the drying process as can be seen in Figure 24.

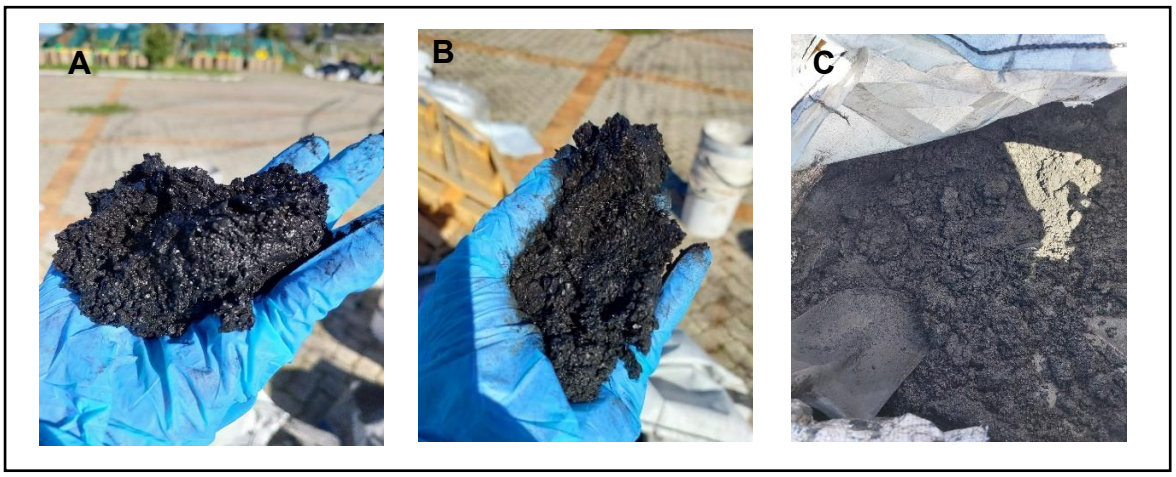

Figure 23: Wet coal received from the Highveld Coalfield with a thick slurry paste consistency

After drying the coal, the large coal chunks and agglomerated particles were broken down using a de-lumping mill. The coal was then manually screened using a 3.35 mm screen. The received coal had a top size of 5 mm which was not suitable for a 100 mm diameter hydrocyclone. A total of 750 kg of the screened fine coal (<3.35 mm) fraction was transferred into 40 buckets for temporal storage.

Figure 24: Damp coal air drying in the laboratory

The coal was then blended to obtain a uniform composition. The forty buckets of coal were initially grouped into four sub-sets of 10 buckets each (subsets A, B, C and D) as shown in Figure 25.

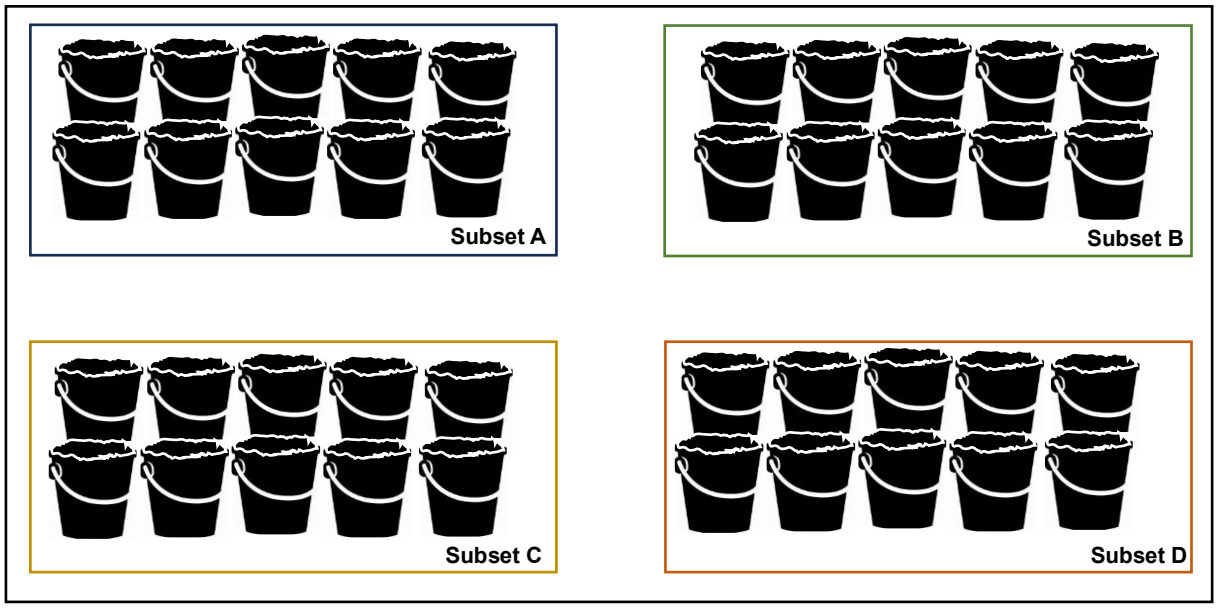

Figure 25: Initial grouping of coal into four groups

In phase one of the blending process, each subset (A, B, C, and D) was individually blended, as illustrated in Figure 26. Starting with subset A, each of the ten buckets of coal was emptied onto a 2 m x 2 m metal trough. Using a shovel, the coal underwent a process of coning, quartering, and blending, as shown in steps 1 and 2 in Figure 26. This was done to make each of the batches of coal of each subset homogeneous.

The blended coal was then fed in batches through a ten-way rotary splitter as shown by step 3 in Figure 26. After the ten-way material split of the blended coal was obtained, each split material was then transferred into ten separate empty 20L buckets as shown by step 4 in Figure 26. Steps 3 and 4 were repeated until all the blended material produced in step 2 was split and transferred to the ten buckets. This step was important to help further blend and make the coal homogenous. The same process was repeated for subsets B, C and D of the coal feed sample.

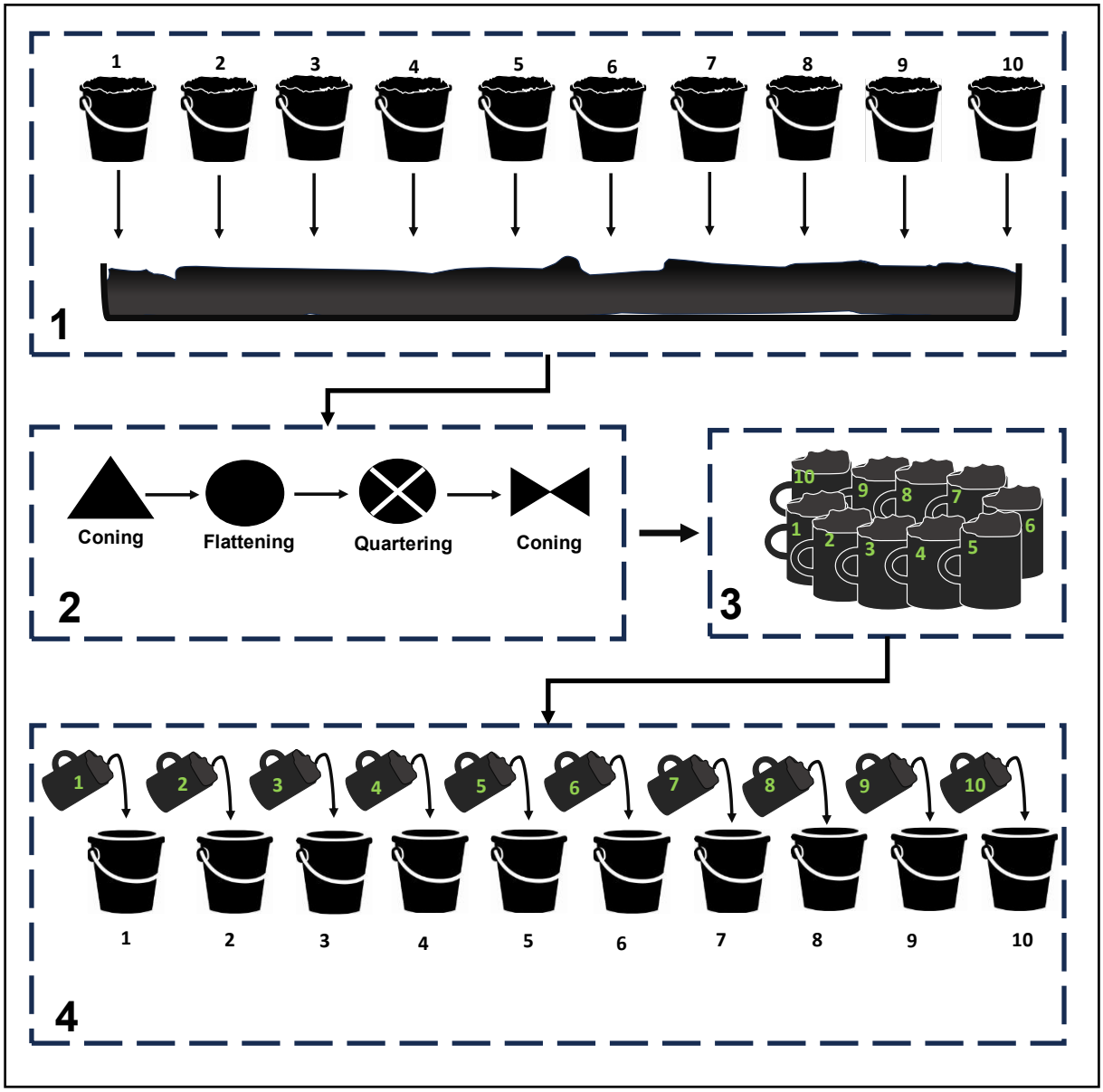

Figure 26: Phase one of coal blending and splitting for subsets A, B, C and D

After completing the homogenisation process of each subset samples, half of the blended coal from subset A was combined with half of the blended coal from subset B. Half of the blended coal from subset C was combined with half of the blended coal from subset D. The remaining buckets of subset A were combined with subset C, and the remaining buckets of subset B were combined with subset D as shown in Figure 27.

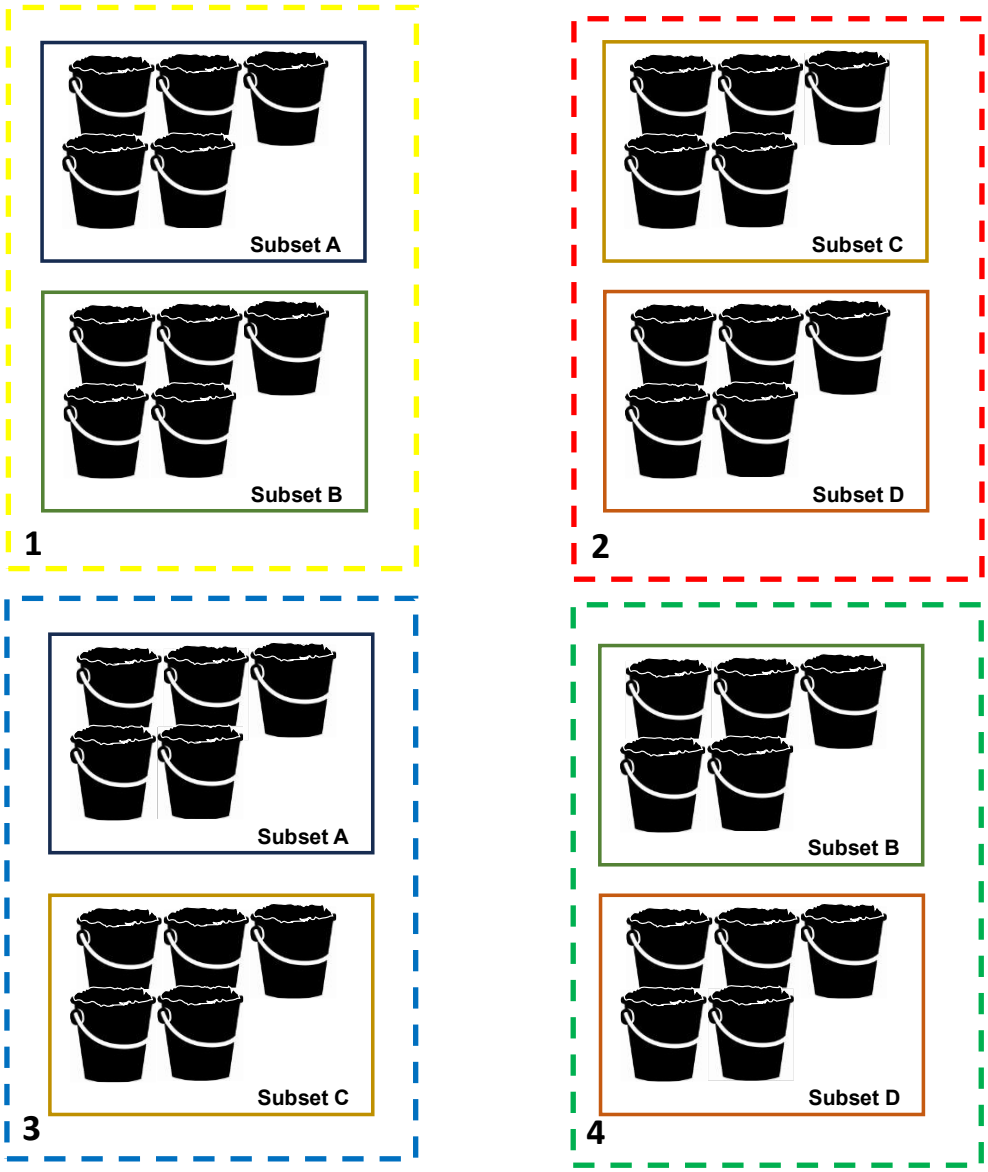

Figure 27: Phase two: re-grouping of the blended coal into groups 1,2, 3 and 4

The new groups (one to four), each comprising ten buckets of coal, underwent the same blending and splitting methodology as shown in steps 1 to 4 in Figure 26. This process resulted in 10 buckets from each group, producing a total of 40 buckets of coal.

3.4 Experimental Method

3.4.1 Flat-bottom Cyclone Tests

3.4.1.1 Selection of Test Variables

The efficiency of a FBC in separating fine coal is influenced by a range of factors related to its design and operation. This research focused on investigating the influence of the solids concentration, vortex finder diameter (VFD), and spigot diameter (SPD) on the coal yield and ash content. The FBC experiments were developed based on a study by Hembrom and Suresh (2018), and the work of Majumder and Barnwal (2011).

Table 6: Flat-bottom cyclone experiments test variables

Design Parameter	Dimensions	Units
Vortex finder diameter	26, 35 and 41	mm
Spigot diameter	25, 28 and 35	mm
Solids concentration	17, 23 and 29	% wt

The cone angle and vortex finder length remained fixed, while the vortex finder diameter, spigot diameter, and solids concentration were varied across three levels (see Table 6). The selected parameter ranges were chosen to assess the performance response at both lower and upper operational limits. This will enable a comprehensive analysis of their effects on the separation performance of the FBC. The experimental matrix was designed using CCRD, as outlined in Table 7.

Table 7: Design of experiment for the flat-bottom cyclone using CCRD

Experiment	Vortex Finder Diameter (mm)	Spigot Diameter (mm)	Solids Concentration (wt%)
1	26	25	17%
2	26	25	29%
3	26	35	17%
4	26	35	29%
5	34	25	17%
6	34	25	29%
7	34	35	17%
8	34	35	29%
9	34	28	23%
10	41	28	23%
11	41	16	23%
12	41	35	23%
13	41	28	12%
14	41	28	32%
15	41	28	23%
16	41	28	23%
17	41	28	23%
18	41	28	23%
19	41	28	23%
20	41	28	23%

3.4.1.2 Hydrocyclone Test Procedure

To run the hydrocyclone test rig, the sump tank was emptied and valves 1 to 4 in Figure 14 were closed. Forty-five litres of water was then added to the sump tank. After activating the agitator, valve 3, the by-pass line shutoff valve was opened to allow fluid flow and valve 2, the pump inlet shutoff valve, was opened to allow for the flow of liquid to the pump. The variable speed drive (VSD) of the pump was turned on to control the pump speed, feed pressure and flowrate. The VSD was operated and

maintained at 28 Hz for all the experiments which corresponded to a feed pressure of 14 kPa. A determined quantity of coal was then gradually added to the water, depending on the target solids concentration. Ten minutes were allowed for the coal and water to mix and achieve a steady state condition.

Subsequently, valve 4 was opened, and valve 3 was closed to stop the flow going back to the bypass line and to direct the slurry to the hydrocyclone. The rig operated for an additional ten minutes to stabilize before sampling the feed, overflow and underflow at the sampling points labelled 1, 2 and 3 respectively in Figure 14. Each of the streams was cut five times at five-minute intervals and the cut samples were combined to form a composite sample used for product analysis. Multiple samples help assess the consistency and reliability of the separation performance of the classifier. The experiment was conducted over a period of thirty minutes.

The flowrates of the feed, underflow and overflow were measured directly using a stopwatch and a 5000 mL beaker to determine the flow split in the hydrocyclone. The mass of each of the feed, underflow and overflow samples collected was measured. After all test work was completed, the system was drained to recover all remaining sample material. It was then flushed with water to prevent the solids build-up and pump clogging.

The composite sample was weighed to determine the wet mass. The wet-weighted samples obtained from the sampling were filtered using a filter press. The product filter cake was then dried overnight in the oven at 80°C. A medium to low temperature was used to avoid introducing any chemical change to the coal samples. The mass of the dry sample was then measured to determine the dry mass. The dry and wet mass was used to determine the solids concentration and to perform a mass balance over the hydrocyclone. An example of the mass balance over the DMC and FBC is provided in Appendix A.

The dried-up samples were then de-lumped over a 1000 µm sieve and split ten-way in a rotary splitter in preparation for ash content analysis and wet screening of the coal samples. The ASTM D3174-12 test standard method for the coal ash analysis was used. 1 g from the split sample of the underflow and overflow from each experiment test underwent ash analysis in a muffle furnace at 850°C (ASTM D3174−12, 2018). A

sample of the data generated from the experiments is shown in Table 8 and Table 9. Summarized experimental data is provided in Appendix A.

Table 8: Sample data collected from FBC experiments

Test conditions	VSD frequency (Hz)	28
	Spigot to VFD ratio	30/26
	Solids Concentration (wt%)	28.6
Feed	Mass (t/hr)	0.103
	Volume (m^3/hr)	0.092
	Water (t/hr)	0.073
	Solids concentration (wt%)	28.7
Overflow	Mass (t/hr)	0.011
	Volume (m^3/hr)	0.019
	Water (t/hr)	0.010
	Solids concentration (wt%)	11.7
Underflow	Mass (t/hr)	0.093
	Volume (m^3/hr)	0.124
	Water (t/hr)	0.061
	Solids concentration (wt%)	34.7

Table 9: Particle size distribution sample data for the FBC

Spigot to VFD ratio			30/26
Solids concentration (wt%)			28.6
Sieve size (µm)	**Feed (wt%)**	**Overflow (wt%)**	**Underflow (wt%)**
2800	100	100	100
2000	97.9	100	96.5
1400	85.1	100	80
1000	70.9	100	60.5
850	58.4	100	46.9
600	53.8	100	41.3
425	45.1	100	31.8
300	37.1	95	25.4
212	28.9	90.4	19.8
150	23.3	84.4	16.1
90	16.7	79.2	12.7
75	7.4	75.9	9.6
63	5.9	71.5	8.4
45	3.8	69.9	7.7
<45	1.1	64.6	7.5

3.4.2 Dense Medium Cyclone Tests

3.4.2.1 Selection of Test Variables

The experimental method of the dense medium cyclone (DMC) followed the standard approach reported by Ma et al. (2021) and Sahu et al. (2019). This study investigated the effect of the relative density of the separating medium, the spigot diameter, and the vortex finder diameter on the separation performance of a DMC. All other design and operational variables, including the cone angle and vortex finder length, were kept constant.

The diameter of the dense medium cyclone (DMC) significantly affects the distribution of material between the underflow and overflow, as well as the throughput capacity, product quality, and maximum particle size processed (Osborne, 2013b). Standard

DMC design parameters specify that the feed inlet diameter should be 15–20% of the cyclone diameter, while the vortex finder should be 43–50%. Furthermore, Osborne (2013b) recommends that the spigot diameter be 30–40% of the cyclone diameter and reiterates that the feed inlet may also be sized at approximately 50% of the cyclone diameter, depending on the specific application.

The upper and lower bounds for the vortex finder and spigot diameters were selected based on standard Dense Medium Cyclone (DMC) design principles. The chosen range for the relative density used in this experiment is based on the work of Ma et al. (2021). It was observed that this relative density range yielded improved coal ash reduction in the DMC. These limits were further refined using the Central Composite Rotatable Design (CCRD) employed in this study to generate a coded experimental matrix comprising 20 runs (refer to Table 10). This parameter range will enable a comprehensive analysis of their effects on the separation performance of the DMC.

Table 10: Design of experiment for the dense medium cyclone using CCRD

Experiment	Vortex Finder Diameter (mm)	Spigot Diameter (mm)	Medium Density (kg/m^3)
1	26	16	1350
2	26	16	1450
3	26	30	1350
4	26	30	1450
5	41	16	1350
6	41	16	1450
7	41	30	1350
8	41	30	1450
9	26	23	1400
10	41	23	1400
11	34	12	1400
12	34	30	1400
13	34	23	1320
14	34	23	1480
15	34	23	1400
16	34	23	1400
17	34	23	1400
18	34	23	1400
19	34	23	1400
20	34	23	1400

3.4.2.2 Hydrocyclone Test Procedure

The same approach discussed in section 3.4.1.2 was followed for the dense medium cyclone experiments. The only difference was the addition of dense media to effect separation by density. The media used was fine magnetite, Fe_3O_4, with a 95.20% purity. After allowing the coal and water to mix in the sump tank, a calculated quantity of magnetite was added to the slurry in the sump tank. The ratio of magnetite suspension to coal used in the experiment was maintained at 4:1 (volume basis) as recommended by Osborne (2013). Ratios above this may improve separation

efficiency. However, they can cause overcrowding of coal and magnetite particles in the DMC due to solids concentration exceeding its design capacity. Ratios below the recommended limit of 3:1 would culminate in reduced separation efficiency (Osborne, 2013).

After de-lumping the dried samples from the feed, overflow and underflow, the magnetite was extracted from each sample using a magnet. The recovered magnetite was sieved through a 100 µm screen to remove any entrained coal particles, after which the magnetite and separated coal were weighed individually. The coal sample was then analysed for ash content and particle size distribution. An example of the data obtained is shown in Table 11 and the corresponding particle size distribution in Table 12. A full data set from the DMC experimental work is provided in Appendix A.

Table 11: Sample data collected from DMC experiments

Test conditions	Op. VSD frequency (Hz)	28
	Spigot to VFD ratio	23/41
	Medium-to-coal ratio	4/1
	Operational density (kg/m^3)	1400
Feed	Mass (t/hr)	0.175
	Volume (m^3/hr)	0.127
	Water (t/hr)	0.096
	Solids concentration (wt%)	45.4
Overflow	Mass (t/hr)	0.083
	Volume (m^3/hr)	0.071
	Water (t/hr)	0.064
	Solids concentration (wt%)	23.0
Underflow	Mass (t/hr)	0.093
	Volume (m^3/hr)	0.055
	Water (t/hr)	0.034
	Solids concentration (wt%)	63.6

Table 12: Particle size distribution sample data for the DMC

Spigot to VFD ratio			23/41
Medium to coal ratio			4/1
Operational density (kg/m^3)			1400
Sieve size (µm)	**Feed (wt%)**	**Overflow (wt%)**	**Underflow (wt%)**
2800	100	100	100
2000	100	100	100
1400	97.6	100	96.7
1000	85.3	100	80.4
850	71.7	100	62.2
600	59.7	100	37.1
425	55.0	100	26.3
300	46.5	100	15.5
212	38.6	100	9.9
150	30.5	82.6	6.4
90	24.9	71.3	3.5
75	18.3	52.6	2.5
63	13.0	37.3	1.8
45	8.7	25.3	1.1
<45	6.8	21.8	0

3.4.3 Optimization

The flat-bottom cyclone and dense medium cyclone tests were conducted to identify the optimal operating conditions for the classifiers, that can be applied for the objective of minimizing the ash content in the overflow coal yield. Three-dimensional response surface plots and empirical response models were used to analyse the ash content and coal yield recovered to the overflow. CCRD numerical optimization, implemented using Design Expert and Statistica, was also applied to refine the operating parameters and minimize ash in the final coal product.

The identified optimal conditions were validated through experiments, in which the classifiers were operated under the optimized parameters, as outlined in sections 3.4.1.2 and 3.4.2.2. The overflow and underflow samples were subjected to float-and-

sink tests and ash content analyses to assess the separation performance of the classifiers.

3.5 Material Characterisation

3.5.1 Magnetite Quality Tests

The magnetite sample was split in a ten-way rotary splitter in preparation for the particle size distribution through laser diffraction and elemental carbon, hydrogen, nitrogen and sulphur (CHNS) composition analyses. These analyses are necessary as the quality of magnetite used in DMC tests affects the stability of the separating medium, which influences the separation performance classifier (He & Laskowski, 1994).

3.5.1.1 Particle Size Distribution

The particle size distribution of the magnetite sample was characterized using laser diffraction. The aim was to determine if approximately 50% of the particles fell within the -10 µm size range, with a particular preference for a size range where 90% of the magnetite particles were -5 µm, as recommended by King and Juckes (1988) for heavy media separation. The analysis was conducted with the Malvern Mastersizer 2000G at the UCT Chemical Engineering Analytical Laboratory.

The magnetite was analysed as a wet slurry. The magnetite sample preparation involved mixing 1 g of magnetite with distilled water, acting as the dispersant with a refractive index of 1.33, to create a paste in the sample dispenser. The Mastersizer was operated with a refractive index setting of 2.42 to ensure optimal particle size measurement. Data interpretation was conducted using the Malvern Software on the accompanying computer system.

3.5.1.2 Magnetite Composition

The chemical composition of the magnetite was determined using X-ray diffraction (XRD) from the UCT Chemical Engineering Catalysis Institution. The magnetite was

analysed in a dry state. The aim was to identify the presence of any clay-bearing minerals, such as kaolinite. If the magnetite contains high levels of clay, this can impact the separation performance of the dense medium cyclone by increasing the viscosity of the separating medium, which can lower the separation efficiency of the classifier (Firth, O'Brien & McNally, 2011).

3.5.2 Coal Quality Tests

Understanding the properties of the low-grade fine coal used in this study is important to assess its impact on classifier separation performance and to optimize classifier operating conditions. Float-and-sink tests and ash content analyses were performed to evaluate the washability of the coal. Proximate and ultimate analyses, calorific value, and total sulphur content were also assessed to determine the inherent properties of the fine coal and how these properties change as the specific gravity of coal washing changes. These analyses were conducted at an external analytical laboratory.

3.5.2.1 Proximate and Ultimate Analysis

The fraction of ash, moisture, volatile matter, and fixed carbon content contained in the coal samples was determined using the ASTM D7583-15 test standards under a nitrogen atmosphere. These coal analyses were conducted at Noko Analytical Services, an external analytical lab in Mpumalanga. The CHNS analyser was used to determine the carbon, hydrogen, nitrogen, sulphur, and oxygen content in the coal as per ASTM D3176-15 test standard. The analysis was done at the UCT Chemistry Department.

3.5.2.2 Calorific Value and Total Sulphur Test

The calorific value and the total sulphur content of the coal were determined at Noko Analytical, an external analytical lab in Mpumalanga. A bomb calorimeter was used to determine the calorific value of the coal. The sulphur content was determined using a sulphur analyser according to the ASTM D4239-18 test standards.

3.5.2.3 Float and Sink Tests

Washability tests were performed on the coal samples to determine the amenability of the coal to washing. The float and sink tests were outsourced to Noko Analytical Services in Emalahleni, Mpumalanga. Initially, 29 kg of the blended coal was air-dried to remove moisture and screened using a 0.5 mm screen to remove the sub-0.5 mm coal particles. The remaining 20 kg of coal, sized between 3.35 mm and 0.5 mm, was used for the float and sink test. A clear 40 L cylindrical tank was filled with a mixture of bromoform and zinc chloride solutions to achieve the target relative density, which was verified with a hydrometer. The float and sink tests were conducted across a relative density range of 1.3 to 2.0 in increments of 0.1.

Starting with a separating medium of 1.3 relative density (RD), the 20 kg of screened coal was gradually added and gently stirred to ensure that all the coal particles were suspended in the bromoform and zinc chloride solution mixture. After a 30-minute settling period, the particles less dense than the separating medium floated while the denser particles sank. A woven mesh strainer was used to carefully skim the floating coal fraction without disturbing the settled particles (sink fraction). The float fraction was placed on a collection tray and air-dried to evaporate the organic solution.

The inner mesh lining was then retracted to recover the sink fraction from the bottom, which was also air-dried. The dense organic solution was then incrementally adjusted with a denser solvent to increase the relative density to 1.4. The recovered sink fraction from the previous test was subjected to the same procedure. This process was repeated with relative density increments of 0.1 as shown in Figure 28. This resulted in nine float fractions.

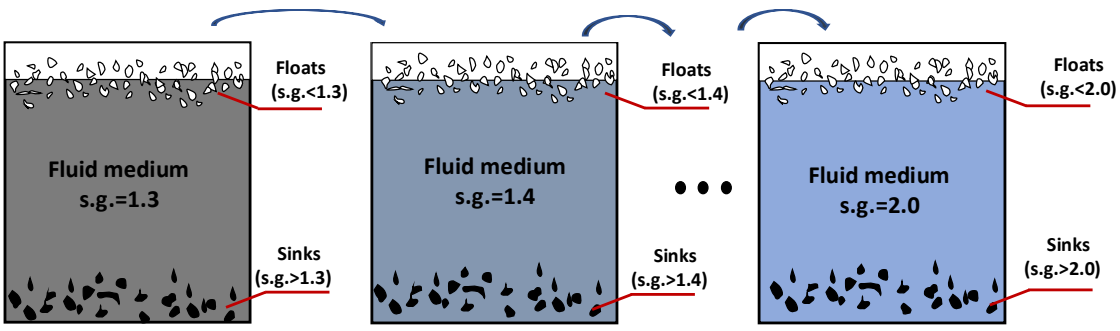

Figure 28: Illustration of the float and sink test

Each air-dried float and sink fraction was weighed to determine the proportion of coal that floats or sinks at each relative density. Proximate analyses were performed on each fraction to determine the ash, moisture, volatile matter, and fixed carbon content. Additionally, the float fractions were tested for calorific value and total sulphur content. This data was used to determine the ash content and near-gravity material in the coal. The ash content for each density float fraction, described in section 3.5.2.5, was also determined. The breakdown of the float and sink calculations from the density float analysis is presented in Table 30 (Gupta & Yan, 2016). This data was then used to determine the washability curves of the coal.

3.5.2.4 Particle Size Distribution

A particle size distribution (PSD) was determined for the bulk feed fine coal using dry screening. A mechanical sieve shaker was used with 17 screen sizes that were within the -3.35 +0.045 mm particle size range. Six sieves were stacked at a time in descending order of size. The mass of each sieve was measured before the screening process. 325 g of coal was measured and was screened through the stack of sieves from aperture sizes 3.35 mm to 32 µm. After the screening process, the mass of each sieve with retained coal was measured. The difference between the sieve mass with and without the retained coal was the size fraction of the coal relative to the feed mass.

Wet screening was used to determine the particle size distribution of both the overflow and underflow sample products. A predetermined mass of the coal sample was mixed with water to form a wet paste, which was then poured over the stack of sieves. Three sieves were used simultaneously, stacked in descending order of aperture size. A low-pressure water supply was used to wash the paste through the sieves, pushing the particles to the subsequent sieve. Low-pressure supply water was used to avoid particle breakage.

The water and coal passing through the sieves were collected in a 20L bucket at the base of the stacked sieves. Once the water running through the sieves became clear, the screening process was considered complete. The process was repeated with another stack of sieves. The slurry collected in the 20L bucket was gently poured over the sieves again, and the excess water and coal that were not retained were collected

at the base in a 20L bucket. This procedure continued until the slurry had passed through all the sieves, ranging from 3.35 mm to 45 µm. The retained coal in each screen was decanted onto a clean tray, dried in the oven overnight at 80°C and weighed. The mass was used to determine the partition curves and analyse the performance of the classifier.

3.5.2.5 Ash Analysis

The float fractions of coal from the float and sink tests and the size fractions from the particle size distribution analysis of the coal were subjected to ash analysis according to ASTM D3174-12 test standards. A maximum mass of about 1 g of the coal sample was placed in a crucible and then incinerated in a muffle furnace. The coal mass required was measured on an analytical balance with a precision of 0.01 mg.

During the first hour, the furnace temperature was increased by 125°C every 15 minutes until it reached 500°C. In the second hour, the temperature was further increased by 88°C every 15 minutes until it reached 850°C. For the remaining two hours, the furnace was maintained at 850°C to ensure complete calcination of the coal. The ash content was determined using equation 27:

$$Ash\ content = \frac{Mass_{crucible\ and\ coal} - Mass_{crucible\ and\ ashed\ coal}}{Mass_{crucible\ and\ coal}} \qquad 27$$

4 Results and Discussion

This chapter discusses the results from the testwork performed to compare the efficiency of a dense medium cyclone and a flat-bottom cyclone. The focus is on their application in washing coal with high near-gravity material and ash-bearing impurities to produce clean coal with significantly reduced ash content. The magnetite and low-grade fine coal used in the experiments were characterised to assess if their properties met the requirements set out for the thesis experimental work.

Twenty tests were conducted for each classifier. This chapter presents and discusses the effects of feed solids concentration, spigot diameter, and vortex finder diameter on ash reduction and coal yield in the flat-bottom cyclone. For the dense medium cyclone, the focus was on the influence of the separating medium density, spigot diameter, and vortex finder diameter on ash reduction and coal yield.

4.1 Material Characterisation

Various techniques were employed to characterize the raw materials, which were the coal and magnetite used in the experimental work. The characterisation was conducted to determine the physical and chemical properties of these materials. These properties are known to have direct influence on the composition and stability of the separating medium and, consequently, the separation efficiency of both the dense medium cyclone and the flat-bottom cyclone (He & Laskowski, 1994). This section discusses the results of the particle size distribution (PSD) and chemical composition analysis of the magnetite. It also covers the feed coal quality assessment, which includes PSD, proximate and ultimate analyses, calorific value, float and sink tests, and ash content analysis.

4.1.1 Magnetite Quality Analysis

An X-ray diffraction (XRD) analysis was performed on the bulk magnetite to determine its chemical composition and detect the presence of clay minerals. This analysis is important as clay minerals impact the separation efficiency of the dense medium cyclone by increasing the separating medium viscosity (He & Laskowski, 1995). High

concentrations of clay contaminants in magnetite have been reported to destabilize the separating medium, resulting in reduced separation efficiency (Firth, O'Brien & McNally, 2011). The outcome of the XRD analysis is presented in Table 13.

Table 13: XRD results of minerals in magnetite sample

Mineral	**Crystalline Phase (wt %)**
Magnetite	95.15*
Calcite	1.28
Dolomite	0.72
Mica	2.85
*main mineral	

The magnetite has a purity of 95.1% with other minor mineral impurities. Low quantities of clay impurities, in the form of mica, were detected in the magnetite sample. The XRD diffractogram provided in Figure 53 in Appendix A confirms that magnetite (Fe_3O_4) was the main compound present in the sample.

A study by O'Brien, Firth and McNally (2014) showed that the presence of impurities in magnetite, even at concentrations up to 20 wt%, has a negligible impact on the stability of the separating medium when used in a DMC with a relative density exceeding 1.4. Therefore, an assumption was made in this work that a 5 wt% magnetite impurities concentration would not significantly impact medium viscosity and stability during the dense medium cyclone experiments.

The particle size distribution of the magnetite used in the experimental work is shown in Figure 29. The particle size distribution was determined by laser diffraction using the Malvern Mastersizer 2000G. The magnetite has a d_{90} and d_{50} of 88.46 µm and 34 µm, respectively. Fine magnetite should be used for optimal coal beneficiation in dense medium cyclone experiments. According to England et al. (2002) coarse magnetite can cause the separating medium to be unstable as it segregates inside the DMC, which lowers its separation efficiency. Fourie and Van Der Waltt (1980) recommend that at least 50% of the magnetite be finer than 10 µm for efficient separation in a 150 mm DMC. The magnetite utilised in this study is relatively coarser than the optimal ultrafine magnetite grade (d_{10} passing size of 10 µm) recommended

for fine coal cleaning. Its selection was driven by budgetary constraints, as ultrafine magnetite is more expensive than the coarse grade (d_{50} passing size of 45 µm).

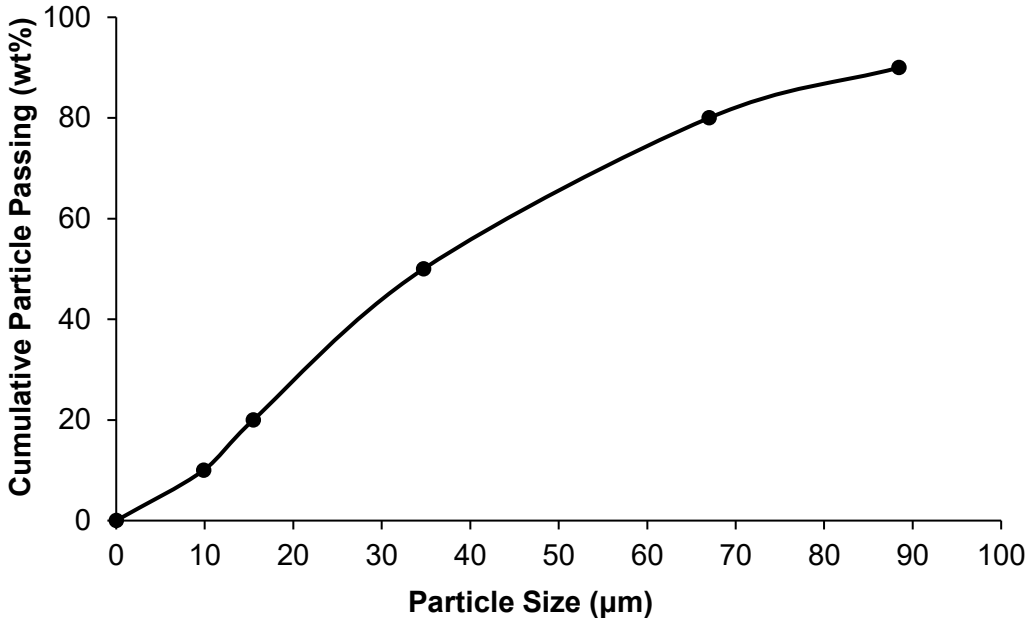

Figure 29: Magnetite particle size distribution curve

4.1.2 Coal Quality Analysis

Characterization analyses were conducted on the feed coal, which included proximate and ultimate analyses, float and sink tests, particle size distribution, ash content analysis, calorific value and total sulphur tests. The proximate analysis measured fixed ash content, moisture content, volatile matter, and fixed carbon. The ultimate analysis determined the elemental composition of carbon, hydrogen, nitrogen, and sulphur. These analyses are essential in evaluating coal rank, assessing its value, and understanding how its inherent properties influence coal cleaning processes and efficiency.

4.1.2.1 Proximate and Ultimate Analysis

The feed coal has a fixed carbon content of 44.5% and an ash content of 30.3%, which is a characteristic of low-grade bituminous coal from the Highveld Coalfields (L. S.

Jeffrey, 2005; North, Engelbrecht & Oboirien, 2015). This is further supported by the observed low coal volatile matter content of 21.7%, and moisture content of 3.5%, as shown in Table 14.

Table 14: Proximate analysis for the fine coal

Parameter	Quantity (wt%)
Inherent moisture	3.5
Ash	30.3
Volatile matter	21.7
Fixed carbon	44.5

The coal has a low total sulphur content of 0.72% and a calorific value (CV) of 20 MJ/kg. This data aligns with the proximate analysis and CV data for coal from the Highveld Coalfields reported by L. S. Jeffrey (2005). The data from the ultimate analysis shown in Table 15 show that the low-grade coal has 30.12% carbon, 5.18% hydrogen, 11.68% nitrogen, 26.89% sulphur and 26.13% oxygen. The relatively low carbon content and CV value suggest that this coal can be classified as low-grade bituminous coal. Therefore, for the objectives of this study, the coal is suitable for this experimental study.

Table 15: Ultimate analysis for the fine coal

Element	Quantity (wt%)
Carbon	30.12
Hydrogen	5.18
Nitrogen	11.68
Sulphur	26.89
Oxygen	26.13

4.1.3 Particle Size and Ash Analysis

Dry screening of the bulk coal was performed over a size range of 3.35 mm to 32 µm. A size-by-size ash analysis was conducted to determine the distribution of ash-bearing

impurities in the coal feed. The results are shown in Table 16 and the PSD curve in Figure 30.

Table 16: Particle size distribution and ash analysis of the fine coal

Sieve Size (µm)	Differential		Cumulative	
	Mass (%)	Ash (%)	Mass (%)	Ash (%)
-3350 +2800	2.10	28.01	2.10	28.01
-2800 +2000	12.77	28.15	14.87	28.13
-2000 +1400	14.26	29.46	29.13	28.78
-1400 +1000	12.45	29.45	41.59	28.98
-1000 +850	4.57	29.53	46.16	29.04
-850 +600	8.70	29.77	54.86	29.15
-600 +425	8.00	29.81	62.86	29.24
-425 +300	8.26	29.98	71.12	29.32
-300 +212	5.57	29.98	76.69	29.98
-212 +150	6.62	30.91	83.31	30.91
-150 +106	5.22	31.51	88.53	31.18
-106 +90	4.05	31.58	92.57	31.28
-90 +75	1.55	31.69	94.12	31.31
-75 +63	2.10	31.73	96.23	31.36
-63 +53	2.04	32.56	98.27	31.47
-53 +45	0.60	33.41	98.87	31.53
-45 +32	0.43	39.87	99.30	31.69
<32	0.70	42.78	100.00	32.02

The coal has a top size of 3.35 mm, which is suitable for efficient separation in a 100 mm diameter hydrocyclone. Table 16 shows that 83.31% of the bulk coal is made up of fine coal particle sizes ranging between 3.35 mm to 0.15 mm and has an average ash content of 29.61%. The remaining ultrafine coal fraction makes up close to 16% of the bulk coal and has an average ash content of 32.21%. Table 16 shows that ash content increases as particle size decreases across the respective size fractions.

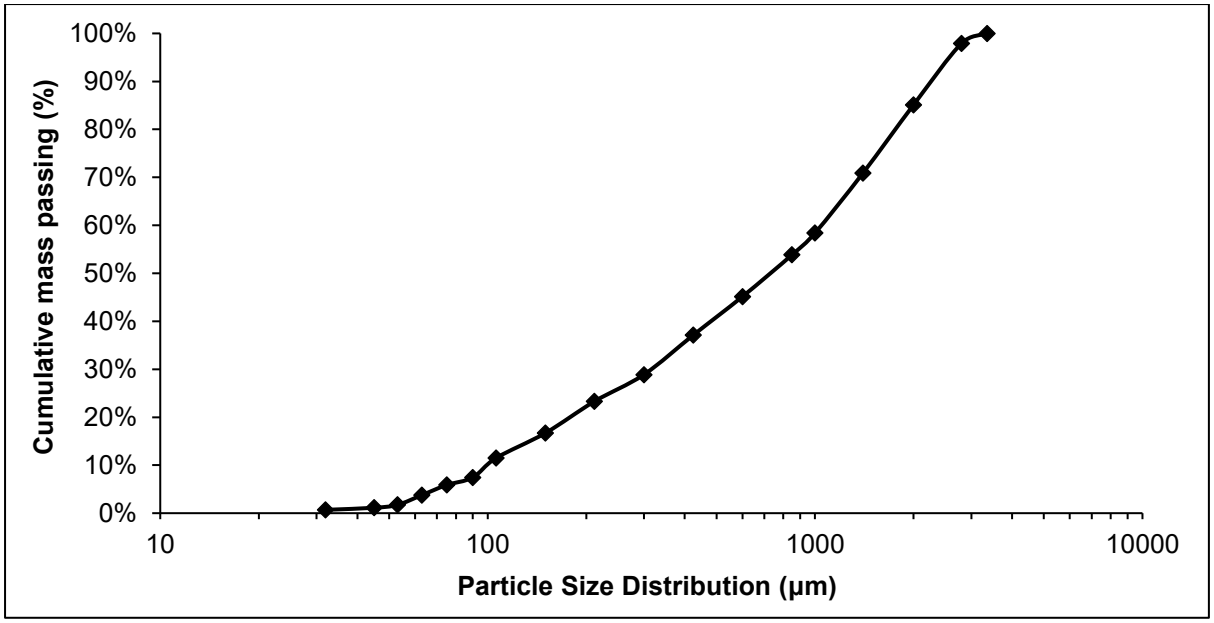

Figure 30: Particle size distribution curve for the fine coal

4.1.4 Float and Sink Test

Float and sink tests were performed to evaluate the washability of the coal. These tests are important in determining the appropriate coal-washing processes and the specific gravity values that maximize ash reduction in the clean coal product while maintaining reasonable yield and economic viability (Mukherjee, 2009). The washability of the coal is influenced by the proportion of NGM present (Bhattacharya, Maheshwari & Panda, 2016b). The float and sink test data are used to generate washability curves and indexes, which are applied to estimate the theoretical coal yield achievable for a given coal quality.

4.1.4.1 Washability Index

Washability indices are used to evaluate the amenability of the coal to washing, and two indices are discussed in this section, namely the S-value and near gravity material index (NGMI). The S-value index ranges from 0 to 1, where values close to one indicate that the coal is easy to wash, and lower values indicate that the coal is generally challenging to beneficiate. The NGMI determines the optimal cut-point density for which the coal will be most amenable to washing and is calculated per

density float fraction. The NGMI ranges between 0 to 100%, where the closer the value to 100%, the more amenable the coal is to washing.

The S-value was calculated using equation 8, while the cumulative non-ash recovery (RNA) and cumulative ash recovery (RA) were determined from equations 1 and 2 as outlined in section 2.1.1, respectively. A third-order polynomial was applied to the cumulative ash and non-ash recovery data, generating the plots shown in Figure 31. The recovery trends of the ash and non-ash components were modelled using this polynomial, maintaining the format of equations 3 and 4 for the non-ash and ash recovery, respectively shown in Table 17. A sample calculation is provided in Appendix A.

Table 17: Calculated cumulative ash recovery (R_A) and non-ash recovery (R_{NA}) curves

Specific Gravity	Cumulative		S-Value	NGMI
	R_A	R_{NA}		
kg/m³	wt%	wt%	%	%
F1.3	0.38	2.83		-
F1.4	4.28	17.17		16.86
F1.5	13.20	38.18		60.01
F1.6	41.68	73.41		62.21
F1.7	53.17	84.13	57.84	24.86
F1.8	62.68	90.38		13.93
F1.9	70.55	94.07		7.59
F2.0	76.28	96.16		6.92
Sink at 2.0	100	100		-

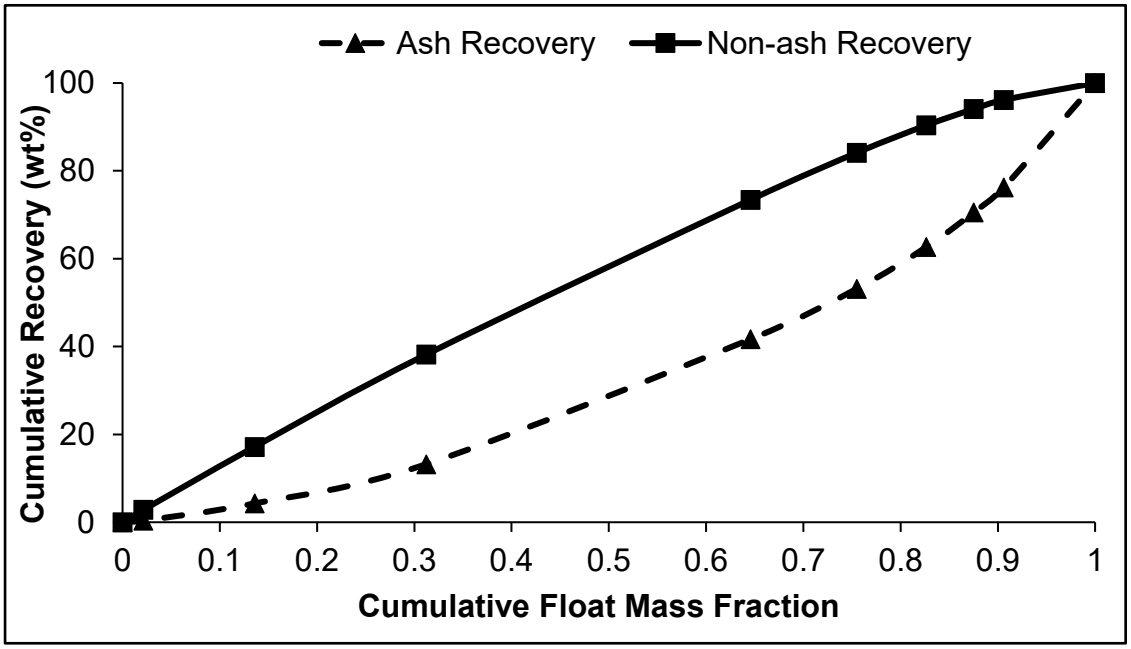

Figure 31: Cumulative ash and non-ash recovery plots

The coefficients for these recovery curves presented were determined through the application of the least squares method, as shown in Table 18 from the recovery plots shown in Figure 31. Subsequently, these coefficients were utilised to calculate the near-gravity material index for the coal using equation 7. A sample calculation is provided in Appendix A.

Table 18: Coefficients for the recovery of ash and non-ash plots

RA	**r**	**q**	**p**
	77.948	-22.489	42.446
RNA	**c**	**b**	**a**
	-30.124	8.6912	122.4
Variance	**c-r**	**b-q**	**a-p**
	-108.072	31.1802	79.954

The S-value, determined from coal washability data, is 57.84%, indicating that the coal is moderately amenable to washing. The NGMI results of the coal used in this study are shown in Table 17.

4.1.4.2 Washability Curves

Coal washability improves the quality of run-of-mine coal by removing gangue minerals via density-based separation, as run-of-mine coal consists of varying proportions of coal and minerals with different densities (Kumar & Saxena, 2014). The washability data for the coal in this study, shown in Table 19, illustrates the correlation between the mass of each float fraction and the ash content at specific relative densities.

Table 19: Float and sink test results and calculated near-gravity material for fine coal

Relative density	Differential float (wt%)		Cumulative float (wt%)		NGM (%)
	Mass	Ash	Mass	Ash	
F1.3	2.15	5	2.15	5	-
F1.4	11.43	9.5	13.58	8.79	29.07
F1.5	17.64	14.1	31.22	11.79	50.99
F1.6	33.35	23.8	64.56	17.99	44.28
F1.7	10.94	29.3	75.50	19.63	18.10
F1.8	7.16	37.0	82.66	21.14	12.01
F1.9	4.85	45.2	87.51	22.47	7.96
F2.0	3.11	51.4	90.62	23.46	-
Sink at 2.0	9.38	70.5	100	27.87	-

Float and sink test data were utilised to determine the NGM content in the coal. For low-density coal particles, specifically those with a relative density (RD) of 1.3 to 1.5, the near-gravity material content initially increases from 29.07% at 1.4 RD to an observed maximum of 50.99% at 1.5 RD. Beyond an RD of 1.5, the NGM content decreases.

Figure 32 shows the float curve for the fine coal representing the cumulative mass of floats against cumulative coal ash. It was observed that the ash content increases proportionally with coal yield. The maximum ash content observed at full clean coal recovery (100%) is 27.87%.

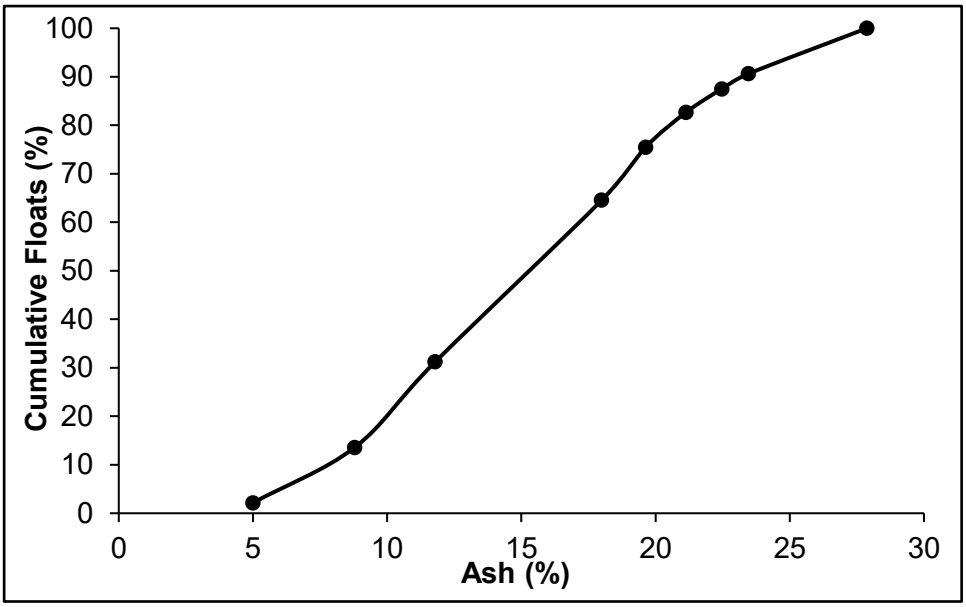

Figure 32: Float curve for the fine coal

Figure 33 shows the near-gravity material index and yield curve for the coal. The yield curve is a function of the cumulative mass of floats and specific gravity of the separating medium of the fine coal. The NGMI curve shows the relationship between the near-gravity material index for the coal and the specific gravity of separation. The yield curve in Figure 33 follows a conventional 's-shape' curve. It has a steep initial incline within the specific gravity range of 1.3 to 1.6, followed by a gentle slope beyond a specific gravity (SG) of 1.6. This shows that a substantial fraction of coal has a specific gravity range below 1.6.

From the float and sink tests performed on the coal, 65% of the bulk clean coal was obtained at a separation specific gravity of 1.6, with a 23.8% ash content. The observed yield and float curves reflect a comparable pattern to that identified by Ma et al. (2021) for -1 + 0.125 mm fine coal.

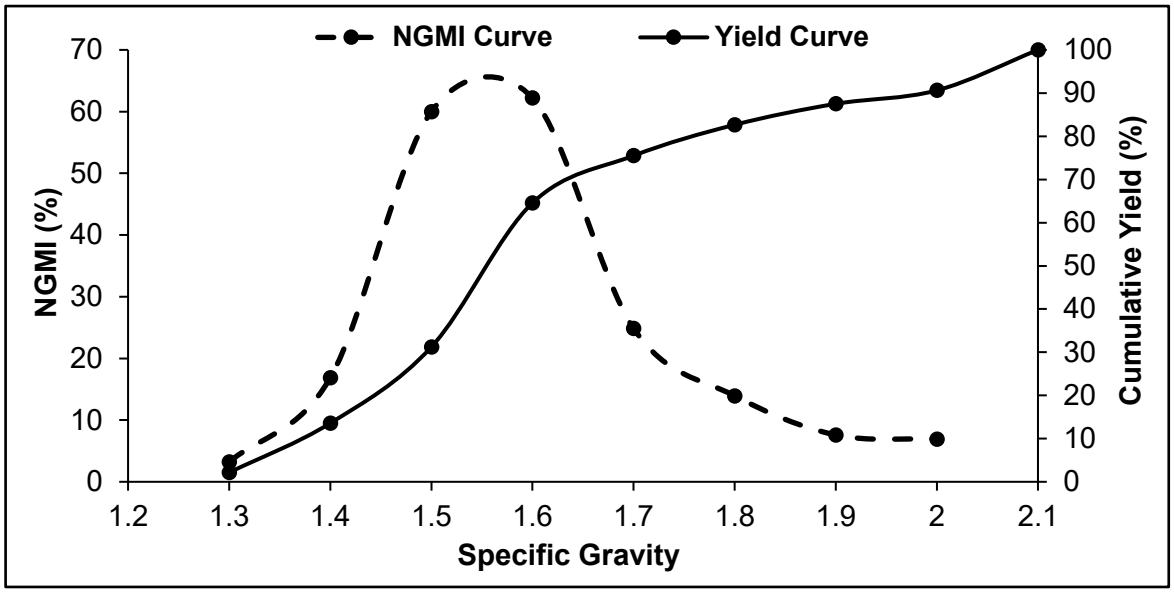

Figure 33: NGMI and yield curves for fine coal

Figure 33 shows the NGMI curve. It has a bell shape, which is closely comparable to a trend that has been observed in the work of Majumder and Barnwal (2004). The critical specific gravity of separation for the coal is between 1.5 to 1.6, corresponding to the maximum NGMI value of 60% to 62.2%. This showed that washing the coal at this specific gravity range would be challenging.

The coal is amenable to washing at specific gravities below 1.4 and above 1.8 because of the low NGMI values. At a specific gravity below 1.4, it corresponds to an NGMI of 16.9%, and this produces a low coal yield of 13.58% and ash content of 8.79% (see Figure 32). Conversely, washing at specific gravities greater than 1.8 corresponds to an NGMI of 13.9%, resulting in higher coal yields exceeding 82% and generating coal with a cumulative ash content greater than 21%.

Figure 34 shows the calorific value curve, a function of the specific gravity of separation for the coal. It was observed that the calorific value decreased as specific gravity increased. The trend observed is consistent with observations made on South African coal from Witbank (Botha, 2016). The coal achieves a maximum calorific value of 29.53 MJ/kg at a separation specific gravity of 1.3. However, when washed at a higher separation specific gravity of 2.0, the calorific value decreases to 20.26 MJ/kg.

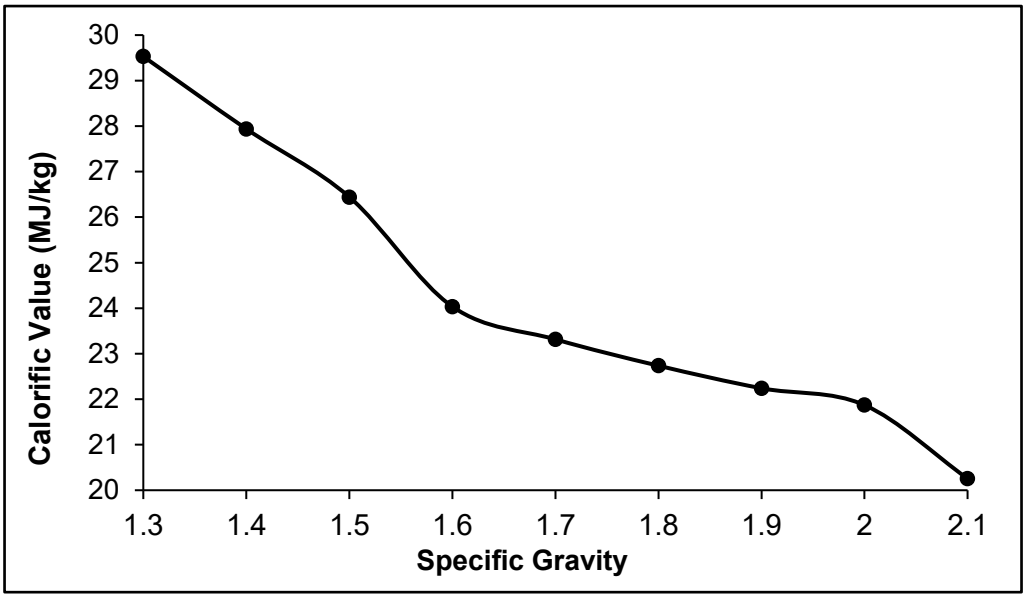

Figure 34: Calorific value curve for the fine coal

The ash content distribution is presented in Figure 35. The observed trend shows that the ash content for this coal increases with an increase in the specific gravity of washing. This could be because at higher specific gravity values of coal washing, the high-density gangue particles in the coal, such as shale and pyrite, are recovered with the float fraction during coal washing.

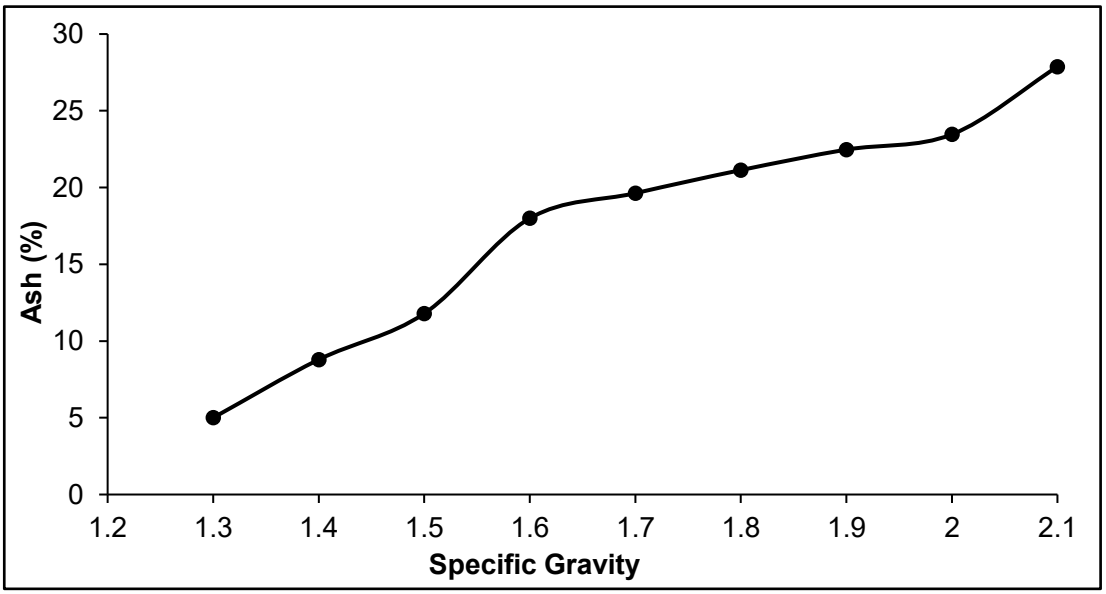

Figure 35: Ash distribution curve for the fine coal

Therefore, in this experimental study, the selected separating medium specific gravity for the classifier tests was 1.4. Under these conditions, the NGMI value is relatively low at 16.9%, indicating favourable washability of the coal. At this specific gravity, a

theoretical coal yield of 13.58% is achieved, with an ash content of 8.79% and an increased calorific value of 27.94 MJ/kg. This represents an improvement from the initial ash content of the raw bulk coal of 30.3% and a calorific value of 20 MJ/kg.

4.2 Flat-bottom Cyclone Experiments

Flat bottom cyclone (FBC) tests were performed to assess the influence of the spigot diameter, vortex finder diameter, and solids concentration on the separation performance of the classifier. This cyclone is sometimes called a water-only cyclone (WoC) in coal washing because no dense media is used. The quality and quantity of the coal recovered to the overflow were investigated as part of the performance criteria for this study.

Using Statistica 12 and Design Expert Software, three-dimensional (3D) response plots were developed to investigate the combined effect of the independent variables, vortex finder diameter, spigot diameter and solids concentration on the ash content and coal yield. The response surface plots utilize a colour map ranging from intense red to dark green (hottest to a cold colour). The intense red represents the highest concentration of either ash content or coal yield, while dark green signifies the lowest levels.

Statistical analysis of the experimental data was conducted using analysis of variance (ANOVA) and significance tests to develop empirical regression models for predicting coal ash content and coal yield. Numerical optimization of coal ash content and coal yield was performed by applying the desirability function in Design Expert Software.

4.2.1 Effect of Solids Concentration and Spigot Diameter

The study investigated the influence of feed solids concentration and spigot diameter on a flat bottom cyclone with a 34 mm vortex finder diameter on ash content and clean coal yield. Figure 36A and B show the developed three-dimensional (3D) response plots illustrating the interaction effects of solids concentration and spigot diameter on ash content and coal yield, respectively. Figure 36A showed the coldest dark green colour at a high solids concentration of 33%. This cold dark green colour implies that

the coal produced has the lowest ash content. The solids concentration had a more substantial influence on product ash content compared to spigot diameter, with an increase in the latter correlating with higher ash content in the coal product to the overflow. These findings contradicted prior research by Abbas and Muhammad (2016) and Hacifazlioglu (2012).

Abbas and Muhammad (2016) studied 2 mm top-size coal at solids concentrations from 10% to 20%, using a flat-bottom cyclone with a fixed spigot diameter of 26 mm and a vortex finder diameter of 54 mm. The ash content increased from 9% to 19%, and the coal yield increased from 54% to 78%. Similarly, Hacifazlioglu (2012) examined 2 mm top-size coal with solids concentrations ranging from 10% to 30%, reporting an increase in clean coal ash content from 8.5% to 14% and coal yield from 22% to 26% when using a cyclone with a fixed spigot diameter of 50 mm and a vortex finder diameter of 75 mm.

The observed results may be attributed to the combined effect of high solids concentration and a reduced spigot diameter. Operating the cyclone at a higher solids concentration promotes reasonable autogenous medium formation within the conical section of the hydrocyclone, which would increase the separation density (Abbas & Muhammad, 2016). Under these conditions, the restricted underflow discharge increases internal cyclone pressure, promoting the upward transport of fine, low-density coal particles to the overflow (Wills & Finch, 2016). This flow bias enhances the separation of coal from denser mineral matter, thereby potentially explaining the observed outcome.

Figure 36B shows that increasing spigot diameters from 25 mm to 35 mm causes a reduction in the clean coal yield recovered to the overflow. This is indicated by the change in the colour gradient from an intense red to a yellow. This could be due to the considerable pressure decrease encountered across the cyclone body associated with larger spigot diameters. This low-pressure drop causes more slurry to report to the underflow, reducing the feed residence time inside the flat-bottom cyclone and preventing the formation of an autogenous bed medium. Consequently, separation efficiency and clean coal yield in the overflow decrease, as observed by Hacifazlioglu (2012).

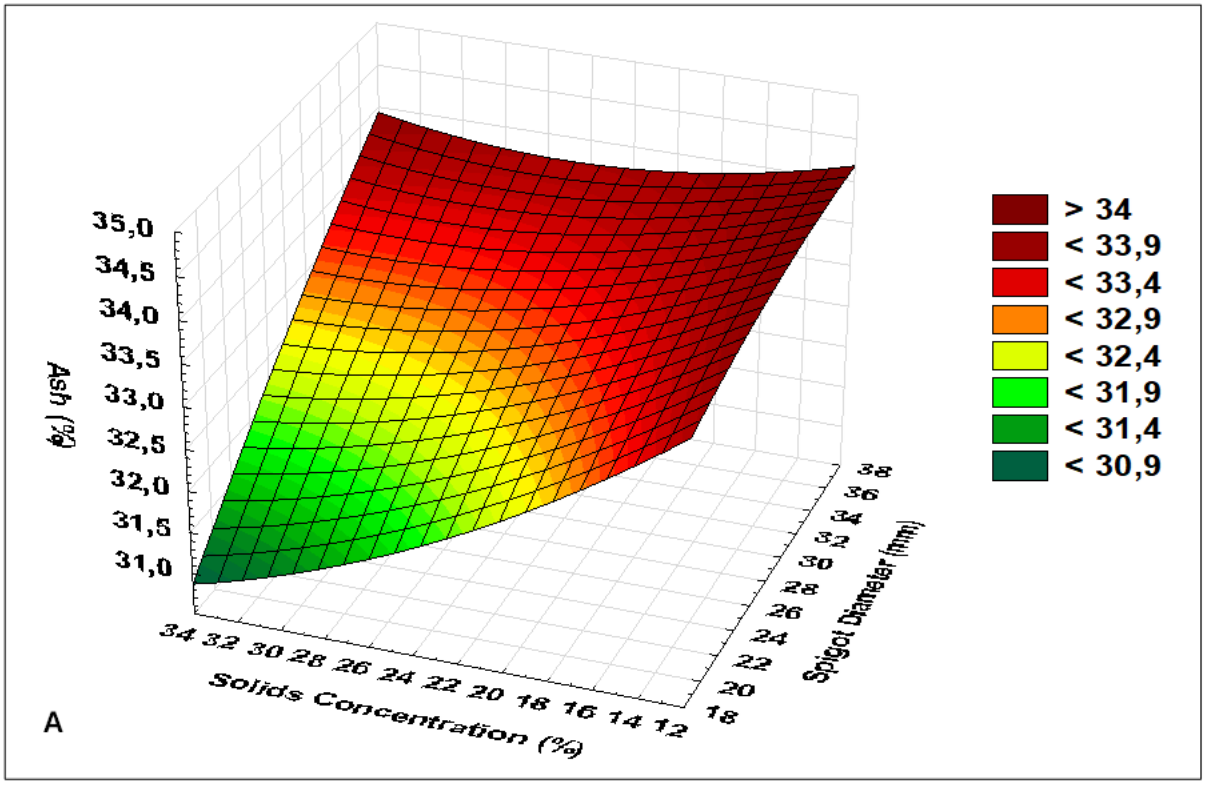
Ash (%)
35,0
34,5
34,0
33,5
33,0
32,5
32,0
31,5
31,0
34 32 30 28 26 24 22 20 18 16 14 12
Solids Concentration (%)
18 20 22 24 26 28 30 32 34 36 38
Spigot Diameter (mm)
> 34
< 33,9
< 33,4
< 32,9
< 32,4
< 31,9
< 31,4
< 30,9
A

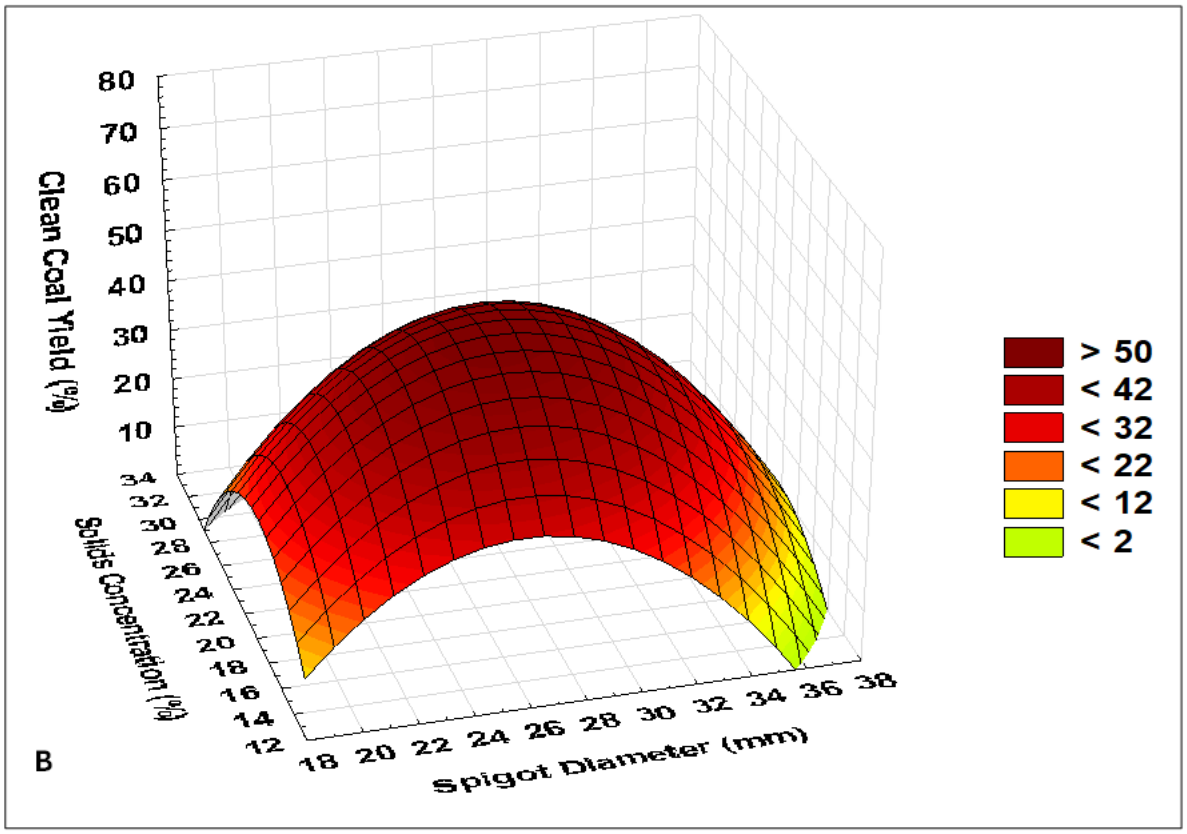
Clean Coal Yield (%)
80
70
60
50
40
30
20
10
34 32 30 28 26 24 22 20 18 16 14 12
Solids Concentration (%)
18 20 22 24 26 28 30 32 34 36 38
Spigot Diameter (mm)
> 50
< 42
< 32
< 22
< 12
< 2
B

Figure 36: Flat-bottom cyclone 3D surface response plot of the interaction effect of the solids concentration and the spigot diameter on the ash content (A) and clean coal yield (B)

However, a low coal yield was also observed at a spigot diameter of 16 mm, as shown in Figure 36B (highlighted in warm orange hues). Undersized spigot diameters restrict the underflow stream, leading to pressure buildup within the flat-bottom cyclone. This increases the density of the underflow stream and periodically overloads the lower cone section with solids (Izquierdo et al., 2023). According to Sanders (2007), surging can cause low-density particles to report to the underflow, leading to poor separation efficiency.

4.2.2 Effect of Solids Concentration and Vortex Finder Diameter

This study investigated the combined effects of feed solids concentration and vortex finder diameter on coal ash content and yield, using a 100 mm flat-bottom cyclone with a 25 mm spigot diameter. Figure 37A and B show the developed three-dimensional (3D) response plots illustrating the interaction effects of solids concentration and vortex finder diameter on ash content and coal yield, respectively. As shown in Figure 37A, ash content decreased from 34.5% to 31.7% as the solids concentration increased from 12% to 32%. This is indicated by the colour shift from a bright red at a maximum ash content of 34.5% to a dark green colour at an ash content of 31.7%.

The observed trends can be attributed to the minimal particle-to-particle interactions occurring at low solids concentrations, leading to the predominance of the free-settling regime within the flat-bottom cyclone. Effective density-based separation in the flat-bottom cyclone requires the establishment of an autogenous medium, which necessitates a dominant hindered-settling regime. As noted by Wills and Finch (2016), hindered settling becomes significant when the solids concentration exceeds 15% by weight. This explains why the ash content decreases as the solids concentration increases in Figure 37A. At low solids concentrations, the separation efficiency decreases, resulting in poor density-based separation and elevated ash content in the coal.

Figure 37B shows that the coal yield increased from 11.44% to 61.22% as the vortex finder diameter expanded from 26 mm to 41 mm. This is indicated by the change in colour gradient from light green to an intense red. A wider vortex finder diameter creates an oversized air core, reducing short-circuit flow distance. This promotes the misplacement of a larger proportion of the coal feed, bypassing density-based separation, into the overflow stream. The observed trend in clean coal yield aligns with findings reported by Su and Zhang (2022) and Maharana and Suresh (2020).

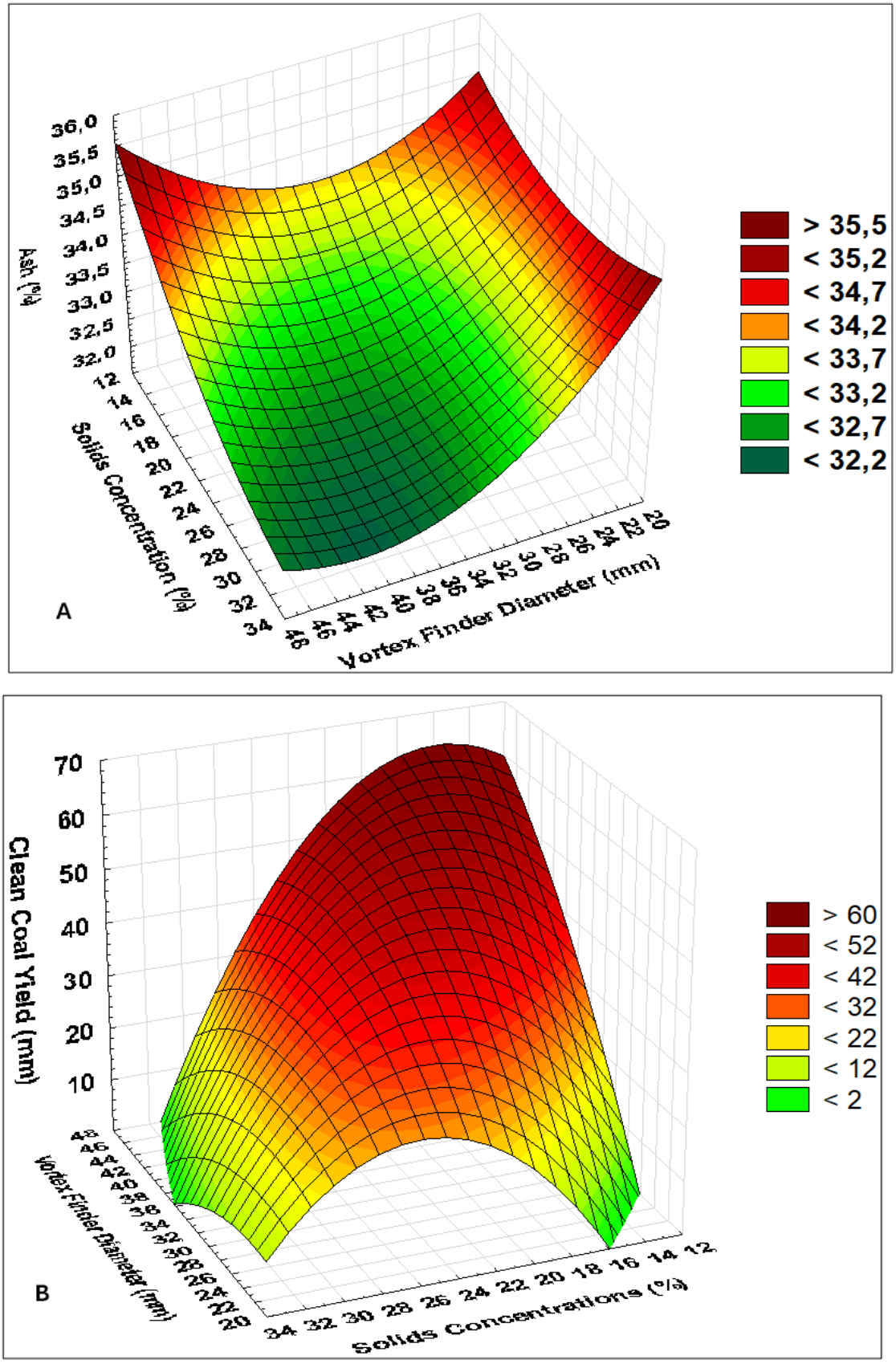

Figure 37: Flat-bottom cyclone 3D surface response plot showing the Interaction effect of the solids concentration and the vortex finder diameter on the ash content (A) and clean coal yield (B)

4.2.3 Effect of Vortex Finder Diameter and Spigot Diameter

The investigation focused on the combined influence of a spigot diameter and vortex finder diameter on ash content and coal yield at a constant feed solids concentration of 23% in a 100 mm diameter flat-bottom cyclone. Figure 38A and B show the developed three-dimensional (3D) response plots illustrating the interaction effects of the spigot diameter and the vortex finder diameter on ash content and coal yield, respectively. Figure 38A shows that reducing the spigot diameter from 35 mm to 16 mm results in a decrease in the ash content from 34.4% to 31.7%. This is indicated by a colour shift from red to green.

Figure 38B indicates that decreasing the spigot diameter from 35 mm to 25 mm results in an increase in coal yield from 16.4% to 59%. The maximum coal yield is achieved at a spigot diameter of 26 mm, as indicated by the intense red colour. As outlined in section 4.2.1, an increase in the spigot diameter results in an increase in the mass split of coal feed, that has not undergone density-based separation, directed to the underflow stream. This leads to a reduction in the proportion of clean coal particles recovered to the overflow. This could be the reason behind the observed trend in the flat-bottom cyclone. The observed trends in coal yield and ash content are consistent with findings by Hacifazlioglu (2012c) and Hembrom and Suresh (2018).

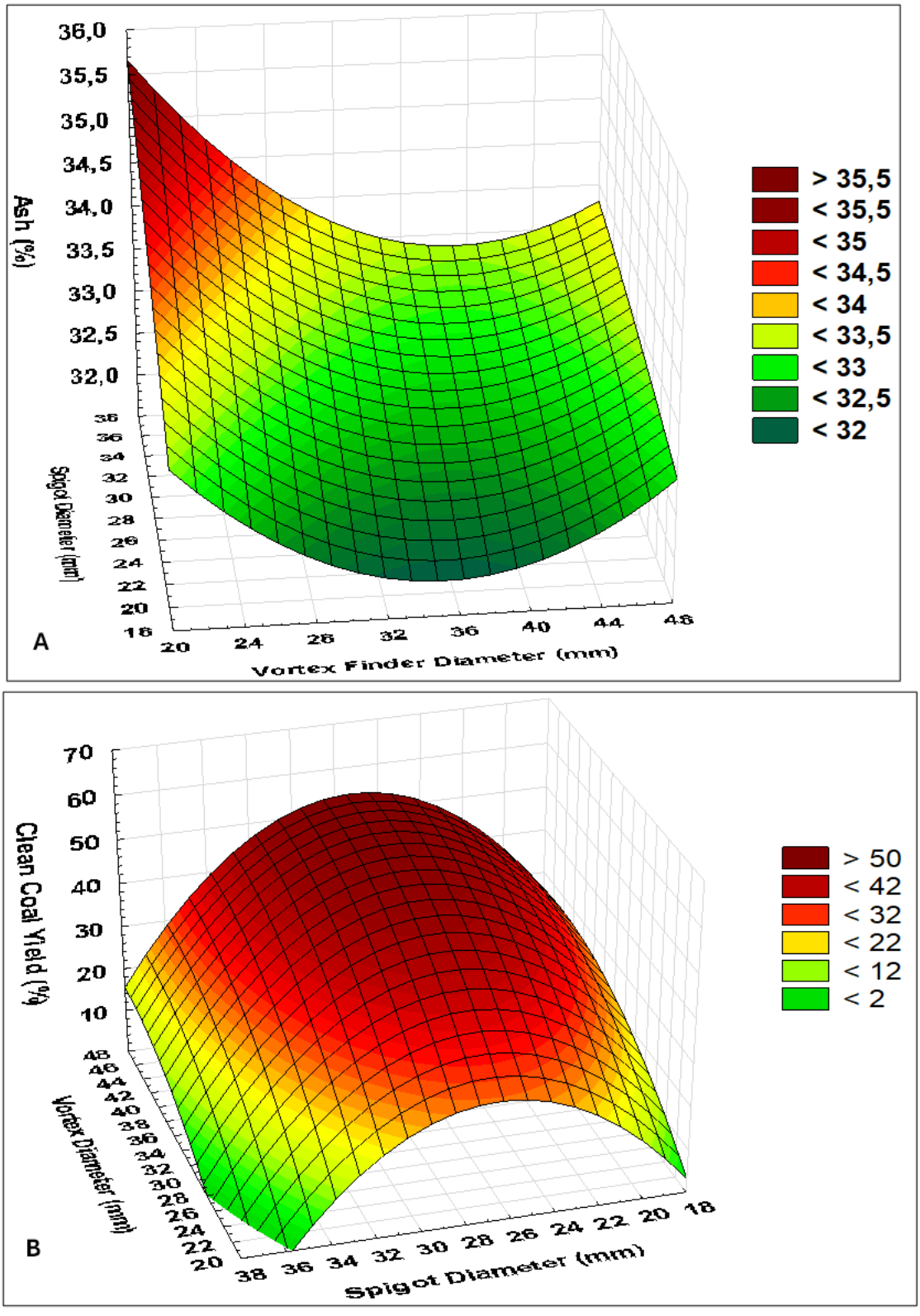

Figure 38: Flat-bottom cyclone 3D surface response plot showing the Interaction effect of the spigot diameter and the vortex finder diameter on the ash content (A) and clean coal yield (B)

4.2.4 Performance Analysis: Particle Size Distribution

The observed change in the ash content of the coal in the overflow stream was minimal, it ranged from 34.4% to 31.7% (see Appendix B). This outcome may be attributed to the limited efficiency of the flat-bottom cyclone in separating coal primarily based on density rather than size. Consequently, additional particle size distribution analyses were conducted to investigate the underlying mechanisms responsible for these experimental outcomes. The particle size analysis data was used to generate partition curves to evaluate the extent to which separation of the coal in the flat-bottom cyclone is size-based.

Figure 39 shows the corrected partition curves developed for the selected tests for experiments, corresponding to the spigot-to-vortex finder diameter and solids concentration ratios detailed in Table 20. The corrected partition curves were modelled using the Reid-Plitt equation. These experimental conditions were selected to represent the extremes of the design variables, as they demonstrated the most desirable impact on ash reduction in the flat-bottom cyclone.

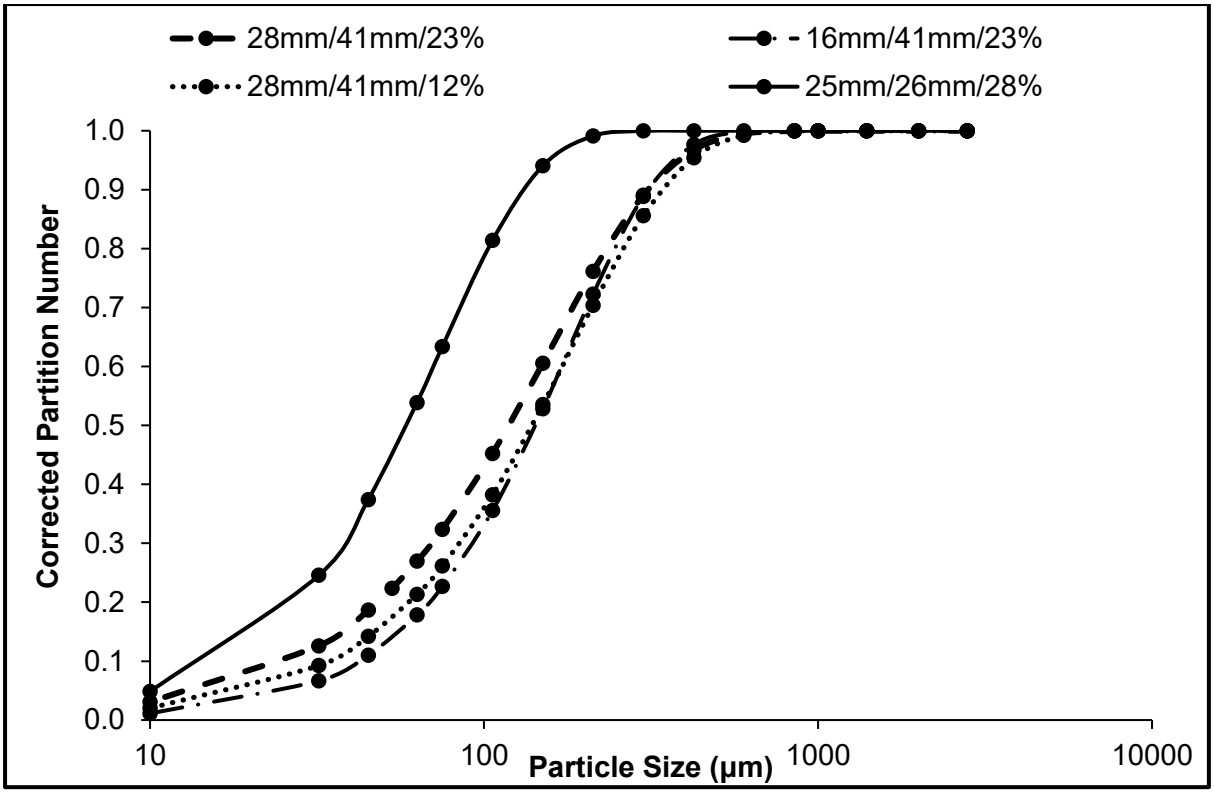

Figure 39: Partition curves for FBC tests performed at different operating conditions

The properties of the partition curves for the selected tests are given in Table 21. All the partition curves in Figure 39 have steep gradients, indicating sharp separation, which is further supported by the low E_{pm} values ranging from 0.03 to 0.08, in Table 21. Lower E_{pm} values signify higher classifier separation efficiency which corresponds to steep slopes around the cut-size region.

Table 20: Operating conditions of selected FBC experiments for particle size analysis

Experiment ID	Vortex Finder Diameter (mm)	Spigot Diameter (mm)	Solids Concentration (%)
2	26	25	28
11	41	16	23
13	41	28	12
17	41	28	23

The flat-bottom cyclone cut size, d_{50c} obtained from the partition curves ranged from 58 to 142 µm. For coal feed with a wide particle size distribution and most particles above 300 µm, the d_{50c} values observed in the selected flat-bottom cyclone experiments suggest a significant portion of ultrafine coal reports to the overflow during separation. Ultrafine coal is coal particles with a particle size less than 250 µm (Ramudzwagi, Tshiongo-Makgwe & Nheta, 2020).

Reported experimental data in Table 17 showed that the ultrafine coal fraction in the bulk coal has the highest ash content, as discussed in Section 4.1.3. This may explain the limited reduction in ash content observed in the coal recovered to the overflow. Therefore, the experimental dataset suggests that the flat-bottom cyclone primarily classified particles by size rather than by density. A similar trend has been observed in a study by Pyka and Wierzchowski (2022) on fine coal with a top size of 6 mm in a 300 mm flat-bottom cyclone.

These findings also agree with the work of Majumder and Barnwal (2011) and Hacifazlioglu (2012) who reported that separation in water-only or flat-bottom cyclones was primarily influenced by particle size rather than density. This mechanism results in ultrafine coal with high ash content reporting to the overflow, while the underflow exhibits a lower ash content. Comparable trends were observed in this study, with summarised ash content data provided in Appendix B.

Table 21: Size-based flat-bottom cyclone separation performance analysis

Experiment ID	E_{pm}	D_{50c} (µm)
2	0.03	58
11	0.07	142
13	0.08	139
17	0.07	119

4.2.5 Prediction Response Model

The experimental data of the flat bottom cyclone experiment were utilised to formulate a multivariable polynomial equation, that predicts the ash content (y_{ash}, %) in the

product coal and the coal yield (y_{yield}, %). The key variables include the vortex finder diameter (x_1, mm), spigot diameter (x_2, mm), and feed solids concentration (x_3, %). These mathematical regression models facilitate the determination of optimal design parameters for minimising ash content while maximising coal yield in the FBC. The CCRD approach taken is based on the polynomial equation 28:

$$y = (b_o + \varepsilon) + \sum_{i=1}^{3} b_i x_i + \sum_{i=1}^{3} b_{ii} {x_i}^2 + \sum_{i=1}^{3}\sum_{j=1}^{3} b_{ij} x_i\, x_j \qquad 28$$

The experimental data was statistically analysed using Statistica 12 and Design Expert Software. Statistical tests for model significance, analysis of variance (ANOVA), coefficient of variation, lack-of-fit, and predicted multiple regression coefficients, pure error and corrected total were computed to compare and choose a statistically significant model.

Pure error is the portion of residual variation arising from replicated observations at identical parameter levels, reflecting inherent variability under constant experimental conditions. Corrected total represents the total variation in the response variable after removing the effect of the overall mean, serving as the benchmark against which model and residual variation are compared.

4.2.5.1 Ash Content

An analysis of variance and a test of significance (see Table 22) was conducted to evaluate the model fit. The evaluation used the F-value and the P-value statistic with X_1, X_2 and X_3 and treatments of variables combination of these variables were inputs shown in Table 22. Several permutations were tried, and the final model is presented in equation 29.

Table 22: Flat-bottom cyclone ANOVA and test significance analysis for the ash content response model

Source	Regression coefficients	Sum of Squares	Degrees of Freedom	Mean Square	F-value	P-value

Model	**-**	9.19	4	2.30	13.28	< 0.0001*
Intercept	27.5	-	-	-	-	-
X_1	0.15	2.78	1	2.78	16.05	0.001*
X_2	0.06	1.67	1	1.67	9.64	0.007*
X_3	0.27	0.9926	1	0.99	5.74	0.03*
X_1X_3	-0.01	1.69	1	1.69	9.75	0.007*
Residual	-	2.59	15	0.17	-	-
Lack of Fit	-	1.96	9	0.22	2.04	0.2
Pure Error	-	0.64	6	0.11	-	-
Cor Total	-	11.78	19	-	-	-

Significant*

The developed model had a P-value of less than 0.0001 and an F-value of 13.28, indicating statistical significance since the P-value is below 0.05. According to Quanhong and Caili (2005), a P-value less than 0.05 suggests that the model term has a statistically significant impact on the response variable, while a larger F-value represents a stronger overall effect, which indicates that the response model is adequate and valid. The F-value statistic is computed at the probability of less than 0.05.

The independent variables: vortex finder diameter (x_1), spigot diameter (x_2), solids concentration (x_3) and the interaction model term, vortex finder diameter and solids concentration, (x_1x_3), all have P-values below 5% (0.001, 0.007, 0.03, and 0.007, respectively) and large F-values (16.05, 9.6, 5.74 and 9.75, respectively). The lack of fit P-value of the regression model is 0.2 showing it is not statistically significant. This shows that the model is valid and is a good fit. Consequently, the regression model equation is as follows:

$$y_{ash} = 27.5 + 0.15x_1 + 0.06x_2 + 0.27x_3 - 0.01x_1x_3 \quad (29)$$

The ash content data predicted by the chosen regression model was compared against the actual experimental data on a parity plot in Figure 40. A parity plot was constructed to show the correlation between the observed and predicted data points. The plot showed a satisfactory correlation, as most data points closely align with or cluster along the diagonal line.

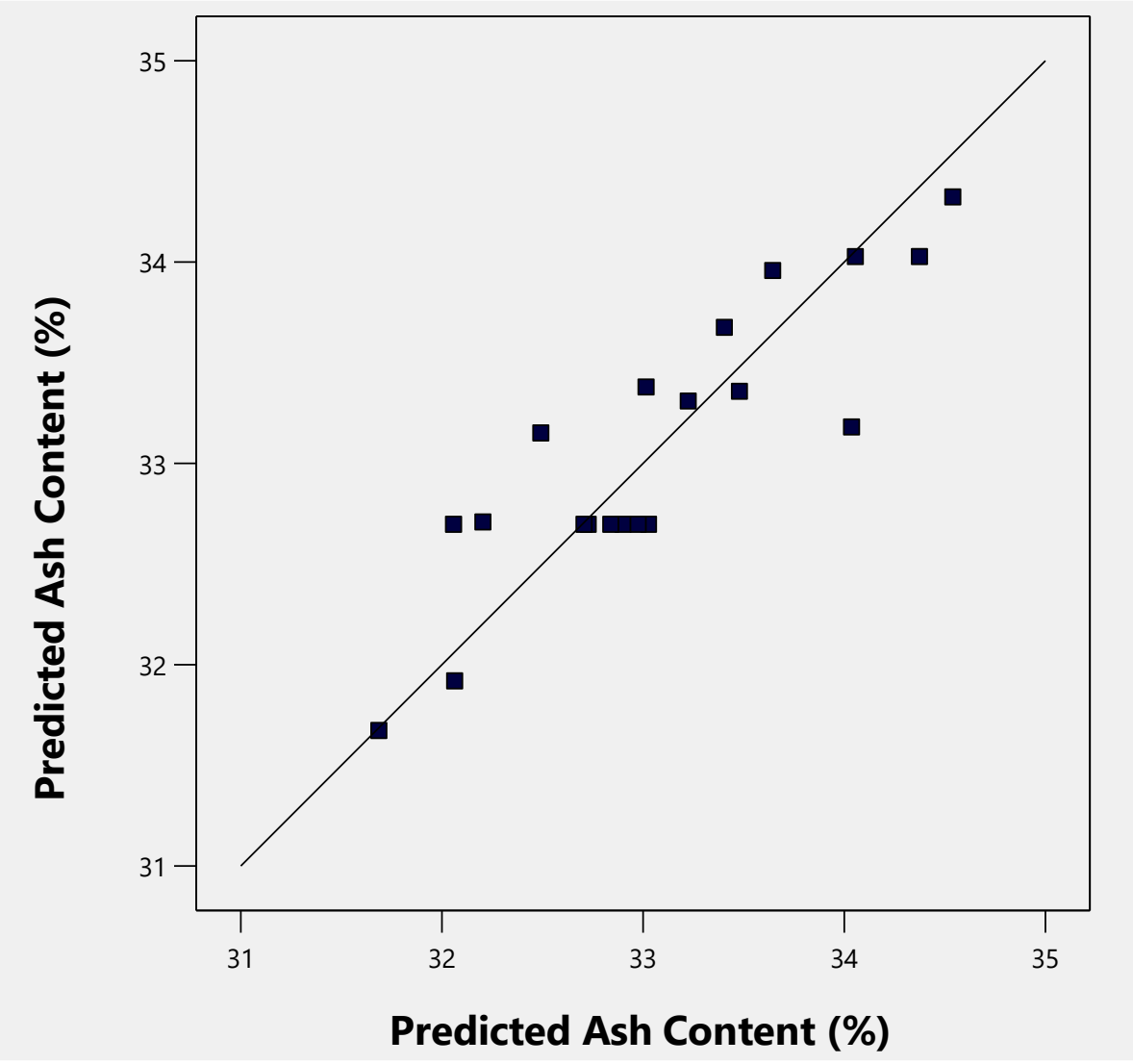

Figure 40: Parity plot showing experimental and predicted values for ash content in the flat-bottom cyclone

Figure 41 shows the residuals against the predicted ash content plot. Residuals are the difference between the actual experimental ash content data point and the ash content predicted by the response model. The residuals show a random distribution

around the y = 0 axis, with no discernible pattern. This shows that the regression model has no discernible bias.

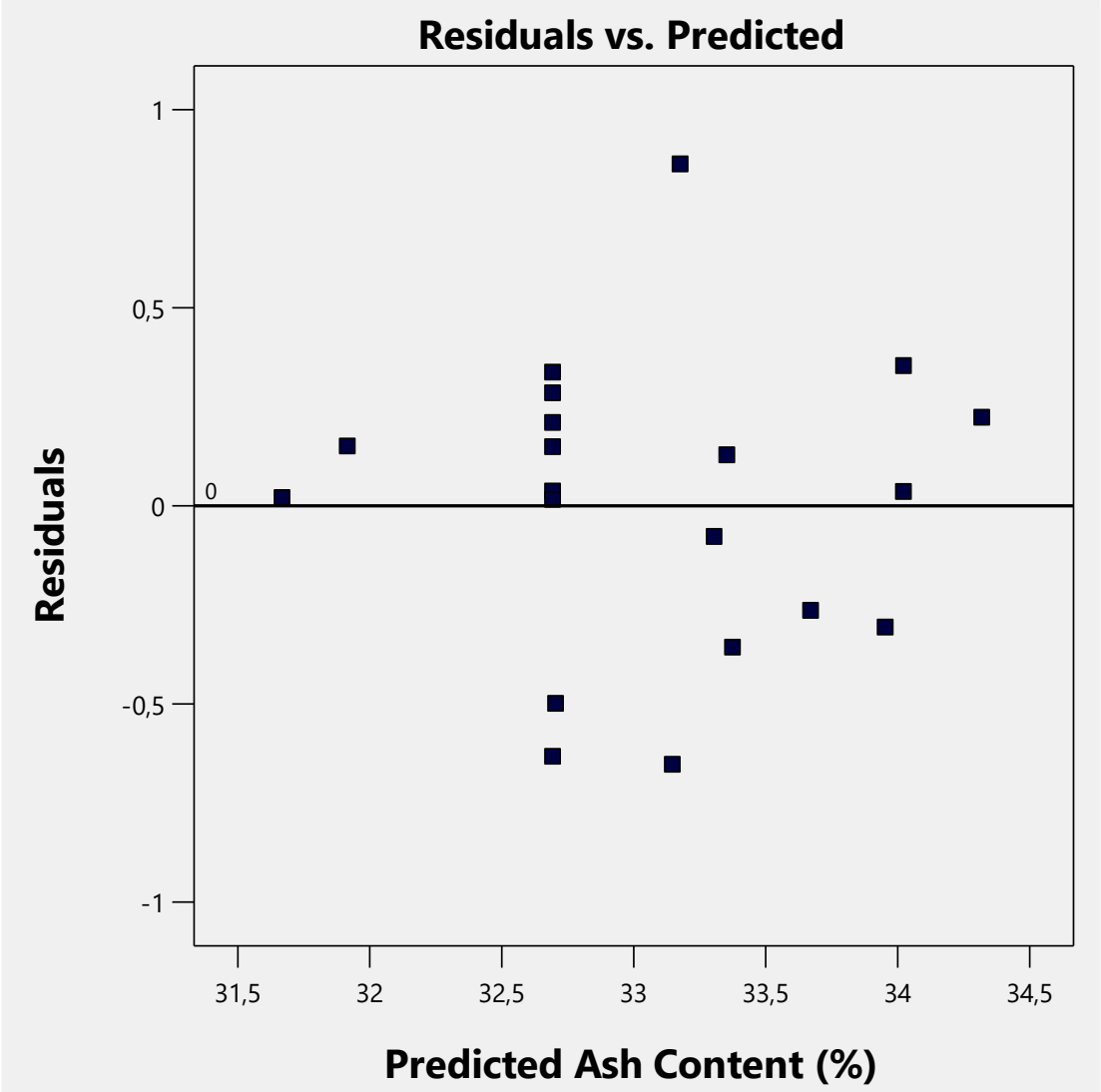

Figure 41: Plot of residuals for the developed model and the observed experimental data for the flat-bottom cyclone ash content model

The model has an R^2 value of 0.78. This suggests that 78% of the variation in the experimental response is explained by the spigot diameter, vortex finder, feed solids concentration, and their interaction effect. The adjusted R^2_{adj} value of the model is 0.72, which is 0.06 less than the R^2 value. This demonstrates a high degree of model accuracy, further supporting the reliability and significance of the developed response model.

4.2.5.2 Clean Coal Yield

An empirical regression model for predicting the response coal yield produced by the flat bottom cyclone was developed. X_1 represents the vortex finder diameter, X_2 the spigot diameter, and X_3 the feed solids concentration. An ANOVA was conducted to evaluate the fit of the model.

Table 23: FBC ANOVA and test significance for the coal yield response model

Source	Regression Coefficient	Sum of Squares	Degrees of Freedom	Mean Square	F-value	P-value
Model	-	6281.80	11	571.07	33.57	< 0.0001*
Intercept	508	-	-	-	-	-
X_1	5.33	242.72	1	242.72	14.27	0.0054*
X_3	-8.27	271.13	1	271.13	15.94	0.0040*
X_1X_2	-12.6	983.24	1	983.24	57.79	< 0.0001*
X_1X_3	-6.37	267.64	1	267.64	15.73	0.0041*
X_2X_3	6.90	215.78	1	215.78	12.68	0.0074*
X_1^2	-8.35	230.49	1	230.49	13.55	0.0062*
X_2^2	-9.98	1756.97	1	1756.97	103.27	< 0.0001*
X_3^2	-7.20	698.44	1	698.44	41.05	0.0002*
$X_1X_2\ X_3$	10.57	254.55	1	254.55	14.96	0.0048*
$X_1^2\ X_2$	-16.16	1609.01	1	1609.01	94.57	< 0.0001*
$X_1^2\ X_3$	8.16	162.98	1	162.98	9.58	0.0148*
Residual	-	136.11	8	17.01	-	-
Lack of Fit	-	78.39	2	39.20	4.07	0.0763
Pure Error	-	57.72	6	9.62	-	-
Cor Total	-	6417.91	19	-	-	-
				Significant*		

The ANOVA in Table 23 shows that the clean coal yield regression model and all model terms have a P-value less than 0.05 and hence are significant. Additionally, the model has a p-value of 0.0001 and a lack of fit p-value of 0.076. This shows that the model is statistically significant. The regression model has a goodness of fit R^2 value of 0.93 and an adjusted R^2_{adj} value of 0.87. All model terms have an F-value greater than 0.05. The large F-value represents a stronger overall effect, which indicates that

the model is valid. Several permutations were tried, and the final model is presented in equation 30:

$$y_{yield} = 508 + 5.33x_1 + 8.27x_3 - 8.35{x_1}^2 - 9.98{x_2}^2 - 7.20{x_3}^2 - 12.6x_1x_2 - 6.37x_1x_3 + 6.90x_2x_3 + 10.6x_1x_2x_3 - 16.2{x_1}^2x_2 + 8.16{x_1}^2x_3 \quad (30)$$

Figure 42 shows a plot of the actual coal yield against the predicted coal yield. The parity plot indicates a good agreement between the predicted ash content values against the actual experimental data. The data points are close to the diagonal line and have a positive correlation.

Figure 43 presents the residuals plotted against the predicted ash coal yield. It shows that the model has noticeably higher residuals when compared to the ash content model for the same FBC. However, the residuals are randomly clustered along the y=0 line and shows no discernible pattern. This indicates that the model is statistically significant and has no bias. However, the presence of an outlier in the plot could be indicative of a measurement or data capturing error during the testwork.

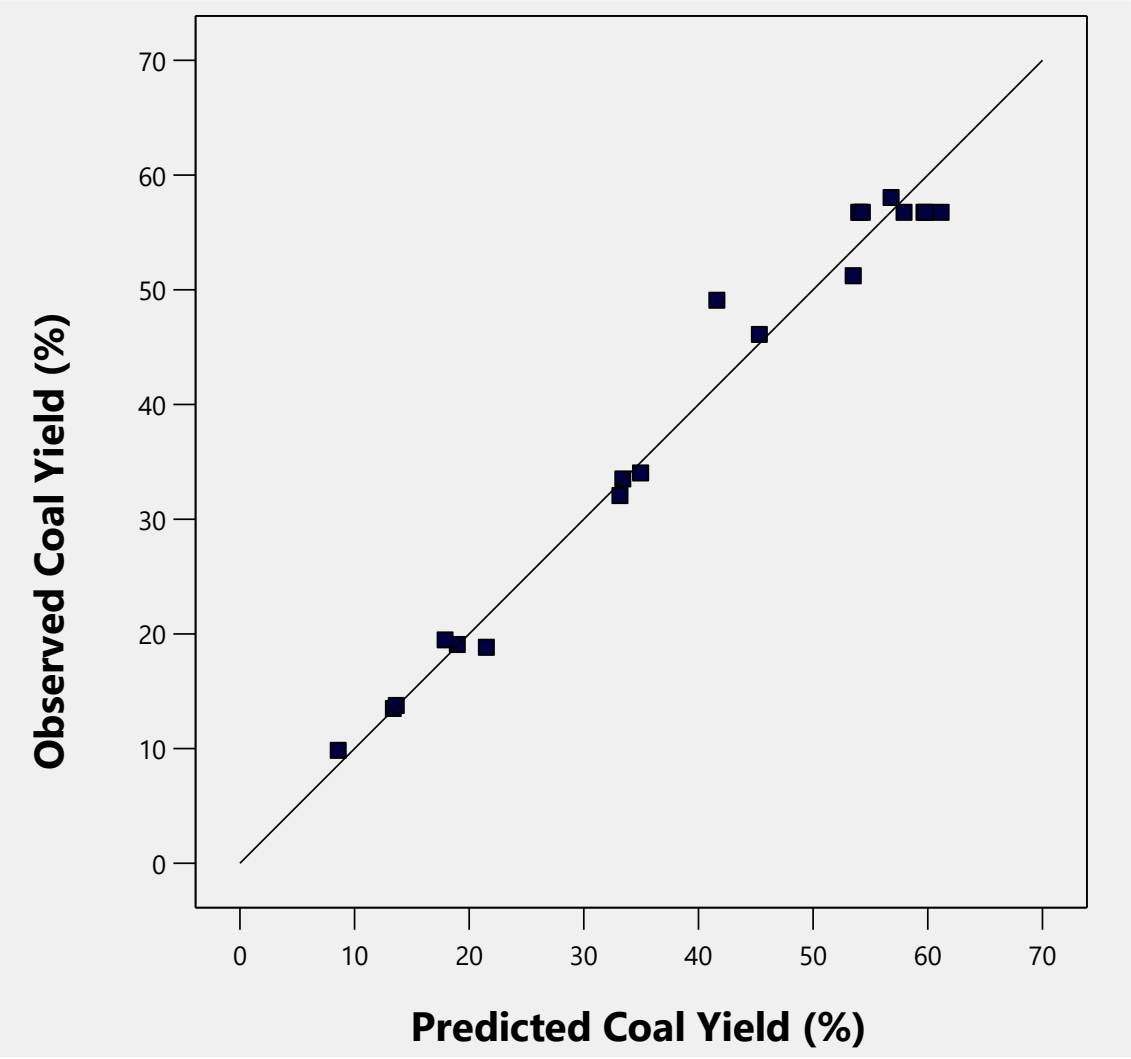

Figure 42: Parity plot showing experimental and predicted values for achievable coal yield in the flat-bottom cyclone

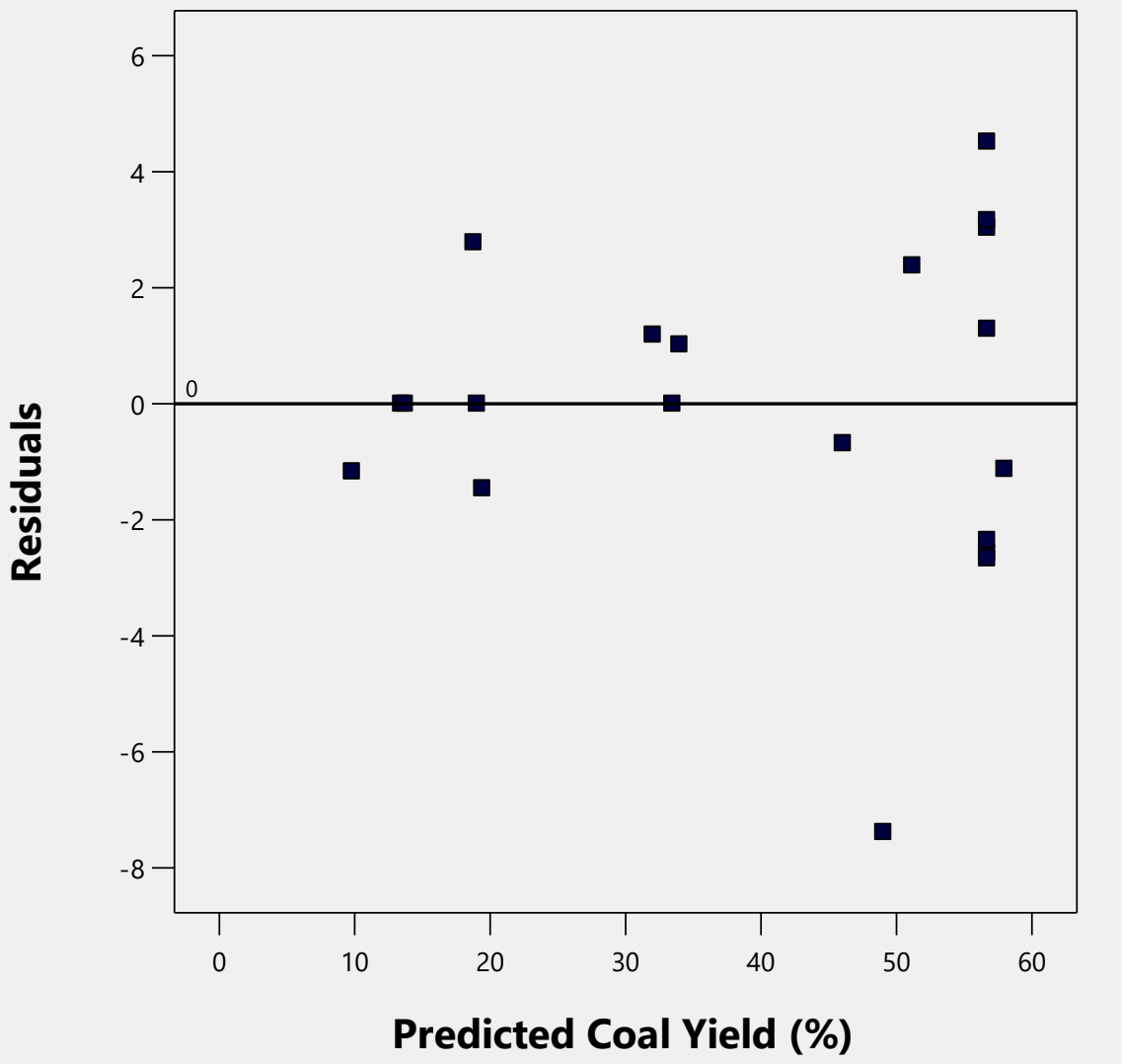

Figure 43: Plot of residuals for the developed model and the observed experimental clean coal data in flat-bottom cyclone

4.3 Dense Medium Cyclone Experiments

Dense medium cyclone tests were conducted to evaluate the effects of spigot diameter, vortex finder diameter, and medium density on separation performance, as well as the quality and quantity of coal recovered to the overflow. Three-dimensional (3D) response plots were developed to show the combined effect of the three variables on the ash content and coal yield.

4.3.1 Effect of Medium Density and Spigot Diameter

This study investigated the combined impact of separating medium density and spigot diameter on ash content and clean coal yield, with the vortex finder diameter fixed at 34 mm. Figure 44A and B shows the three-dimensional (3D) response plots depicting the interaction effects between the spigot diameter and separating medium density on coal yield and ash content , respectively. Figure 44A shows that as the spigot diameter increases from 16 mm to 30 mm, the coal yield decreases from 81% to 41%. This trend is visually represented by a shift in colouration, transitioning from bright red at 81% yield to dark red at 41%.

As discussed in section 4.2.1, enlarging the spigot diameter increases the mass split of coal feed directed to the underflow stream. This leads to a reduction in the proportion of feed recovered to the overflow. This could potentially explain the trend observed in the experimental dataset. Furthermore, it agrees with the findings reported by Sahu, Chaurasia and Suresh (2019a). They studied the effect of the SPD in a 76 mm diameter dense medium cyclone at a VFD of 33 mm. The coal yield decreased from 35% at a spigot diameter of 18 mm to around 30% at a spigot diameter of 22 mm.

Figure 44B illustrates that ash content decreases as the separating medium density increases. The lowest ash content was observed at a medium density of 1450 kg/m³, represented by the dark green colouration. However, as noted in Section 4.1.4, the ash content in the recovered coal increases with higher washing specific gravity. These findings contradict those of Sahu, Chaurasia, and Suresh (2019a), who reported that ash content increased with rising medium density for all spigot diameters tested (16, 25, and 35 mm) in a 76 mm diameter cyclone. The coal that was used in their study had a top size of 3 mm, 2% of the bulk coal had a density of less than 1300 kg/m³ and a magnetite-to-coal ratio of 5.

The observed trend can be attributed to the composition and inherent properties of the feed coal and the magnetite-to-coal ratio of 4 employed in this study. As discussed under section 4.1.4, the float-and-sink test dataset shows that only 2.15% of the bulk coal possesses a density of 1300 kg/m³ or lower. During separation at low medium densities, the mass split of the coal feed to the overflow is low. This creates an underflow stream with a high solids concentration and density, while the overflow

stream becomes highly diluted. This creates a pronounced density differential between the overflow and underflow streams of the dense medium cyclone, destabilising the separating medium. This reduces the separation efficiency of the dense medium cyclone. The detrimental impact of a pronounced underflow and overflow density difference on medium stability has also been documented in the findings of He and Laskowski (1995).

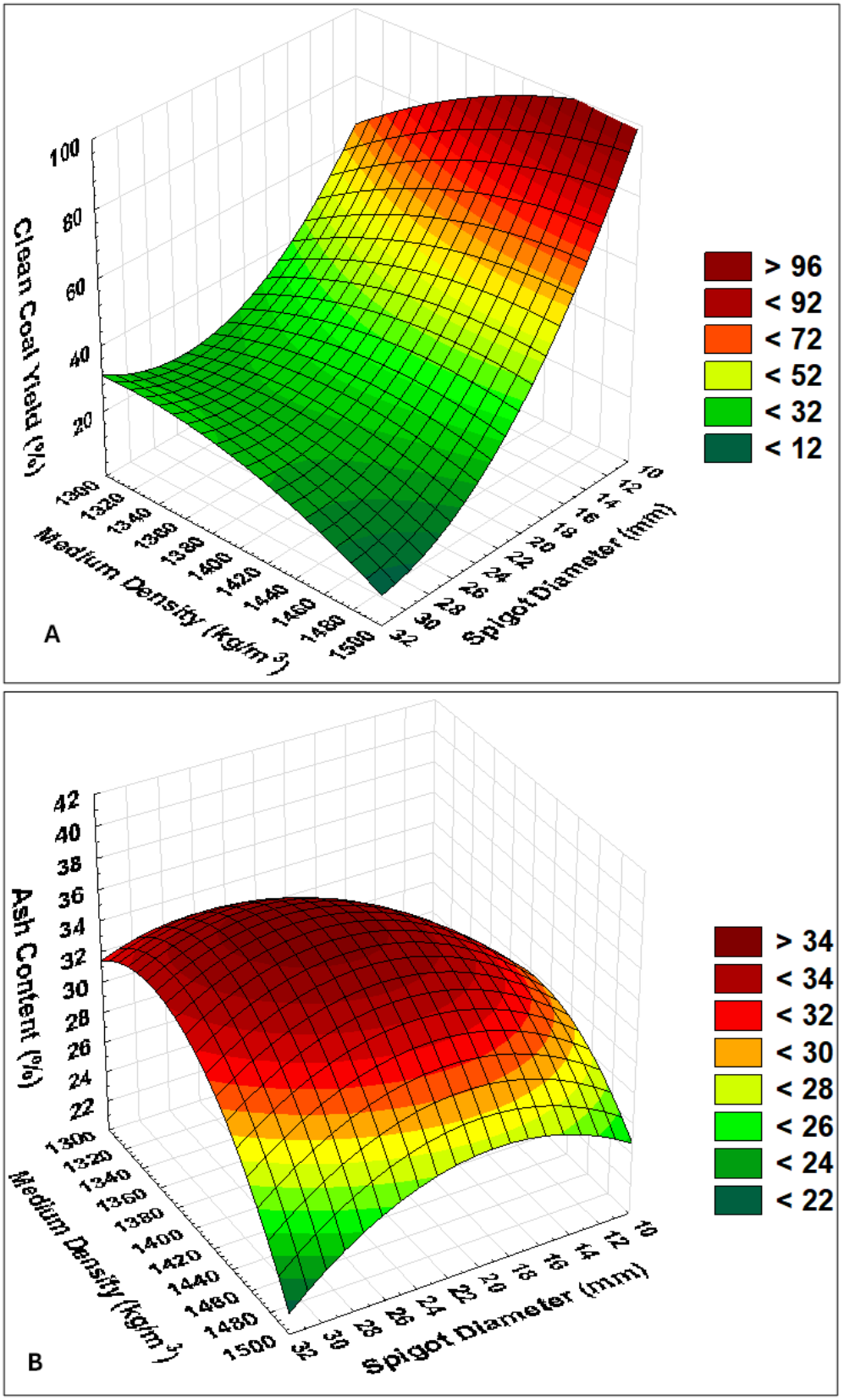

Figure 44: Dense medium cyclone 3D surface response plot showing the Interaction effect of the spigot diameter and the separating medium density on the coal yield (A) and ash content (B)

4.3.2 Effect of Medium Density and Vortex Finder Diameter

The impact of the medium density and vortex finder diameter, measured at a fixed vortex finder diameter of 23 mm, on coal quality and yield were investigated. Figure 45A and B show the developed three-dimensional (3D) response plots illustrating the interaction effects of the separating medium density and the vortex finder diameter on coal yield and ash content, respectively. It was observed that as the vortex finder diameter and the separating medium density increased, the coal yield increased in Figure 45A. A peak coal yield of 43% was observed at the maximum spigot diameter of 41 mm, which is highlighted by the intense red colour. An increase in the vortex finder diameter results in an increase in the fraction of the coal feed that reports to the overflow as discussed in section 4.2.2.

Figure 45B shows that when the vortex finder diameter decreases in size from the tested levels (30, 25 to 16 mm), the ash content decreases to a minimum of 23%. This is indicated by a dark green colour. Conversely, a larger vortex finder diameter leads to higher ash content in the overflow stream. This increase can be attributed to the increase in the short-circuiting of the feed to the overflow before undergoing separation by density. Therefore, high-density gangue particles are misplaced to the overflow. This results in an increase in the ash content of the overflow stream. The trend observed for the ash content aligns with the findings of Sahu, Chaurasia and Suresh (2019).

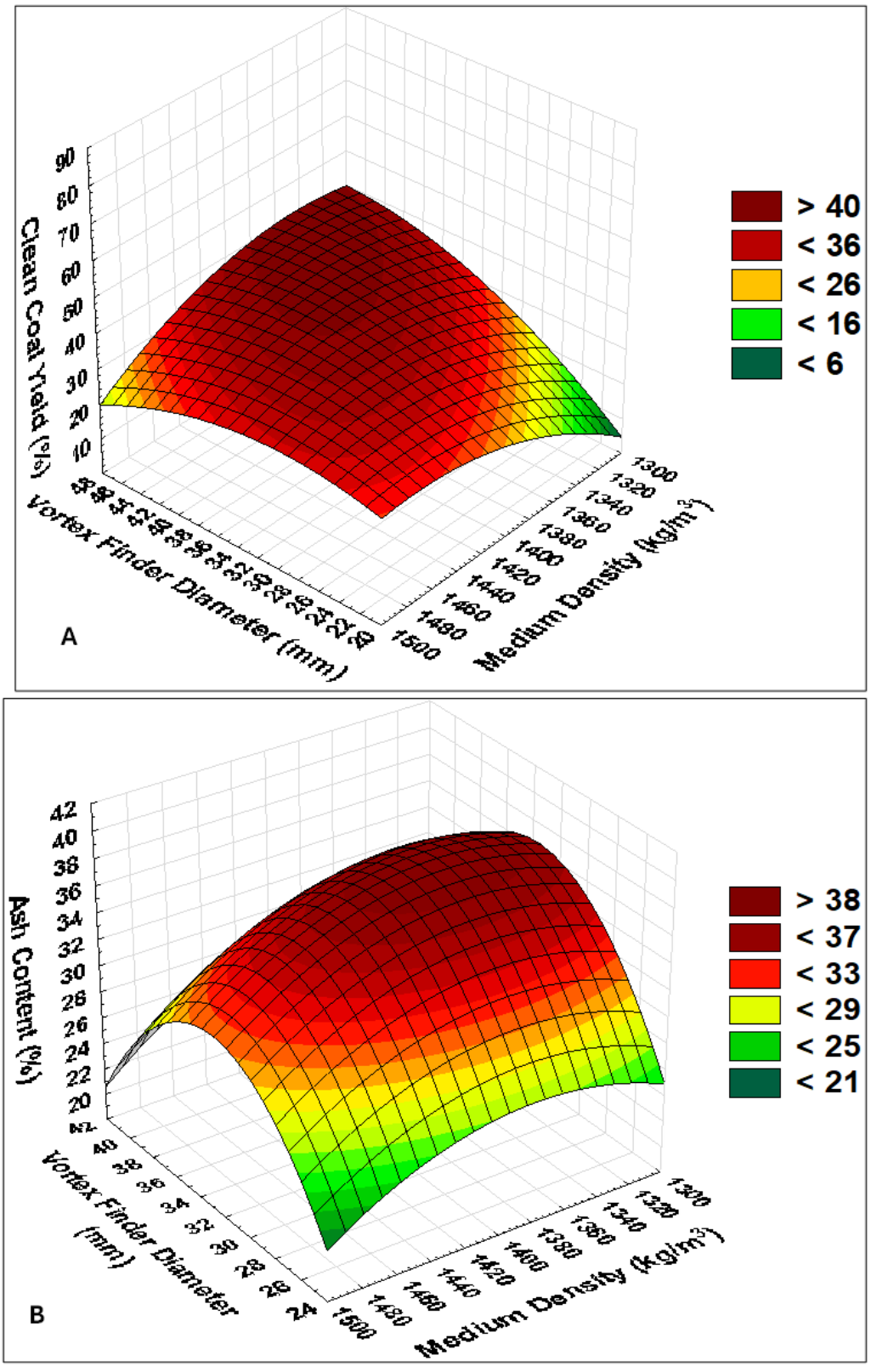

Figure 45: Dense medium cyclone 3D surface response plot showing the Interaction effect of the vortex finder diameter and the separating medium density on the coal yield (A) and ash content (B)

4.3.3 Effect of Vortex Finder Diameter and Spigot Diameter

The combined effects of vortex finder diameter and spigot diameter on the ash content and coal yield were analysed at a fixed medium density of 1400 kg/m^3. Figure 46A and B present the three-dimensional (3D) response plots depicting the interaction effects between the spigot diameter and vortex finder diameter on coal yield and ash content, respectively.

It was observed in Figure 46A that increasing the spigot diameter from 23 mm to 35 mm results in a decrease in coal recovery to the overflow from 55% to 35%. This is indicated by the change in the colour from an intense red at high coal yield to a dark green colour at low levels of coal yield recovered at the overflow. A maximum coal yield of 55% was observed at a spigot diameter of 23 mm. A wider spigot diameter increases the mass fraction of coal feed directed to the underflow, reducing the proportion of clean coal recovered to the overflow.

Figure 46B shows that the ash content increased as the vortex finder diameter increased from 26 to 34 mm. This is reflected in the colour shift from dark green, indicating a low ash content of approximately 26% at a spigot diameter of 26 mm, to an intense red at 34 mm at a maximum ash content of 35%. This can be as a result of the increased short-circuiting of coal particles, including gangue particles, to the overflow. A larger vortex finder diameter generates an oversized air core, which diminishes separation efficiency by reducing the short-circuit flow distance, thereby increasing the likelihood of unseparated feed reporting to the overflow. The observed trend is in agreement with the findings reported by Su and Zhang (Su & Zhang, 2022b).

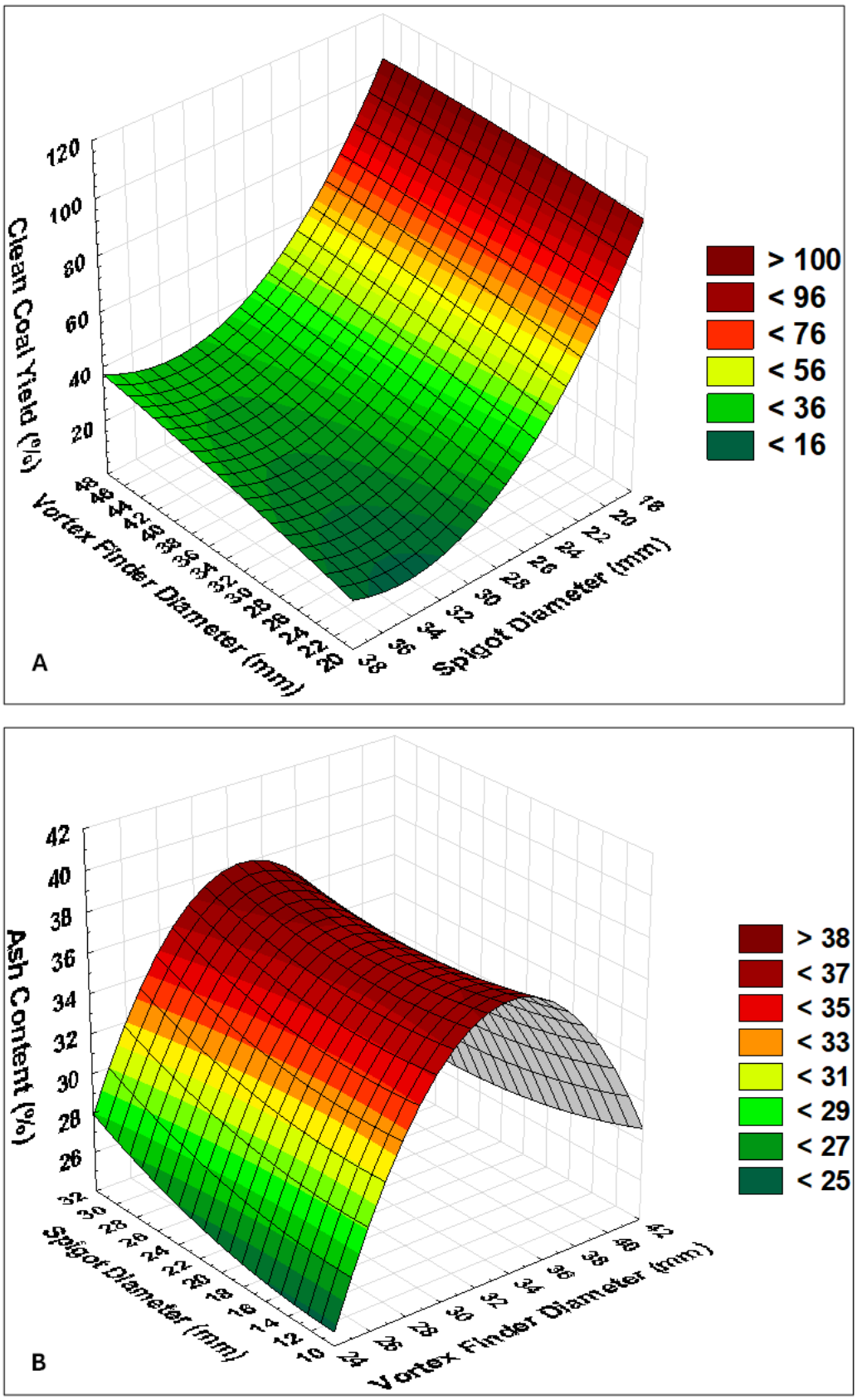

Figure 46: Dense medium cyclone 3D surface response plot showing the Interaction effect of the vortex finder diameter and the spigot diameter on the clean coal yield (A) and ash content (B)

4.3.4 Response Prediction Model

The dense medium cyclone experimental data was statistically analysed using Statistica 12 and Design Expert Software. Statistical tests for model significance, such as ANOVA, coefficient of variation, lack-of-fit, and predicted multiple regression coefficients, were computed to compare and choose a statistically significant model.

The regression model predicts the ash content (y_{ash}, %) and coal yield (y_{yield}, %) based on the independent variables: vortex finder diameter (x_1, mm), spigot diameter (x_2, mm), and relative medium density (x_3, %). These regression models assist in the determination of optimal design parameters for minimizing ash content while maximizing coal yield in the DMC.

4.3.4.1 Ash Content

Regression coefficients for the empirical response model were computed from the experimental data produced by the dense medium cyclone to predict ash content in the coal. The model fit was evaluated using ANOVA and significance tests, as shown in Table 24, with F-value and P-value statistic. The F-value tests were computed at the probability of less than 0.05 to determine the significance of the model and the model terms.

Table 24: ANOVA for the dense medium cyclone ash content response model

Source	Regression Coefficient	Sum of Squares	Degrees of Freedom	Mean Square	F-value	p-value
Model	-	286.39	3	95.46	21.21	< 0.0001*
Intercept	72.4	-	-	-	-	-
X_3	-26.9	24.26	1	24.26	5.39	0.034*
X_2X_3	-0.002	6.65	1	6.65	1.48	0.24
X_1^2	0.009	255.49	1	255.49	56.78	< 0.0001*
Residual	-	72	16	4.50	-	-
Lack of Fit	-	49.44	11	4.49	0.9964	0.54
Pure Error	-	22.56	5	4.51	-	-
Cor Total	-	358.39	19	-	-	-
Significant*						

The ANOVA analysis in Table 24 shows that the experimental coal ash content can be used to develop a regression model. The model has a p-value < 0.0001 which indicates that the model has a strong statistical significance and reliability. The relative medium density model term (X_3) and the quadratic vortex finder diameter model term (X_1) were also significant, with p-values of 0.034 and less than 0.0001, respectively. Several permutations were tried, and the final model is presented in equation 31:

$$y_{ash} = 72.4 - 26.9x_3 - 0.002{x_2}^2 + 0.009x_2x_3 \quad 31$$

The regression model has a lack-of-fit F-value of 0.996 and a p-value of 0.54, indicating that the lack of fit is nonsignificant (p > 0.05) relative to the pure error. This indicates that the model is reasonable and fits the experimental ash content data. A small p-value (< 0.05) suggests that the model term has a statistically significant impact on the response variable, while a larger F-value represents a stronger overall effect, which shows that the response model is valid (Quanhong & Caili, 2005).

The R^2 of the model is 0.8, with an adjusted R^2_{adj} of 0.76, demonstrating close agreement. The small difference (< 0.04) between these values indicates a strong model fit. R^2 values range from 0 to 1, where a value closer to 0 indicates a poor fit. A high R^2 value implies that the model effectively accounts for the variance in the response variables (Myers, Montgomery & Anderson-Cook, 2016).

A parity plot was used to show the correlation between the observed and predicted ash content data points. This data is presented Figure 47. The plot showed a satisfactory correlation, as the majority of data points closely align with or cluster around the diagonal line. Overall, this further supports that the mathematical model is reliable, it fits the response ash content experimental data.

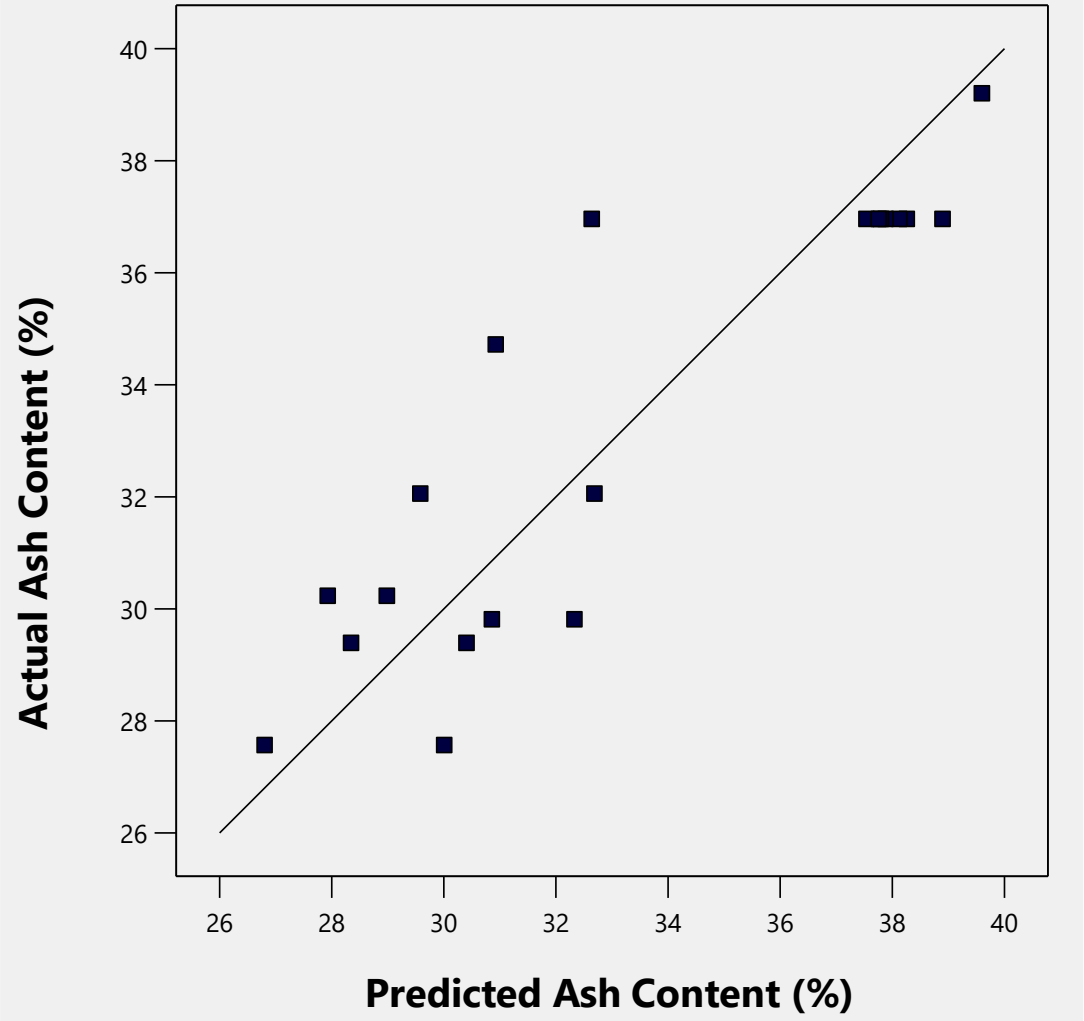

Figure 47: Parity plot showing experimental and predicted values for ash content in a dense medium cyclone

Figure 48 presents the residuals plotted against the predicted ash content. The model residuals are scattered in almost a pattern that follows a linear a negative correlation. This indicates that the model may have some degree of bias. However, after multiple tried permutations, this was the most statistically reliable model achievable. The model was selected based on its overall performance and tests of significance of key model terms.

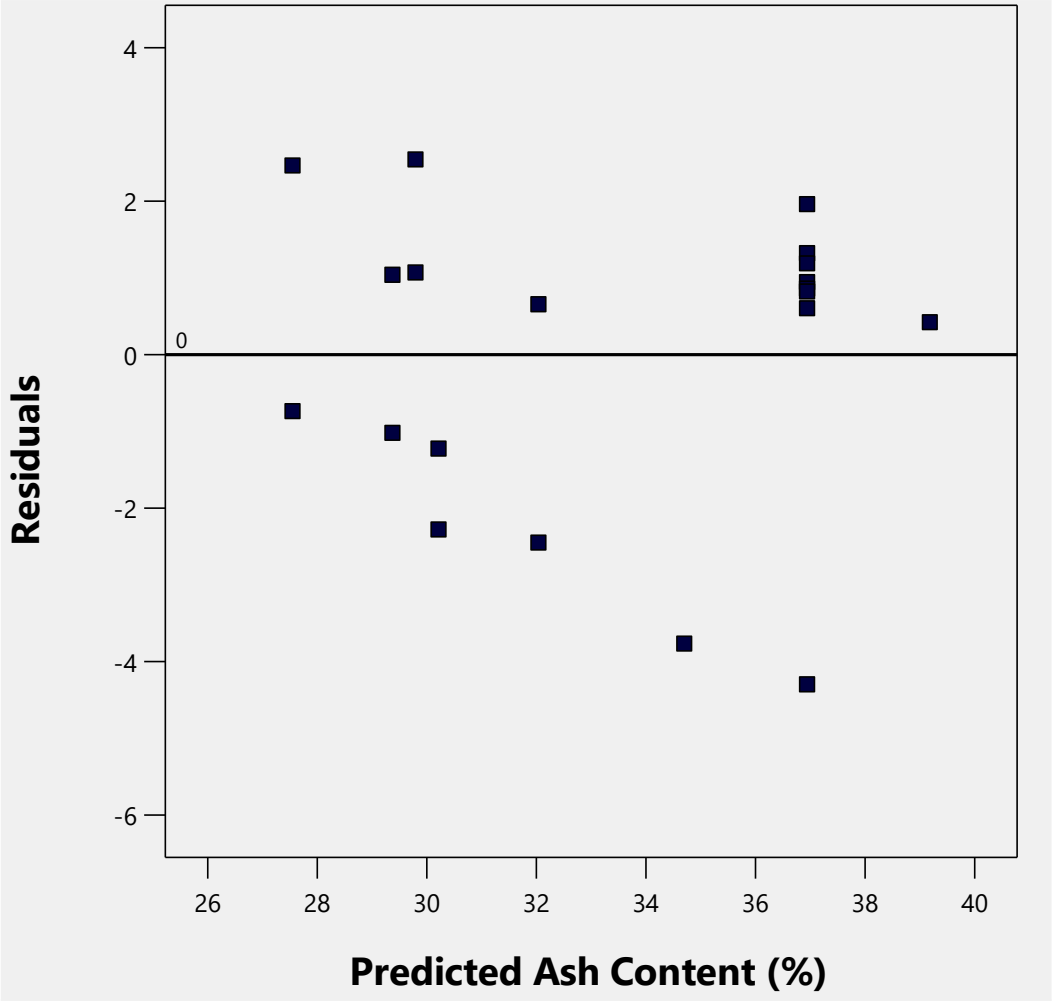

Figure 48: Residuals vs predicted ash content values in the dense medium cyclone

4.3.4.2 Clean Coal Yield

The experimental coal yield data was analysed to develop a response model using Statistica 12 and Design Expert Software. Table 25 shows the ANOVA analysis data of the developed mathematical model. Statistical significance, including tests for lack

of fit, p-values, and F-values were used to evaluate whether the mathematical model provides a good fit for the data.

Table 25: ANOVA for the coal yield response model for the dense medium cyclone

Source	Regression Coefficient	Sum of Squares	Degrees of Freedom	Mean Square	F-value	P-value
Model	-	4563.47	5	912.69	60.3	< 0.0001*
Intercept	81.6	-	-	-	-	-
X_1	6.0	148.38	1	148.38	9.8	0.007*
X_2	-11.3	2446.09	1	2446.09	161.6	< 0.0001*
X_2X_3	-0.1	185.9	1	185.9	12.3	0.004*
X_1^2	-0.1	89.62	1	89.62	5.9	0.03*
X_2^2	0.2	676.28	1	676.28	44.7	< 0.0001*
Residual	-	211.97	14	15.14	-	-
Lack of Fit	-	206.71	9	22.97	21.8	0.002*
Pure Error	-	5.26	5	1.05	-	-
Cor Total	-	4775.44	19	-	-	-
Significant*						

Table 25 shows the model has a significant p-value of 0.0001, a high F-value of 60.3 and all the model terms have a p-value less than 0.05. This indicates that the model fits and is a reliable predictor for the coal yield produced via the overflow. The model has a lack-fit test of 0.002 which is significant. Multiple model permutations and transformations were tried. This model was selected based on its overall statistical reliability. The final model is presented in equation 32:

$$y_{yield} = 81.6 + 6x_1 - 11.3x_2 - 0.1{x_1}^2 + 0.2{x_2}^2 - 0.1x_2x_3 \quad 32$$

To further evaluate the predicted response model, a parity plot was generated (see Figure 49). The observed pattern on the parity plot reveals a close alignment of data points with the diagonal line, signifying a positive correlation. Figure 50 presents the residuals plotted against the predicted coal yield. The residuals plot shows a bending pattern. This shows that the model is biased. Multiple permutations and model transformation were tried, and this was the most statistically reliable model attainable. The selection was based on its overall performance and the significance tests of key model terms. The model has an R^2 value of 0.96 and an adjusted R^2_{adj} value of 0.94, and the model terms are significant.

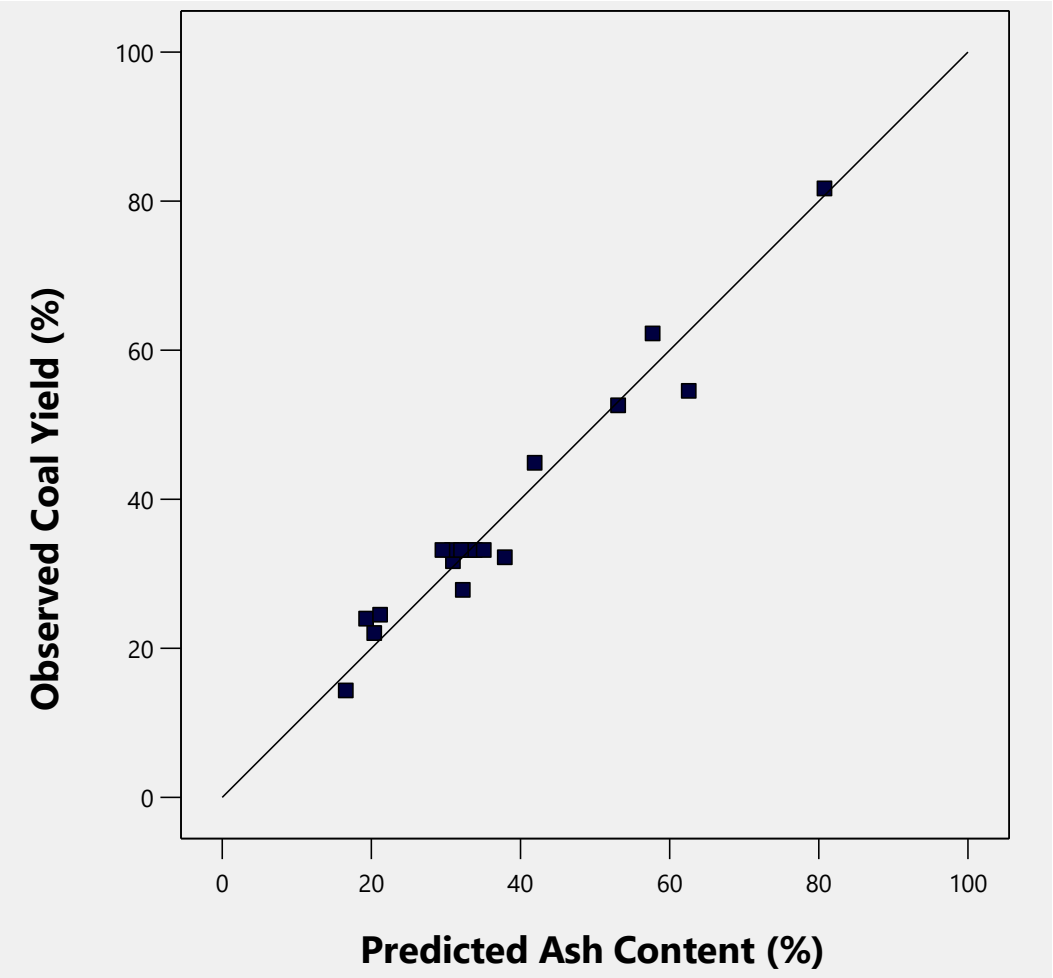

Figure 49: Parity plot showing experimental and predicted values for the coal yield in the dense medium cyclone

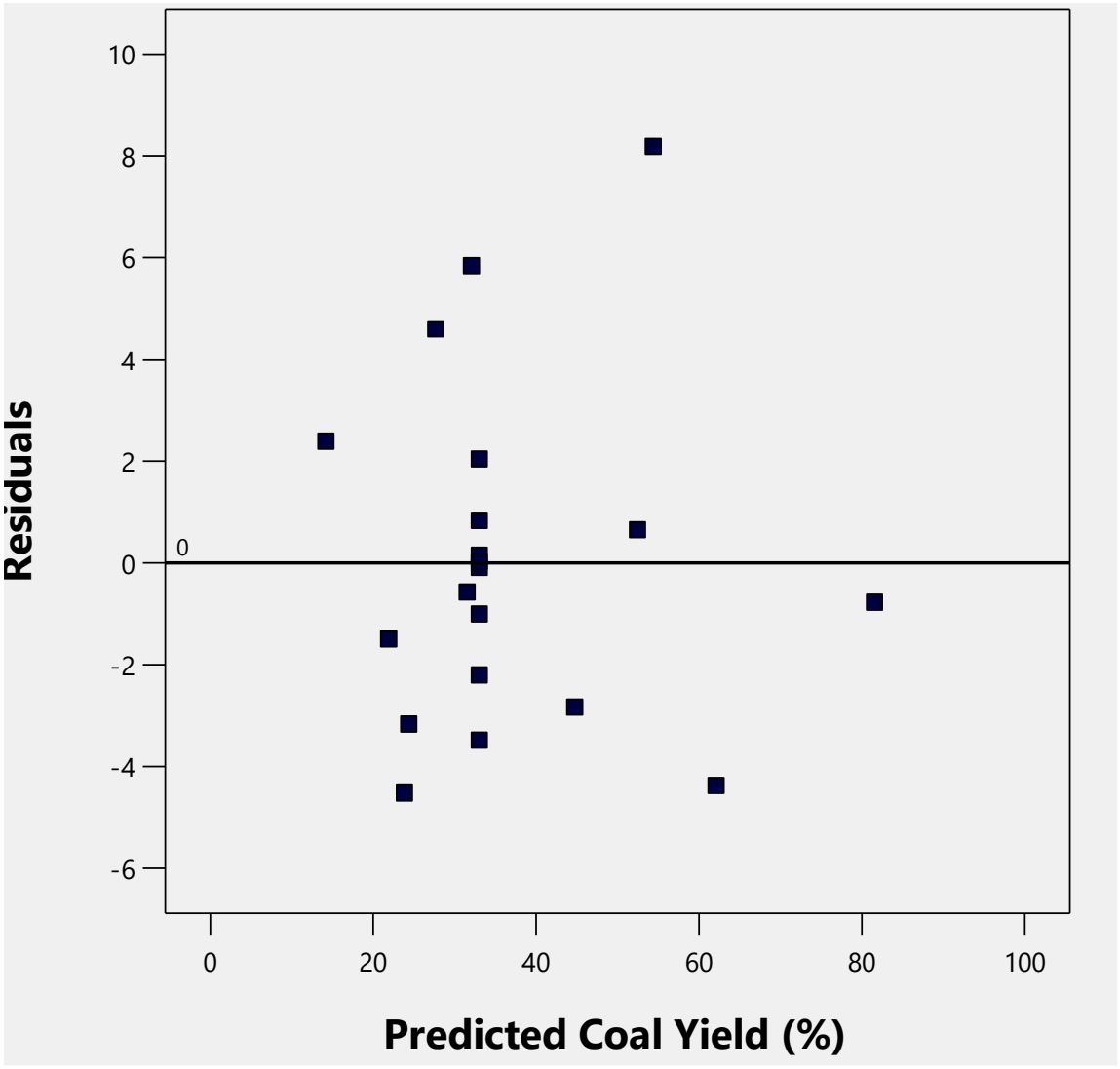

Figure 50: Residuals vs predicted cola yield for the dense medium cyclone

4.4 Classifier Experiments Optimisation

The ash content and coal yield response models for the flat-bottom cyclone and dense medium cyclone were optimized numerically using the desirability function in Design Expert Software. This approach assigns a value between 0 and 1 to each outcome, where values closer to 1 indicate higher desirability based on predefined optimization criteria, such as minimizing, maximizing, or targeting specific responses or independent variables. This method is applied to assess response variable desirability in multivariate optimization problems.

The optimisation objective for the dense medium cyclone and flat-bottom cyclone was to minimise ash content while maintaining vortex finder diameter, spigot diameter, and the medium density for the DMC or the solids concentration for the FBC within the specified experimental ranges described in section 3.4. The optimal response variables were selected based on desirability values approaching 1.

For the DMC, an optimal desirability of 0.942 was chosen from 80 possible outcomes, with a predicted ash content of 27.6% and yield of 20.8%. The FBC optimisation yielded a maximum desirability of 0.925 (out of 57 possible outcomes; see Appendix B), with a predicted ash content of 31.7% and a yield of 35.4% (see Table 26).

Table 26: Predicted optimum response variables and experimental values at optimum classifier operating conditions

Parameter	**Optimum Conditions**			
	DMC		**FBC**	
Vortex finder diameter (mm)	41		41	
Spigot diameter (mm)	30		25	
Solids Concentration (wt%)	-		29	
Medium Density (kg/m^3)	1450		-	
Response	**Actual**	**Predicted**	**Actual**	**Predicted**
Ash Content (%)	26.8	27.6	31.7	31.9
Coal Yield (%)	20.5	20.8	32.3	35.4

The classifiers were operated at these optimal conditions to validate the model predictions, and the close agreement between predicted and actual values shows that the model is valid and fits the experimental data.

4.5 Classifier Performance Analysis

This section evaluates the separation performance of the dense medium cyclone and flat-bottom cyclone under optimal operating conditions when beneficiating the same

coal feed with a high near-gravity material content and ash-bearing impurities content. The separation efficiency was determined and compared by applying partition curves, separation density cut-points of the classifiers, sharpness of separation, and the probable error of separation (E_{pm}).

High NGM coal feed with an ash content of 30.3% was beneficiated in the dense medium cyclone and the flat-bottom cyclone. The dense medium cyclone produces a clean coal yield with a 19.1% ash content and a 20.5% yield (see Table 27). The classifier achieves an ash rejection of 85.6%. The flat-bottom cyclone achieves a comparatively lower ash rejection of 64.2%, a product ash content of 31% and a relatively higher yield of 32.2%.

Table 27: Performance data for the optimised classifiers

	DMC	**FBC**
Feed ash content (%)	30.3	30.3
Clean coal ash content (%)	19.1	31
Coal yield (%)	20.5	32.3
Ash rejection (%)	85.6	64.2

The partition curve graph is typically an S-shaped curve, where the curve steepness indicates separation efficiency. Figure 51 shows the corrected partition curves of the optimised dense medium cyclone and flat-bottom cyclone. The partition curves were modelled using the modified Whiten equation. The dense medium cyclone exhibits a steeper partition curve than the flat-bottom cyclone. This means that the dense medium cyclone has a higher separation efficiency. This analysis is further supported by the determined probable error of separation (E_{pm}) values.

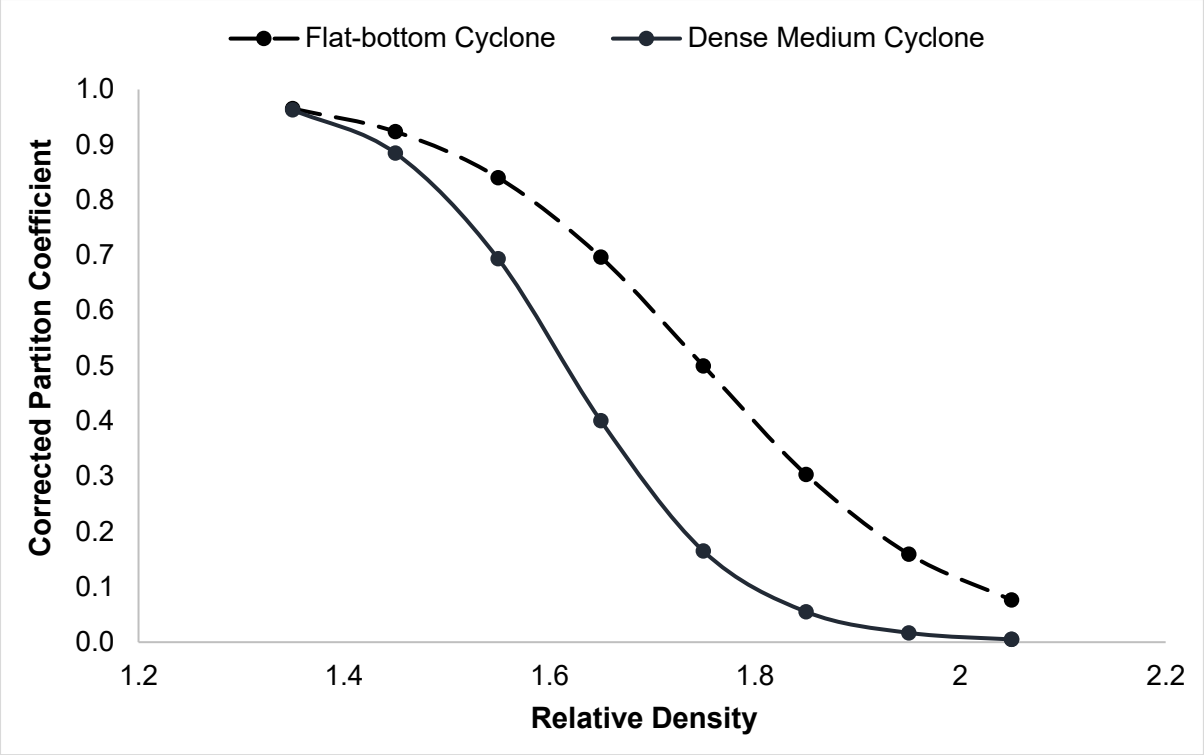

Figure 51: Partition curves for the dense medium cyclone and the flat-bottom cyclone operating at optimised conditions

The DMC and FBC have an E_{pm} of 0.09 and 0.13, respectively. They are consistent with the expected range for dense medium classification (Osborne, 1988). E_{pm} is a dimensionless value that mainly provides a measurement of how much the actual partition curve has shifted from the ideal curve (Paul & Bhattacharya, 2021). According to Wills and Finch (2016), the E_{pm} should ideally range from 0.01 to 0.10 for dense medium separation to maintain an efficient separation process.

This indicates that the DMC achieves a sharper separation than the FBC. This is further corroborated by the separation density cut points and the sharpness of separation or imperfection values of the classifiers. The sharpness of separation value is 0.056 for the DMC and 0.074 for the FBC. Lower values closer to zero indicates efficient separation performance in the classifier (Kumar & Kumar, 2018). The DMC exhibits a relative density cut point of 1.61, while the FBC has a cut point of 1.75, implying that the DMC is more efficient in producing a final coal product with lower ash content. This is attributed to the fact that a higher relative density cut point results in a greater proportion of ash-bearing impurities being directed to the overflow.

Consequently, 12.4% of clean coal particles in the DMC are misplaced to the underflow, compared to 14.6% in the FBC. Furthermore, the DMC achieves an organic efficiency of 62.7%, whereas the FBC achieves 42.8%. An organic efficiency (E_{org}) value approaching 100% signifies a state of efficient separation, where no coal material is misplaced or directed into the wrong stream during the separation process.

4.5.1 Comparison of Density-Based and Size-Based Classification in the Flat-Bottom Cyclone

The separation performance of the optimised flat-bottom cyclone was assessed using both density-based and size-based classifications. This aimed to determine whether the minimal ash rejection in the final coal product results from suboptimal beneficiation based on density or if the separation is primarily driven by particle size. Figure 52 presents the size-based partition curve for the flat-bottom cyclone, operated with a vortex finder diameter of 41 mm, a spigot diameter of 25 mm, and a solids concentration of 29%. The corrected partition curves were modelled using the Reid-Plitt equation.

The partition curve is steep which indicates a high sharpness of separation. For density-based classification, the probable error (E_{pm}) was 0.13, while for size-based classification, E_{pm} was significantly lower at 0.03. Sripriya et al. (2001) explains that a lower E_{pm} value shows a high separation efficiency. This indicates that size-based separation is sharper than density-based separation, which may explain the minimal ash reduction in the final coal product, as the process is predominantly influenced by particle size rather than density.

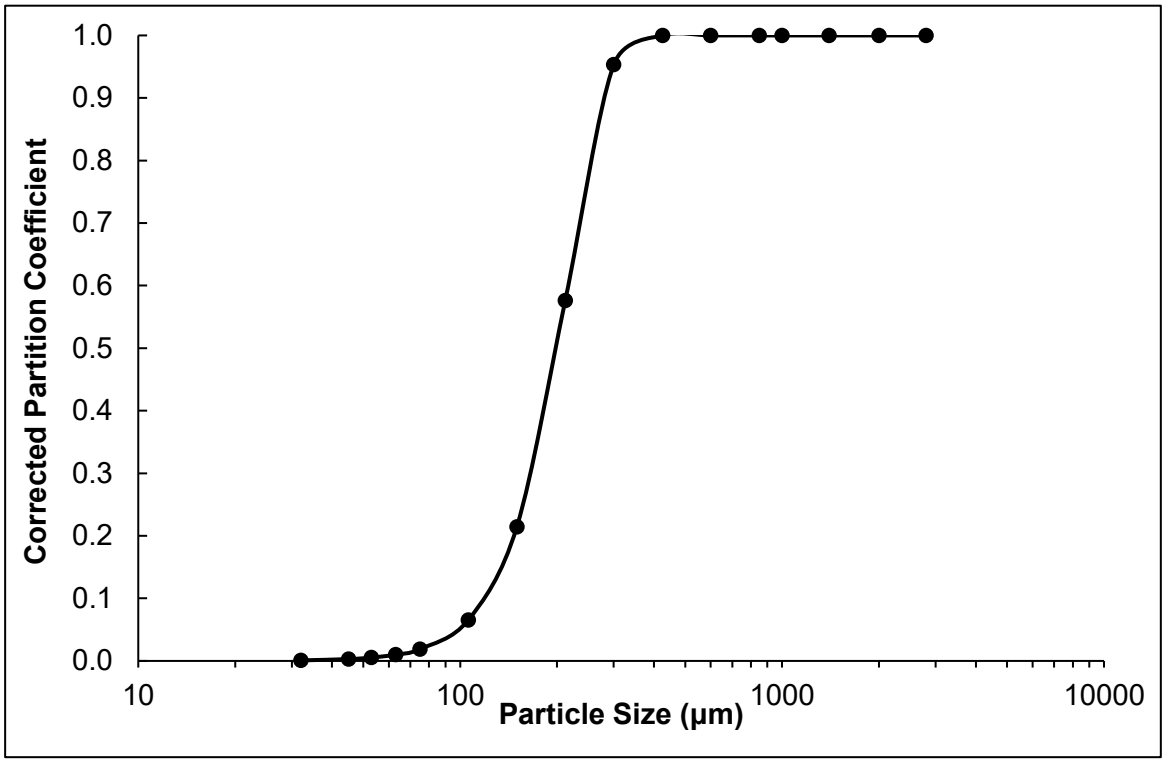

Figure 52: Size-based partition curve for the flat-bottom cyclone operating at optimised conditions

5 Conclusion and Recommendations

This chapter focuses on presenting the key observations made and the main conclusion from the study. The study examined the separation efficiency of a dense medium cyclone and a flat-bottom cyclone in beneficiating low-grade fine coal with high ash-bearing impurities and near-gravity material content. It also highlights the challenges associated with the density-based classification of coal containing a high proportion of near-gravity material and ash-bearing impurities.

5.1 Observations Made From The Study

The key findings from this study are as follows:

- The use of heavy media in the dense medium cyclone results in a steeper density gradient between the clean coal particles and separating medium. This results in a sharper density-based separation.
- An increase in the vortex finder diameter in the flat-bottom cyclone and the dense medium cyclone results in an increase in the ash content and coal yield recovered to the overflow. This increase can be attributed to the increase in the short-circuiting of the coal feed to the overflow before undergoing separation by density.
- An increase in the size of the spigot diameter leads to a decrease in the coal yield and an increase in the ash content in the coal product recovered from the overflow. This is attributed to the increased mass split of the coal feed to the underflow. This leads to a decrease in the proportion of the coal feed recovered to the overflow.
- Increasing the relative density of the separation medium results in an increase in the coal yield and the ash content recovered to the overflow of the dense medium cyclone. This is because a high medium density during separation may result in a higher separation density cutpoint, which results in an increase in the fraction of high-density gangue coal particles that report to the overflow.
- Float-and-sink test data from this study highlighted that the coal has significant amounts of near-gravity material and ash content. These properties have an impact on the separation performance of the classifier. The high near-gravity

material in the coal presented challenges for the flat-bottom cyclone over the dense medium cyclone. The ability of the flat-bottom cyclone to achieve a steep density difference during separation was limited. High near-gravity material content increases particle misplacement during beneficiation, reducing separation efficiency and producing a low-quality coal product.

5.2 Conclusions

5.2.1 Findings in Response to Hypothesis 1

The hypothesis proposed that incorporating heavy media in the classification of high NGM and ash-bearing impurities in low-grade fine coal would enhance the separation efficiency of the classifier.

The study showed that increasing the density of the separating medium resulted in an increase in the ash content of the coal recovered to the overflow stream. Enlarging the spigot and vortex finder diameters reduced the separation efficiency, yielding a coal product with higher ash content.

The testwork showed that coal recovery to the overflow decreased with reduction in spigot diameter size and increased with larger vortex finder diameters. Therefore, the spigot and vortex finder diameter can be used to optimise coal recovery to the overflow. Optimal conditions for maximum ash rejection and separation efficiency were achieved using a combination of a 41 mm vortex finder diameter, 30 mm spigot diameter and a relative density of 1.45 which yielded an ash content of 19.1% and 20.5%. Under these conditions, the dense medium cyclone achieved enhanced separation efficiency, as indicated by a steep partition curve and a reduced probable error of separation (E_{pm}).

5.2.2 Findings in Response to Hypothesis 2

The hypothesis stated that the separation process in a flat-bottom cyclone is predominantly influenced by density rather than particle size.

The flat-bottom cyclone has limited ability to achieve effective density-based separation, with particle size emerging as the primary factor governing the separation process. The study showed that the size partition curves had a steeper curve and a low E_{pm} value of 0.03 compared to the density partition curve with an E_{pm} of 0.13. Therefore, the separation mechanism inside the flat-bottom cyclone fails to efficiently separate the gangue material from the clean coal particles using density but rather both the coal feed is separated by size.

An increase in coal feed solids concentration enhanced coal yield recovery to the overflow and reduced the ash content of the recovered coal. The study showed that using a combination of large vortex finder and spigot diameters and intermediate solids concentration leads to producing clean coal to the overflow but at an increase in ash content.

The optimal conditions for maximum ash reduction were determined to be a vortex finder diameter of 41 mm, a spigot diameter of 25 mm, and a solids concentration of 29%. However, these adjustments resulted in a slight decrease in the overall ash reduction efficiency of the flat-bottom cyclone. Under these conditions, the flat-bottom cyclone produced a 32.3% coal yield with a 31% ash content.

5.3 Recommendations

The following recommendations are suggested for future work:

- Conduct a computational fluid dynamics (CFD) study to examine coal particle-fluid interactions within the classifier. This will help evaluate how fluid flow patterns influence separation efficiency in the DMC and FBC. This approach could reveal zones where, during separation, particle density or size exerts greater influence on separating near-gravity material-rich low-grade coal. This can clarify how density and particle size affect settling rates, particularly in the FBC, where hindered sedimentation facilitates density-based classification.
- Investigate particle residence times in both classifiers under varied coal feed flow rates to analyse how the feed quantity affects separation performance and particle misplacement within the classifiers. Changes in feed rates correspond to varying amounts of near-gravity material introduced per unit of time in the

coal beneficiation circuit during processing. This analysis could aid in optimising classifier operating conditions for enhanced separation accuracy.

- Investigate the effects of breaking the feed into multiple, defined size fractions and performing similar classifier experiments on each size fraction. This could help clarify the effect of particle size in density-based classification.
- The impact of structurally positioning the DMC and FBC at an incline to the horizontal should be investigated. This will provide insight into the influence of the position of the cyclone on the separation efficiency.
- Conduct further experiments to increase the dataset for both the dense medium cyclone and the flat-bottom cyclone. This will facilitate the refinement of the regression models and address the significant lack of fit observed, particularly in the ash model for the dense medium cyclone.

6 References

Abbas, N. & Muhammad, K. 2016. Optimization of Operating and Design Parameters of Water only Cyclone using Cherat Coal in Pakistan. *Journal of Nuclear Energy Science & Power Generation Technology*. 05(02). DOI: 10.4172/2325-9809.1000149.

Abbas, N. & Muhammad, K. 2017. Optimization of Operating and Design Parameters of Water only Cyclone using Cherat Coal in Pakistan. *Journal of Nuclear Energy Science & Power Generation Technology*. 2016(02). DOI: 10.4172/2325-9809.1000149.

Aketi, V.A.K., Vakamalla, T.R., Narasimha, M., Sreedhar, G.E., Shivakumar, R. & RajanKumar. 2017. Computational Fluid Dynamic study on the effect of near gravity material on dense medium cyclone treating coal using Discrete Phase Model and Algebraic Slip mixture multiphase model. *Journal of Computational Multiphase Flows*. 9(2):58–70. DOI: 10.1177/1757482X16677755.

Aketi, V.A.K., Teja Reddy, V., Mangadoddy, N., G E, S., Raparla, S.K. & Kumar, R. 2021. Numerical simulation of near-gravity coal particle behavior in a dense medium cyclone using a mixture model coupled with a discrete phase model. *International Journal of Coal Preparation and Utilization*. 41(8):554–576. DOI: 10.1080/19392699.2018.1491844.

Anupam, A., Bhattacharya, S. & de Korte, G.J. 2020. DOI: 10.1080/19392699.2017.1390457.

Aslan, N. 2008. Application of response surface methodology and central composite rotatable design for modeling and optimization of a multi-gravity separator for chromite concentration. *Powder Technology*. 185(1):80–86. DOI: 10.1016/j.powtec.2007.10.002.

ASTM D3174−12. 2018. *Standard Test Method for Ash in the Analysis Sample of Coal and Coke from Coal*.

Bai, T., Chen, Z., Aminossadati, S.M., Rufford, T.E. & Li, L. 2017. Experimental investigation on the impact of coal fines generation and migration on coal permeability. *Journal of Petroleum Science and Engineering*. 159:257–266. DOI: 10.1016/J.PETROL.2017.09.035.

Bhattacharya, S., Maheshwari, A. & Panda, M. 2016a. Coal Cleaning Operations: The Question of Near Gravity Material. *Transactions of the Indian Institute of Metals*. 69(1):157–172. DOI: 10.1007/S12666-015-0737-Z.

Bhattacharya, S., Maheshwari, A. & Panda, M. 2016b. Coal Cleaning Operations: The Question of Near Gravity Material. *Transactions of the Indian Institute of Metals*. 69(1):157–172. DOI: 10.1007/s12666-015-0737-z.

Botha, W. 2016. MANAGEMENT OF THE MINERAL RESOURCE RISK ASSOCIATED MANAGEMENT OF THE MINERAL RESOURCE RISK ASSOCIATED. University of Pretoria.

Box, G.E.P. & Hunter, J.S. 1957. Multi-Factor Experimental Designs for Exploring Response Surfaces. *The Annals of Mathematical Statistics*. 28(1):195–241. DOI: 10.1214/AOMS/1177707047.

Cilliers, J.J., Austin, R.C. & Tucker, J.P. 1992. An Evaluation of Formal Experimental Design Procedures for Hydrocyclone Modelling. 31–49. DOI: 10.1007/978-94-015-7981-0_3.

Clarkson, C.J. & Wood, C.J. 1993. A Model of Dense Medium Cyclone Performance. *Coal Preparation*. 12(1–4):101–115. DOI: 10.1080/07349349308905112.

Crozier, R.D. 1992. Flotation: theory, reagents and ore testing. 343.

Dou, D., Liu, G. & Yang, J. 2022. Particle size-included partition curve model of dense medium cyclones. *International Journal of Coal Preparation and Utilization*. 42(3):565–579. DOI: 10.1080/19392699.2019.1628026.

Electricity Supply Commission (Eskom). 2016. Coal in South Africa. Available: https://www.eskom.co.za/wp-content/uploads/2021/08/CO-0007-Coal-in-SA-Rev-16.pdf [2023, May 01].

England, T. & Horsfall, D.W. 2002. *Coal preparation in South Africa*. 4th ed. South African Coal Processing Society. Available: https://books.google.com/books/about/Coal_Preparation_in_South_Africa.html?id=M1eEQwAACAAJ [2023, March 26].

Firth, B., O'Brien, M. & McNally, C. 2011. Medium quality and DMC performance: Effect of clay and fine coal. *International Journal of Coal Preparation and Utilization*. 31(6):355–372. DOI: 10.1080/19392699.2011.606245.

Fourie, P.J.F. & Van Der Waltt, P.J. 1980. The beneficiation of fine coal by dense-medium cyclone. DOI: 10.10520/AJA0038223X_1190.

Gerald H. Luttrell, Chris J. Barbee, Peter J. Bethell & Chris J. Wood. 2005. *DENSE MEDIUM CYCLONE OPTIMIZATON*. Pittsburgh, PA, and Morgantown, WV. DOI: 10.2172/882213.

GJ de Korte. 2012. *Fine Coal Processing with Dense-Medium Cyclones GJ de Korte Fine Coal Processing with Dense-Medium Cyclones*.

Govindarajan, B. & Rao, T.C. 1994. Indexing the washability characteristics of coal. *International Journal of Mineral Processing*. 42(3–4):285–293. DOI: 10.1016/0301-7516(94)00027-1.

Grobler, J.D., Sandenbergh, R.F. & Pistorius, P.C. 2002. The stability of ferrosilicon dense medium suspensions. *Journal of the Southern African Institute of Mining and Metallurgy*. 102(2):83–86.

Gupta, A. & Yan, D. 2016. Gravity Separation. In *Mineral Processing Design and Operations*. Elsevier. 563–628. DOI: 10.1016/b978-0-444-63589-1.00016-2.

Hacifazlioglu, H. 2012a. Optimization of some parameters in a modified water-only cyclone for metallurgical coal production from high-ash fine coking coals. *International Journal of Coal Preparation and Utilization*. 32(6):290–297. DOI: 10.1080/19392699.2012.717564.

Hacifazlioglu, H. 2012b. Application of the modified water-only cyclone for cleaning fine coals in a Turkish washery, and comparison of its performance results with those of spiral and flotation. *Fuel Processing Technology*. 102:11–17. DOI: 10.1016/J.FUPROC.2012.04.011.

Hacifazlioglu, H. 2012c. Application of the modified water-only cyclone for cleaning fine coals in a Turkish washery, and comparison of its performance results with those of spiral and flotation. *Fuel Processing Technology*. 102:11–17. DOI: 10.1016/J.FUPROC.2012.04.011.

Handayani, I., Rasyid, M.A., Fadhilah, R. & Gusti, H.I.K. 2024. Beneficiation Processing of Magnetite ore from Lampung as Dense Media for Dense Medium Separator in Coal Washing Plant. *E3S Web of Conferences*. 543:01006. DOI: 10.1051/e3sconf/202454301006.

He, Y.B. & Laskowski, J.S. 1994. Effect of dense medium properties on the separation performance of a dense medium cyclone. *Minerals Engineering*. 7(2–3):209–221. DOI: 10.1016/0892-6875(94)90065-5.

He, Y.B. & Laskowski, J.S. 1995. Dense Medium Cyclone Separation of Fine Particles Part 2. The Effect of Medium Composition on Dense Medium Cyclone Performance. *Coal Preparation*. 16(1–2):27–49. DOI: 10.1080/07349349508905240.

He, Y.B. & Laskowski, J.S. 2007. Dense Medium Cyclone Separation of Fine Particles Part 2. The Effect of Medium Composition on Dense Medium Cyclone Performance. *http://dx.doi.org/10.1080/07349349508905240*. 16(1–2):27–49. DOI: 10.1080/07349349508905240.

Hembrom, A.A. & Suresh, N. 2018. DOI: 10.1080/15567036.2018.1511657.

Holtham, P., Brennan, M. & Managadoddy, N. 2008. *Dense Medium Cyclone Research at the Julius Kruttschnitt Mineral Research Centre*.

Holuszko, M.E. & Grieve, D.A. 1994. *WASHABILITY CHARACTERISTICS OF BRITISH COLUMBIA COALS*.

Izquierdo, J., Sukunza, X., Espinazo, P., Vicente, J., Aguado, R. & Olazar, M. 2023. In depth characterisation of hydrocyclones: Ascertaining the effect of geometry and operating conditions on their performance. *Advanced Powder Technology*. 34(6):104025. DOI: 10.1016/j.apt.2023.104025.

J. O. Claassen. 2013. Yield improvement at a mid-sized coal mine in the Witbank coalfields. *The Journal of The Southern African Institute of Mining and Metallurgy*. 113:761–768. Available: http://www.scielo.org.za/pdf/jsaimm/v113n10/07.pdf [2023, August 08].

K. Palanikumar. 2021. *Response Surface Methodology in Engineering Science*. P. Kayaroganam, Ed. IntechOpen. DOI: 10.5772/intechopen.90965.

King, R.P. & Juckes, A.H. 1988. Performance of a dense-medium cyclone when beneficiating fine coal. *Coal Preparation*. 5(3–4):185–210. DOI: 10.1080/07349348808945565.

De Korte, G.J. 2008. The influence of near-dense material on the separation efficiency of dense-medium processes. *International Journal of Coal Preparation and Utilization*. 28(2):69–93. DOI: 10.1080/19392690802053979.

De Korte, G.J. 2015. Processing low-grade coal to produce high-grade products. *Journal of the Southern African Institute of Mining and Metallurgy*. 115(7):569–572. DOI: 10.17159/2411-9717/2015/v115n7a2.

Kumar, D. & Kumar, D. 2018. Coking Coal Washing. In *Sustainable Management of Coal Preparation*. Elsevier. 133–178. DOI: 10.1016/b978-0-12-812632-5.00007-0.

Kumar, V. & Saxena, V. 2014. Studies on the Variation in Coal Properties of Low Volatile Coking Coal after Beneficiation. *International Journal of Computational Engineering Research*||*Vol*. 4(1):1.

Kumari, A.A. 2015. *CFD STUDY ON THE EFFECT OF NEAR GRAVITY MATERIAL ON DMC TREATING COAL USING DPM AND ASM MULTIPHASE MODEL*.

Kumari, A., Narasimha, M., Sreedhar, G.E., Shivakumar, R. & Sharma, S.K. 2015. CFD STUDY ON THE EFFECT OF NEAR GRAVITY MATERIAL ON DMC TREATING COAL USING DPM AND ASM MULTIPHASE MODEL. In *Eleventh International Conference on CFD in the Minerals and Process Industries* .

L. S. Jeffrey. 2005. Characterization of the coal resources of South Africa. *The Journal of The South African Institute of Mining and Metallurgy*. (February):95–102.
Leonard, J.W. & Hardinge, B.C. 1991. Coal preparation. 131.
Liu, B., Sha, J., Liu, Z., Xie, G. & Peng, Y. 2018. Separation of 0.75–0.125 mm Fine Coal Using the Cylindrical Section of a 710/500 mm Three-Product Dense Medium Cyclone. *International Journal of Coal Preparation and Utilization*. 38(1):1–12. DOI: 10.1080/19392699.2015.1088528.
Ma, G., Bu, X., Xie, G., Peng, Y., Sha, J., Xia, W. & Wu, E. 2021. Comparative Study of Separation Performance of a Spiral and Dense-medium Cyclone on Cleaning Coal. *International Journal of Coal Preparation and Utilization*. 41(2):108–116. DOI: 10.1080/19392699.2018.1464001.
Maharana, B.S. & Suresh, N. 2020. Separation characteristics of 100-mm dual-cone water-only cyclone to wash high NGM coal. *International Journal of Coal Preparation and Utilization*. 40(1):37–50. DOI: 10.1080/19392699.2019.1594794.
Majumder, A.K. & Barnwal, J.P. 2004. Development of a new coal washability index. *Minerals Engineering*. 17(1):93–96. DOI: 10.1016/J.MINENG.2003.10.005.
Majumder, A.K. & Barnwal, J.P. 2011a. Processing of coal fines in a water-only cyclone. *Fuel*. 90(2):834–837. DOI: 10.1016/j.fuel.2010.10.038.
Majumder, A.K. & Barnwal, J.P. 2011b. Processing of coal fines in a water-only cyclone. *Fuel*. 90(2):834–837. DOI: 10.1016/j.fuel.2010.10.038.
Malumbazo, N. 2016. Type, Distribution and Use of Coal in South Africa. Cape Town: 35th International Geological Conference GIFT Workshop.
Mukherjee, A.K. 2009. A new method for evaluation of gravity separation processes. *Mineral Processing and Extractive Metallurgy Review*. 30(3):191–210. DOI: 10.1080/08827500802405756/ASSET/A53245E4-6A54-4FFD-8640-AB19E8EA256B/ASSETS/IMAGES/GMPR_A_340743_O_F0005G.GIF.
Myers, R.H., Montgomery, D.C. & Anderson-Cook, C.M. 2016. *Response surface methodology: process and product optimization using designed experiments*. John Wiley & Sons.
North, B., Engelbrecht, A. & Oboirien, B. 2015. Feasibility study of electricity generation from discard coal. *Journal of the Southern African Institute of Mining and Metallurgy*. 115(7):573–580. DOI: 10.17159/2411-9717/2015/v115n7a3.
Nyoni, S., Bwalya, M. & Chimwani, N. 2020. Beneficiation potential of a low-grade coal from the Emalahleni (Witbank) coalfield. *Physicochemical Problems of Mineral Processing*. 56(5):849–859. DOI: 10.37190/PPMP/126242.

Obeng, D.P., Morrell, S. & Napier-Munn, T.J. 2005. Application of central composite rotatable design to modelling the effect of some operating variables on the performance of the three-product cyclone. *International Journal of Mineral Processing*. 76(3):181–192. DOI: 10.1016/j.minpro.2005.01.002.

O'Brien, M., Firth, B. & McNally, C. 2014. Effect of Medium Composition on Dense Medium Cyclone Operation. *International Journal of Coal Preparation and Utilization*. 34(3–4):121–132. DOI: 10.1080/19392699.2014.869924.

Osborne, D.G. 1988. *Coal Preparation Technology*. V. 1. Graham & Trotman.

Osborne, D.G. 2013. *The coal handbook. Volume 2, Coal utilisation : towards cleaner production*. Woodhead Publishing.

Paul, S.R. & Bhattacharya, S. 2021. Performance analysis of coal cleaning operations: Role of Probable Error in Separation and Organic Efficiency. *International Journal of Coal Preparation and Utilization*. DOI: 10.1080/19392699.2021.2000969.

Phengsaart, T., Srichonphaisan, P., Kertbundit, C., Soonthornwiphat, N., Sinthugoot, S., Phumkokrux, N., Juntarasakul, O., Maneeintr, K., et al. 2023. Conventional and recent advances in gravity separation technologies for coal cleaning: A systematic and critical review. *Heliyon*. 9(2):e13083. DOI: 10.1016/j.heliyon.2023.e13083.

Pural, Y.E., Sirkeci, A.A. & Boylu, F. 2023. Simulation and Performance Evaluation of Three Product Dense Medium Cyclone. *International Journal of Coal Preparation and Utilization*. 43(8):1299–1312. DOI: 10.1080/19392699.2022.2110085.

Pyka, I. & Wierzchowski, K. 2022. Influence of equal settling particles on fine coal separation in water-only cyclones. *International Journal of Coal Preparation and Utilization*. 42(3):410–420. DOI: 10.1080/19392699.2019.1608969.

Quanhong, L. & Caili, F. 2005. Application of response surface methodology for extraction optimization of germinant pumpkin seeds protein. *Food Chemistry*. 92(4):701–706. DOI: 10.1016/J.FOODCHEM.2004.08.042.

Ramudzwagi, M. 2020. *Optimization of hydrocyclone classifier in the beneficiation of fine coal using Taguchi approach*.

Ramudzwagi, M., Tshiongo-Makgwe, N. & Nheta, W. 2020. DOI: 10.1016/j.jclepro.2020.122693.

Sahu, D., Chaurasia, R.C. & Suresh, N. 2019a. Statistical studies on high ash Indian coal crushed to (−3 mm) using 76 mm dense medium cyclone. *International Journal of Coal Preparation and Utilization*. 42(3):389–409. DOI: 10.1080/19392699.2019.1605987.

Sahu, D., Chaurasia, R.C. & Suresh, N. 2019b. Mineralogical characterization and washability of Indian coal from Jamadoba. *Energy Sources, Part A: Recovery, Utilization and Environmental Effects*. 41(5):517–526. DOI: 10.1080/15567036.2018.1520336.

Saida, S., Chakravarthy, S., Sahu, R., Mishra, P.R. & Chakravarty, K. 2022. Prediction of Washability Characteristics of Non-coking and Semi-coking Coals. 13–23. DOI: 10.1007/978-981-16-3297-6_2.

Sanders, G.J. 2007. The principles of coal preparation.

Shahzad, M. & Ali, Z. 2021. Development of simple techniques for determining the extent of coal cleaning-part 2: Estimating coal washability characteristics and separator performance. *International Journal of Coal Preparation and Utilization*. 41(8):589–602. DOI: 10.1080/19392699.2018.1496085.

Sobhy, A. 2022. Recent Trends in Mineral Processing Based on Density and Particle Size – A review. *International Journal of Materials Technology and Innovation*. 2(2):13–30. DOI: 10.21608/ijmti.2022.151879.1055.

Sripriya, R., Banerjee, P.K., Rao, P.V.T., Dutta, A. & Rao, M.V.S. 2001. *Critical evaluation of factors affecting the operation of dense medium cyclones treating medium coking coals*. Available: www.elsevier.comrlocaterijminpro.

Sripriya, R., Banerjee, P.K., Soni, Baijal, A.D., Dutta, A., Rao, M.V.S. & Chatterjee, S. 2007. Dense-medium cyclone: Plant experience with high near-gravity material Indian coals. *Coal Preparation*. 27(1–3):78–106. DOI: 10.1080/07349340701249729.

Su, T. & Zhang, Y. 2022a. Effect of the Vortex Finder and Feed Parameters on the Short-Circuit Flow and Separation Performance of a Hydrocyclone. *Processes*. 10(4). DOI: 10.3390/pr10040771.

Su, T. & Zhang, Y. 2022b. Effect of the Vortex Finder and Feed Parameters on the Short-Circuit Flow and Separation Performance of a Hydrocyclone. *Processes*. 10(4). DOI: 10.3390/pr10040771.

Supriya Maharana, B. & Suresh, N. 2020. Taguchi based Grey relational analysis for optimization of design parameters of a 100 mm water-only cyclone. DOI: 10.1080/19392699.2020.1822825.

Waanders, F.B. & Rabatho, J.P. 2005. Recovery of Heavy Minerals by Means of Ferrosilicon Dense Medium Separation Material. *Hyperfine Interactions*. 161(1–4):55–60. DOI: 10.1007/s10751-005-9191-3.

Wang, B., Chu, K.W., Yu, A.B. & Vince, A. 2009. Modeling the multiphase flow in a dense medium cyclone. *Industrial and Engineering Chemistry Research*. 48(7):3628–

3639. DOI: 10.1021/IE801175C/ASSET/IMAGES/LARGE/IE-2008-01175C_0019.JPEG.

Wang, B., Chu, K.W., Yu, A.B., Vince, A., Barnett, G.D. & Barnett, P.J. 2011. Computational study of the multiphase flow and performance of dense medium cyclones: Effect of body dimensions. *Minerals Engineering*. 24(1):19–34. DOI: 10.1016/j.mineng.2010.09.003.

Wang, C., Wei, L.B. & Cui, G.W. 2022. Effects of the operating parameters on the separation results of a three-stage cone water-only cyclone. *International Journal of Coal Preparation and Utilization*. 42(8):2314–2331. DOI: 10.1080/19392699.2020.1837787.

Wills, B.A. & Finch, J.A. 2016. Wills' Mineral Processing Technology- An Introduction to the Practical Aspects of Ore Treatment and Mineral Recovery. In *Wills' Mineral Processing Technology*. Elsevier. DOI: 10.1016/C2010-0-65478-2.

7 Appendix

7.1 Appendix A

7.1.1 Magnetite X-ray Diffraction

The diffractogram below displays sharp, intense red peaks for magnetite at a wavelength of 1.79 Å, indicating that the feed contains a significant amount of pure magnetite. The narrow peak width is directly related to the purity of the magnetite phase in the sample. In contrast, the other compounds, such as dolomite, calcite, and mica, have very small peaks, as shown in Figure 53.

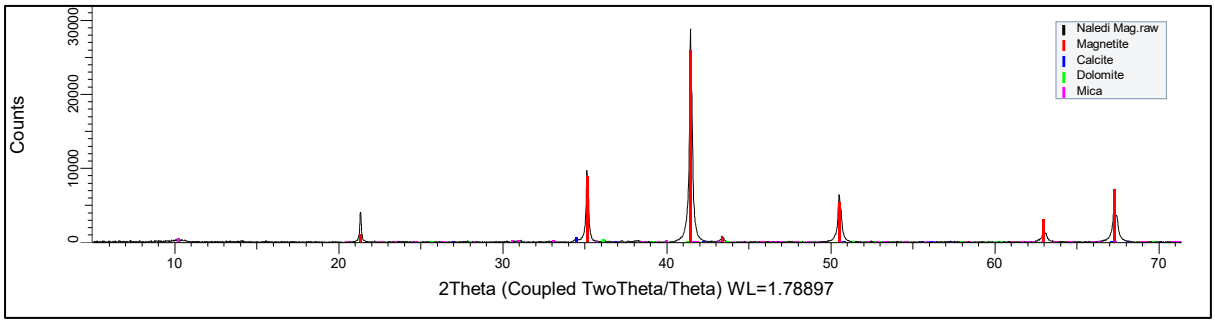

Figure 53: XRD Diffractogram showing the chemical composition of the bulk magnetite sample

7.1.2 Coal Particle Size Analysis

The bulk coal from Mpumalanga has a characteristic distribution shown in Table 28. The coal has a top size of 3.35 mm and a d_{50} of 0.78 mm.

Table 28: Characteristic size distribution of the bulk coal from the Highveld Coalfields, Mpumalanga

Characteristic Distribution	Size (mm)
d_{100}	3.35
d_{90}	2.32
d_{50}	0.78
d_{10}	0.09

7.1.3 Float and Sink Test

7.1.3.1 Near Gravity Material Index

The cumulative non-ash and ash recovery is calculated using equations 1 and 2.

Table 29: Example of cumulative ash and non-ash recovery calculations

Specific Gravity	[1]	[2]	[1]x[2] /Net Ash = [3]	[1]x(100-[2]) = [4]	[4]/(100-Net Ash) = [6]
	Cumulative		Cumulative ash recovery		Cumulative non-ash recovery
	Mass (wt%)	Ash (wt%)			
F1.3	2.15	5.00	0.38	204	2.83
F1.4	13.58	8.79	4.28	1238	17.17
F1.5	31.22	11.79	13.20	2754	38.18
F1.6	64.56	17.99	41.68	5295	73.41
F1.7	75.50	19.63	53.17	6068	84.13
F1.8	82.66	21.14	62.68	6519	90.38
F1.9	87.51	22.47	70.55	6785	94.07
F2.0	90.62	23.46	76.28	6936	96.16
Sink at 2.0	100	27.87*	100	7213	100
Net ash*					

Equation 7 and Table 18 was used to calculate the NGMI over a relative density range of 1.3 to 1.4:

$$NGMI = \frac{\{[6(a-p)X + 4(b-q)X^2 + 3(c-r)X^3]/12\}_\gamma}{[6(a-p) + 4(b-q) + 3(c-r)]/12} - \frac{\{[6(a-p)X + 4(b-q)X^2 + 3(c-r)X^3]/12\}_\alpha}{[6(a-p) + 4(b-q) + 3(c-r)]/12}$$

$$NGMI = \frac{\{[6(79.95)0.312 + 4(31.18)0.312^2 + 3(-108.1)0.312^3]/12\}}{[6(79.95) + 4(31.18) + 3(-108.1)]/12} - \frac{\{[6(79.95)0.02 + 4(31.18)0.02^2 + 3(-108.1)0.02^3]/12\}}{[6(79.95) + 4(31.18) + 3(-108.1)]/12}$$

= 16.86%

7.1.3.2 Near Gravity Material

Column 1 lists the fraction of coal that floats at each relative density, while Column 2 shows the ash content, determined using Equation 27. The actual ash quantity in the density float fraction, Q_{ash}, is shown in Column 3 and was calculated as the product of the float mass fraction and its ash content.

Columns 4 and 5 show the cumulative float fraction mass and cumulative ash quantity, respectively. Column 6 provides the cumulative ash content, calculated as the ratio of the cumulative ash quantity to the cumulative float fraction mass at each relative density. Column 7 is the near gravity material, which was determined as the difference in cumulative mass between the float fractions with relative densities 0.1 less and 0.1 more than the specified float fraction.

Table 30: Example of the float and sink calculations

Relative Density	Differential			Cumulative			NGM (%) (7) = (4) $_{+0.1}$ - (4) $_{-0.1}$
	Mass (%) (1)	Ash (%) (2)	Q_{ash} (%) (3) = (1) · (2)	Mass (%) (4) = Sum (1)	Q_{ash} (%) (5) = Sum (3)	Ash (%) (6) = (5)/(4)	
Float at 1.3	$Mass_{1.3}$	$Ash_{1.3}$	$(Mass \cdot Ash)_{1.3}$	$Mass_{1.3}$	$(Mass \cdot Ash)_{1.3}$	$(Mass \cdot Ash)_{1.3}$ / $Mass_{1.3}$	-
Float at 1.4	$Mass_{1.4}$	$Ash_{1.4}$	$(Mass \cdot Ash)_{1.4}$	$Mass_{1.3} + Mass_{1.4}$	$(Mass \cdot Ash)_{1.3} + (Mass \cdot Ash)_{1.4}$	$[(Mass \cdot Ash)_{1.3} + (Mass \cdot Ash)_{1.4}] / [Mass_{1.3} + Mass_{1.4}]$	$[Mass_{1.3} + Mass_{1.4} + Mass_{1.5}] - [Mass_{1.3}]$
Float at 1.5	$Mass_{1.5}$	$Ash_{1.5}$	$(Mass \cdot Ash)_{1.5}$	$Mass_{1.3} + Mass_{1.4} + Mass_{1.5}$	$((Mass \cdot Ash)_{1.3} + (Mass \cdot Ash)_{1.4} + (Mass \cdot Ash)_{1.5}$	$[(Mass \cdot Ash)_{1.3} + (Mass \cdot Ash)_{1.4} + (Mass \cdot Ash)_{1.5}]/ [Mass_{1.3} + Mass_{1.4} + Mass_{1.5}]$	$[Mass_{1.3} + Mass_{1.4} + Mass_{1.5} + Mass_{1.6}] - [Mass_{1.3} + Mass_{1.4}]$

7.2 Appendix B

7.2.1 Summarized Flat-bottom Cyclone Data

Table 31: Summarised flat-bottom cyclone tests experimental data

Run	Vortex Finder Diameter	Spigot Diameter	Solids Concentration	Feed	Overflow	Underflow	Coal Yield	Ash Content
	mm	mm	%wt	m^3/hr	m^3/hr	m^3/hr	%wt	%wt
1	26	25	17%	0.073	0.010	0.063	13.4%	33%
2	26	25	29%	0.096	0.032	0.064	33.5%	33.4%
3	26	35	17%	0.145	0.020	0.125	13.7%	34.4%
4	26	35	29%	0.149	0.028	0.121	19.0%	34.5%
5	34	25	17%	0.100	0.054	0.046	53.6%	33.2%
6	34	25	29%	0.076	0.016	0.060	21.6%	32.2%
7	34	35	17%	0.159	0.056	0.104	35.0%	33.6%
8	34	35	29%	0.170	0.057	0.114	33.2%	33.5%
9	34	28	23%	0.145	0.061	0.085	41.7%	34%
10	41	28	23%	0.132	0.081	0.051	61.2%	32.9%
11	41	16	23%	0.075	0.034	0.041	45.4%	32.1%
12	41	35	23%	0.125	0.011	0.114	8.6%	32.5%
13	41	28	12%	0.122	0.069	0.052	56.9%	34.1%
14	41	28	32%	0.099	0.018	0.081	18.0%	31.7%
15	41	28	23%	0.137	0.074	0.063	54.1%	32.1%
16	41	28	23%	0.133	0.072	0.061	54.0%	32.7%
17	41	28	23%	0.128	0.069	0.058	54.3%	33%
18	41	28	23%	0.133	0.077	0.056	58.0%	32.7%

Run	Vortex Finder Diameter	Spigot Diameter	Solids Concentration	Feed	Overflow	Underflow	Coal Yield	Ash Content
	mm	mm	%wt	m^3/hr	m^3/hr	m^3/hr	%wt	%wt
19	41	28	23%	0.134	0.080	0.054	59.7%	33%
20	41	28	23%	0.134	0.080	0.054	59.9%	32.8%

Table 32: Summarised flat-bottom cyclone mass balance experimental data

Sample ID		Volume	Mass	Time	Slurry Volumetric Flowrate	Slurry Mass Flowrate
		(ml)	(g)	(mins)	(m^3/hr)	(ton/hr)
		1	2	3	4=1/3	5=2/3
10	Feed	2450	3446.35	1.16	0.127	0.175
	Overflow	2388	2811.13	2.01	0.071	0.083
	Underflow	2477	4214.09	2.68	0.055	0.093
12	Feed	2900	4397.85	1.50	0.116	0.173
	Overflow	2550	2896.71	2.78	0.055	0.062
	Underflow	2050	3124.3	1.65	0.075	0.112
16	Feed	2850	3598.95	1.70	0.101	0.125
	Overflow	2440	2906.15	2.69	0.054	0.064
	Underflow	2100	3971.21	3.85	0.033	0.061

7.2.2 Summarized Dense Medium Cyclone Data

Table 33: Summarised dense medium cyclone tests experimental data

Run	Vortex Finder Diameter	Spigot Diameter	Medium Density	Feed	Overflow	Underflow	Coal Yield	Ash Content
	mm	mm	kg/m^3	m^3/hr	m^3/hr	m^3/hr	%wt	%wt
1	26	16	1350	0.063	0.026	0.036	42.0%	27.9%
2	26	16	1450	0.082	0.051	0.031	62.6%	30.4%
3	26	30	1350	0.122	0.024	0.098	19.4%	32.7%
4	26	30	1450	0.126	0.021	0.105	16.7%	30.0%
5	41	16	1350	0.075	0.040	0.035	53.2%	29.0%
6	41	16	1450	0.080	0.046	0.034	57.8%	28.4%
7	41	30	1350	0.125	0.039	0.086	31.0%	29.6%
8	41	30	1450	0.128	0.026	0.102	20.5%	26.8%
9	26	23	1400	0.090	0.019	0.071	21.3%	30.9%
10	41	23	1400	0.105	0.040	0.065	38.0%	32.3%
11	34	12	1400	0.137	0.111	0.026	80.9%	38.3%
12	34	30	1400	0.135	0.044	0.092	32.4%	38.9%
13	34	23	1316	0.098	0.030	0.068	30.9%	39.6%
14	34	23	1484	0.094	0.028	0.066	29.6%	30.9%
15	34	23	1400	0.095	0.032	0.063	33.3%	38.1%
16	34	23	1400	0.094	0.031	0.063	33.0%	32.6%
17	34	23	1400	0.094	0.031	0.063	33.1%	37.9%
18	34	23	1400	0.098	0.033	0.065	33.9%	37.8%
19	34	23	1400	0.097	0.031	0.066	32.1%	37.5%
20	34	23	1400	0.099	0.035	0.064	35.1%	37.8%

Table 34: Summarised dense medium cyclone mass balance experimental data

Sample ID		Volume	Mass	Time	Slurry Volumetric Flowrate	Slurry Mass Flowrate
		(ml)	(g)	(mins)	(m^3/hr)	(ton/hr)
		1	2	3	4=1/3	5=2/3
4	Feed	1750	1985.56	1.14	0.092	0.103
	Underflow	1802	1367.22	0.87	0.124	0.093
	Overflow	1650	1020	5.28	0.019	0.011
8	Feed	2000	2110.47	1.19	0.101	0.105
	Underflow	1800	1727.15	1.07	0.101	0.095
	Overflow	1300	996.99	6.06	0.013	0.010
12	Feed	2000	2456.62	1.39	0.086	0.104
	Underflow	1800	1232.61	0.81	0.133	0.090
	Overflow	1720	1011.92	4.12	0.025	0.015

7.2.3 Predicted Model Numerical Optimization

Table 35: Desirability outcome for the flat-bottom cyclone

Number	Vortex Finder Diameter (mm)	Spigot Diameter (mm)	Solids Concentration (%)	Ash Content (%)	Coal Yield (%)	Desirability
1	**41**	**25**	**29**	**31.9**	**35.4**	**0.925**
2	41	25	29	31.9	35.5	0.924
3	41	25	29	31.9	35.5	0.924

Number	Vortex Finder Diameter (mm)	Spigot Diameter (mm)	Solids Concentration (%)	Ash Content (%)	Coal Yield (%)	Desirability
4	41	25	29	31.9	35.7	0.923
5	41	25	29	31.9	35.8	0.923
6	41	25	29	31.9	35.0	0.922
7	41	25	29	31.9	35.8	0.921
8	41	25	29	31.9	35.8	0.921
9	41	25	29	31.9	34.7	0.920
10	41	25	29	31.9	36.0	0.920
11	41	25	28	31.9	36.3	0.919
12	41	25	29	31.9	36.0	0.919
13	41	25	29	31.9	36.1	0.918
14	41	25	28	31.9	35.9	0.917
15	41	25	28	31.9	36.6	0.917
16	41	25	29	31.9	34.3	0.916
17	41	26	29	31.9	36.2	0.916
18	41	25	29	31.9	34.4	0.916
19	41	26	29	31.9	36.3	0.915
20	41	25	29	31.9	33.8	0.912
21	41	25	28	31.9	37.4	0.911
22	41	25	28	31.9	37.6	0.910
23	41	26	29	32.0	36.8	0.908
24	41	25	28	32.0	38.3	0.905
25	41	26	29	32.0	37.0	0.904
26	40	25	29	32.0	32.8	0.904
27	40	25	29	32.0	32.5	0.902
28	41	27	29	32.0	37.1	0.900
29	41	27	29	32.0	37.2	0.898
30	41	27	29	32.0	37.3	0.896

Number	Vortex Finder Diameter (mm)	Spigot Diameter (mm)	Solids Concentration (%)	Ash Content (%)	Coal Yield (%)	Desirability
31	41	27	29	32.0	37.3	0.895
32	41	27	29	32.0	37.3	0.891
33	40	25	29	32.0	31.5	0.888
34	40	25	29	32.0	31.1	0.887
35	41	25	28	32.0	38.1	0.884
36	41	28	29	32.0	37.1	0.879
37	41	28	29	32.0	37.1	0.878
38	41	28	29	32.0	37.0	0.876
39	41	28	29	32.0	37.0	0.875
40	39	25	29	32.1	27.8	0.859
41	41	29	29	32.1	35.2	0.854
42	39	25	29	32.1	26.7	0.847
43	41	30	29	32.1	34.3	0.846
44	41	25	27	32.1	46.8	0.843
45	41	31	29	32.2	31.6	0.830
46	41	32	29	32.2	28.6	0.816
47	41	25	26	32.3	52.1	0.800
48	41	33	29	32.3	23.0	0.794
49	41	33	29	32.3	22.5	0.793
50	41	35	29	32.3	14.4	0.769
51	39	25	25	32.5	50.0	0.709
52	41	35	25	32.7	12.1	0.632
53	41	25	22	32.8	70.5	0.617
54	33	25	23	33.0	39.6	0.551
55	33	25	20	33.1	42.5	0.505
56	31	25	19	33.2	37.1	0.481
57	31	25	19	33.2	37.2	0.480

K

L

Table 36: Desirability outcome for the dense medium cyclone

Number	Vortex Finder Diameter (mm)	Spigot Diameter (mm)	Medium Density (kg/m^3)	Ash Content (%)	Coal Yield (%)	Desirability
1	**41**	**30**	**1450**	**27.6**	**20.8**	**0.942**
2	26	30	1450	27.6	16.9	0.942
3	26	30	1450	27.6	16.6	0.939
4	26	30	1450	27.6	16.5	0.939
5	41	30	1450	27.6	20.9	0.938
6	41	30	1449	27.6	21.0	0.936
7	41	29	1450	27.6	21.5	0.936
8	41	30	1448	27.6	21.1	0.935
9	41	29	1450	27.7	21.6	0.935
10	26	30	1450	27.7	17.0	0.934
11	26	29	1450	27.7	15.8	0.932
12	41	30	1447	27.7	21.2	0.932
13	41	30	1450	27.7	20.9	0.930
14	26	29	1450	27.7	15.7	0.930
15	41	29	1450	27.7	22.3	0.929
16	41	29	1450	27.7	22.5	0.928
17	26	29	1450	27.7	16.0	0.927
18	41	29	1450	27.8	22.6	0.927
19	41	28	1450	27.8	22.7	0.926
20	26	30	1445	27.8	17.3	0.925
21	26	28	1450	27.8	15.4	0.925
22	26	30	1445	27.8	17.3	0.923
23	41	28	1450	27.8	23.3	0.923

M

Number	Vortex Finder Diameter (mm)	Spigot Diameter (mm)	Medium Density (kg/m^3)	Ash Content (%)	Coal Yield (%)	Desirability
24	26	30	1450	27.9	17.2	0.917
25	26	27	1450	27.9	15.5	0.914
26	41	27	1450	27.9	24.6	0.914
27	41	27	1450	27.9	25.0	0.912
28	26	27	1450	28.0	15.6	0.911
29	41	27	1450	28.0	25.3	0.910
30	41	27	1450	28.0	25.5	0.909
31	26	27	1450	28.0	15.9	0.907
32	41	26	1450	28.0	26.1	0.906
33	41	30	1440	28.0	22.4	0.905
34	41	26	1450	28.0	26.3	0.905
35	26	26	1450	28.0	16.2	0.904
36	26	30	1439	28.1	17.8	0.903
37	41	25	1450	28.2	29.2	0.891
38	26	30	1435	28.2	18.0	0.888
39	41	24	1450	28.3	30.4	0.885
40	41	30	1433	28.3	23.3	0.883
41	41	24	1450	28.3	31.1	0.882
42	41	28	1437	28.3	25.1	0.882
43	41	24	1450	28.3	31.3	0.881
44	26	27	1439	28.4	16.1	0.878
45	41	23	1450	28.4	33.3	0.873
46	41	23	1450	28.5	34.4	0.869
47	26	23	1450	28.5	24.0	0.869
48	41	23	1450	28.5	34.9	0.867
49	26	30	1428	28.5	18.4	0.866

N

Number	Vortex Finder Diameter (mm)	Spigot Diameter (mm)	Medium Density (kg/m^3)	Ash Content (%)	Coal Yield (%)	Desirability
50	26	22	1450	28.5	25.4	0.865
51	26	22	1450	28.7	28.9	0.856
52	26	21	1450	28.7	29.8	0.854
53	41	21	1450	28.7	38.8	0.853
54	41	21	1450	28.7	39.3	0.852
55	41	21	1450	28.7	39.4	0.851
56	26	30	1423	28.8	18.7	0.848
57	26	21	1450	28.8	32.9	0.847
58	41	20	1450	28.8	41.7	0.844
59	26	30	1421	28.9	18.8	0.841
60	26	20	1450	28.9	36.3	0.840
61	26	20	1450	28.9	37.9	0.837
62	41	18	1448	29.2	50.0	0.818
63	41	17	1450	29.3	53.9	0.810
64	41	30	1412	29.3	26.1	0.808
65	26	17	1450	29.3	57.3	0.807
66	26	16	1450	29.3	60.7	0.802
67	26	19	1422	29.4	36.3	0.796
68	26	17	1421	29.6	50.9	0.785
69	26	25	1408	29.6	17.8	0.785
70	41	30	1405	29.6	26.9	0.784
71	26	16	1420	29.6	54.7	0.781
72	26	30	1404	29.6	19.5	0.780
73	41	16	1417	29.7	57.1	0.778
74	26	16	1416	29.7	57.2	0.777
75	41	16	1413	29.7	57.6	0.775

O

Number	Vortex Finder Diameter (mm)	Spigot Diameter (mm)	Medium Density (kg/m^3)	Ash Content (%)	Coal Yield (%)	Desirability
76	26	19	1406	29.7	36.1	0.774
77	26	16	1409	29.7	55.8	0.773
78	41	16	1406	29.8	57.4	0.770
79	41	16	1397	29.8	57.0	0.764
80	26	16	1385	29.9	50.7	0.757